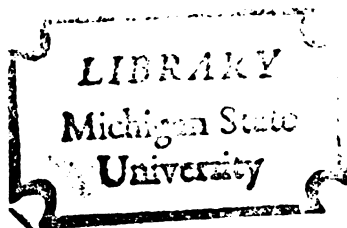




THESIS



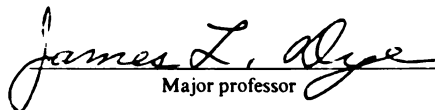
This is to certify that the  
dissertation entitled  
RAPID-SCANNING STOPPED-FLOW STUDIES  
OF THE REDUCTION OF CYTOCHROME c OXIDASE

presented by

Folim G. Halaka

has been accepted towards fulfillment  
of the requirements for

Ph.D degree in Chemistry

  
Major professor

Date October 22, 1981



RETURNING MATERIALS:  
Place in book drop to  
remove this checkout from  
your record. FINES will  
be charged if book is  
returned after the date  
stamped below.

--	--	--

RAPID-SCANNING STOPPED-FLOW STUDIES OF THE  
REDUCTION OF CYTOCHROME c OXIDASE

By

Folim G. Halaka

A DISSERTATION

Submitted to  
Michigan State University  
in partial fulfillment of the requirements  
for the degree of

DOCTOR OF PHILOSOPHY

Department of Chemistry

1981

## ABSTRACT

### RAPID-SCANNING STOPPED-FLOW STUDIES OF THE REDUCTION OF CYTOCHROME c OXIDASE

By

Folim G. Halaka

Rapid scanning and fixed-wavelength stopped-flow spectrophotometry were used to study the anaerobic reduction of cytochrome c oxidase by 5, 10-dihydro 5-methylphenazine (MPH) and by sodium dithionite. In both cases the decay of the oxidized Soret band of the protein was not uniform. With MPH, a neutral molecule, the reduction of the cytochrome a component of the oxidase preceded that of cytochrome a<sub>3</sub>. The kinetics of the reduction were found to be triphasic. The fast phase is a second order reaction between the oxidase and MPH. This is followed by two first order processes, which were interpreted as intramolecular electron redistribution between the oxidase four metal centers. Analysis of kinetic data showed that during the fast phase, the decay at 830 nm, due to the reduction of the copper ion associated with cytochrome a, lags the growth of absorbance at 605 nm (due to cytochrome a).

The method of weighted principal component analysis (PCA) was used to resolve the three dimensional data surface obtained by the scanning stopped-flow method. By using PCA, the wavelength-absorbance-time data surface was resolved to its independent

components, and the spectral shapes and time courses of those components. Time courses obtained by PCA confirmed the assignments of cytochrome a as the site of reduction by MPH.

The properties of MPH and its oxidized form (MPMS) were also studied. The kinetics of the reduction of MPMS to MPH by NADH and the oxidation of MPH by oxygen were investigated. The anaerobic photoreaction of MPMS at pH = 7.4 was found to produce pyocyanine and MPH at nearly equal concentrations.

The reduction of cytochrome oxidase by sodium dithionite was found to involve the  $\text{SO}_2^{\cdot-}$  anion radical as the reducing agent. In contrast to MPH,  $\text{SO}_2^{\cdot-}$  was shown to reduce preferentially the cytochrome a<sub>3</sub> site of the oxidase. This was interpreted on the basis that the cytochrome a surface must be negatively charged.

The reduction of cyanide-bound cytochrome c oxidase by MPH was found to be monophasic, and involving only the cytochrome a site and its associated copper. The reduction of the CN-complex by sodium dithionite was biphasic.

## ACKNOWLEDGMENTS

I would like to thank Dr. James L. Dye for proposing this work on the anaerobic stopped-flow system and for his encouragement, enthusiasm and stimulating discussions.

I am most grateful to Dr. Gerald T. Babcock for his support and ideas, and for acquainting me with the properties of cytochrome oxidase and its biological importance.

I wish to thank the National Science Foundation, National Institute of Health and the Department of Chemistry for financial support as research and teaching assistantships.

I would like to thank Dr. Tom V. Atkinson and Dr. Tom H. Pierce for their help with the computer work that appears throughout this work, and for assisting with computer graphics.

Finally, I am grateful to my wife, Carole, for her encouragement and help in the typing of this manuscript.

## TABLE OF CONTENTS

	Page
LIST OF TABLES . . . . .	vi
LIST OF FIGURES . . . . .	vii
Chapter	
I. INTRODUCTION . . . . .	1
A. Cytochrome <u>c</u> Oxidase . . . . .	1
A.1 Structure and Subunits . . . . .	2
A.2 Physico-Chemical Properties . . . . .	8
A.3 Redox Properties . . . . .	16
A.4 Kinetic Studies . . . . .	19
B. Scanning Stopped-Flow Technique for the Study of Multicentered Enzyme Reactions . . . . .	24
C. Treatment of Scanning Stopped-Flow Data . . . . .	25
C.1 Rate Equations--Program KINFIT4 . . . . .	25
C.2 Weighted Principal Component Analysis . . . . .	26
D. Reducing Agents for the Study of Electron Trans- fer Reactions of Cytochrome Oxidase . . . . .	27
II. EXPERIMENTAL METHODS . . . . .	30
A. Materials . . . . .	30
B. Methods . . . . .	31
B.1 Preparation of Cytochrome Oxidase . . . . .	31
B.2 Activity Assays of Cytochrome <u>c</u> Oxidase . . . . .	32
B.3 Preparation of Anaerobic Solutions . . . . .	32
B.4 Anaerobic Titrations . . . . .	33
C. The Stopped-Flow System . . . . .	35
C.1 Handling and Performance of the Stopped-Flow System . . . . .	36
D. Data Handling, Computations and Computer Graphics . . . . .	41
III. PROPERTIES OF 5-METHYL PHENAZINIUM METHYLSULFATE: REACTION OF THE OXIDIZED FORM WITH NADH AND OF THE REDUCED FORM WITH OXYGEN . . . . .	43
A. Introduction . . . . .	43

Chapter	Page
B. Experimental Section . . . . .	46
C. Results and Discussion . . . . .	48
C.1 Anaerobic Titration and Transient Kinetics of the Reduction of MPMS by NADH . . . . .	48
C.2 Reaction of MPH with Oxygen . . . . .	52
C.3 The Reaction of MPMS with NADH in the Presence of Oxygen . . . . .	52
C.4 Effect of Room Light on the Spectra of MPMS . . . . .	55
D. Conclusions . . . . .	58
IV. REDUCTION OF CYTOCHROME OXIDASE BY MPH . . . . .	59
A. Spectral Shape Analysis . . . . .	60
B. Kinetics of the Reduction of Cytochrome Oxidase by MPH . . . . .	66
B.1 Analysis of the Fast Phase . . . . .	69
B.2 Kinetics of the Slow Processes . . . . .	76
C. Reduction of the Cyanide-Bound Cytochrome Oxidase . . . . .	79
C.1 Spectral Shape Analysis . . . . .	79
C.2 Kinetics . . . . .	82
D. Conclusions . . . . .	85
V. PRINCIPAL COMPONENT ANALYSIS OF THE REDUCTION OF CYTOCHROME <u>c</u> OXIDASE BY MPH . . . . .	90
A. Introduction . . . . .	90
B. The Method of Principal Component Analysis (PCA). B.1 Preparation Steps . . . . .	91
B.2 Number of Components . . . . .	94
B.3 PCA Determination of Real Components . . . . .	98
C. Principal Component Analysis of the Reaction of Cytochrome Oxidase by MPH . . . . .	100
C.1 PCA on the Reduction of the Resting Enzyme by MPH . . . . .	102
C.2 PCA on the Reduction of the Oxygenated Enzyme by MPH . . . . .	102
D. Conclusions . . . . .	115
VI. REDUCTION OF CYTOCHROME OXIDASE BY SODIUM DITHIONITE. A. Introduction . . . . .	123
B. Spectral Shape Analysis . . . . .	130
C. Kinetics of the Reduction of Cytochrome by Sodium Dithionite . . . . .	131
D. Effect of Cholate . . . . .	133
	139

Chapter	Page
E. Reduction of the Cyanide-Bound Cytochrome Oxidase by Dithionite . . . . .	142
F. Discussion . . . . .	145
VII. SUGGESTIONS FOR FUTURE WORK . . . . .	151
A. Effect of Detergents . . . . .	151
B. Partial Reduction of Cytochrome <u>c</u> Oxidase . . . . .	152
C. Aerobic Experiment . . . . .	152
D. Cytochrome <u>c</u> <sub>552</sub> . . . . .	153
E. The Application of Principal Component Analysis to Other Systems . . . . .	154
REFERENCES . . . . .	155

## LIST OF TABLES

Table	Page
IV.1 Analysis of the fast phase of the reduction of cytochrome oxidase by MPH in HEPES buffer containing 0.5% Tween 20, pH = 7.4 at $21 \pm 1^\circ\text{C}$ . $k_1^f$ is the second order rate constant for the process . . . . .	73
IV.2 Summary of studies on the "slow phase" of the reduction of cytochrome oxidase by MPH in HEPES buffer containing 0.5% Tween 20, pH 7.4, $T = 21 \pm 1^\circ\text{C}$ . .	80
IV.3 Rate constant for the reduction of the cyanide-bound cytochrome oxidase by MPH in 50 mM HEPES buffer containing 5% Tween 20, pH = 7.4 at $21 \pm 1^\circ\text{C}$ . Data are collected in fixed-wavelength experiments . . . .	84
VI.1 Rate constant for the reduction of cytochrome oxidase by sodium dithionite in 50 mM HEPES buffer containing 0.5% Tween 20, pH = 7.4, $T = 21^\circ\text{C}$ . Rate constants are the observed first-order constants from the analysis of data by three exponentials . . . . .	136

## LIST OF FIGURES

Figure	Page
I.1 Structure of heme <u>a</u> . . . . .	3
I.2 Optical absorption spectra of cytochrome oxidase: ____, oxidized, and -----, fully reduced . . . . .	10
I.3 Absorption spectra of cytochromes <u>a</u> , <u>a<sub>3</sub></u> and the CN- complex of cytochrome <u>a<sub>3</sub></u> ; _____ . . . . .	11
I.4 EPR reductive titration data for g = 2, 3, and 6 signals . . . . .	14
I.5 The Cu ( <u>a<sub>3</sub></u> ) -- Fe ( <u>a<sub>3</sub></u> ) and Cu ( <u>a</u> )--Fe ( <u>a</u> ) centers in cytochrome oxidase . . . . .	17
II.1 Cells used for preparing anaerobic solution (A) and for anaerobic titrations and preparation of air- sensitive reductants (B) . . . . .	34
II.2 Flow-velocity profile as a function of pressure . . . . .	38
II.3 Test of mixing efficiency in the stopped-flow apparatus . . . . .	40
III.1 Structure of N-methyl phenazine at different pro- tonation and oxidation levels . . . . .	44
III.2 Anaerobic titration of 7 ml of 15.9 $\mu$ M MPMS by successive additions of 0.026 ml increments of 0.527 mM NADH in 50 mM HEPES buffer, pH = 7.4 . . . . .	49
III.3 Spectral changes during the anaerobic reduction 31.9 $\mu$ M MPMS by 39 $\mu$ M NADH . . . . .	50
III.4 Spectral changes which result from mixing NADH with MPMS in the presence of atmospheric oxygen . . . . .	53
III.5 Effect of room fluorescent light on the spectra of 21.2 $\mu$ M aerobic MPMS . . . . .	56
IV.1 Absorbance-time-wavelength surface in the 330-530 region for the anaerobic reduction of cytochrome oxidase by 5, 10-dihydro-5-methyl phenazine (MPH) . . . . .	61

Figure	Page
IV.2 Absorbance-time wavelength surface for the anaerobic reduction of cytochrome oxidase by MPH in the 400 - 630 nm region . . . . .	62
IV.3 Selected spectra from Figure IV.1 . . . . .	64
IV.4 Selected difference spectra constructed from Figure IV.1 by subtracting the oxidized oxidase spectrum . . . . .	65
IV.5 Time dependence of absorbance at 430, 412 and 388 nm; taken from the spectra shown in Figure IV.1 . . . . .	67
IV.6 Selected spectra in the reaction of MPH with cytochrome oxidase, taken from the data shown in Figure IV.2 . . . . .	68
IV.7 (A) Fit of the fast phase for the reduction of cytochrome oxidase by MPH . . . . .	71
IV.8 (A) The decay at 830 nm and 605 nm during the reduction of 10.8 $\mu\text{M}$ cytochrome <u>aa<sub>3</sub></u> by 27 $\mu\text{M}$ MPH . . . . .	75
IV.9 Fit of the "slow phase" to one exponential (a); to a second order process,(b); and to two exponentials (c) . . . . .	77
IV.10 Residual plots for the fit to the data in Figure IV.9 . . . . .	78
IV.11 Spectral changes that resulted on the reduction of 2.4 $\mu\text{M}$ CN-oxidase by 6.5 $\mu\text{M}$ MPH . . . . .	81
IV.12 Time courses for the reduction of the CN-oxidase by MPH followed at 430 nm (A), 605 nm, (B) and at 444 nm (C) . . . . .	83
V.1 Block diagram for main steps in factor analysis . . . . .	93
V.2 Experimental absorbance-wavelength-time surface for the anaerobic reduction of 3.78 $\mu\text{M}$ cytochrome oxidase by 8.4 $\mu\text{M}$ MPH . . . . .	104
V.3 Principal component analysis (PCA) reconstructed surface using three eigenvectors in M-analysis . . . . .	105
V.4 Reconstructed surface using only two M-analysis eigenvectors for the data in Figure V.2 . . . . .	106

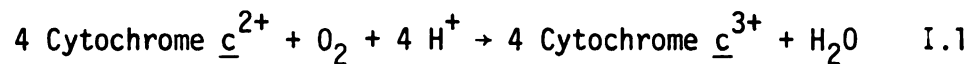
Figure	Page
V.5 Residual surface, resulting from subtracting the matrix in Figure V.3 from the data in Figure V.2 . . . . .	107
V.6 Residual surface . . . . .	108
V.7 M-analysis fit of oxidized cytochrome <u>a</u> spectra from the data presented in Figure V.2 . . . . .	110
V.8 M-analysis fit of oxidized cytochrome <u>a</u> using three eigenvectors . . . . .	111
V.9 M-analysis fit of the reduced oxidase + MPMS contribution . . . . .	112
V.10 Concentration-time profile for the disappearance of oxidized cytochrome <u>a</u> . . . . .	114
V.11 Experimental wavelength-absorbance-time data surface for the anaerobic reduction of the oxygenated form of the oxidase by 26 $\mu\text{M}$ MPH . . . . .	116
V.12 Reconstructed surface for the data presented in Figure V.11 using two eigenvectors . . . . .	117
V.13 Reconstructed surface for the data in Figure V.11 using three eigenvectors . . . . .	118
V.14 Residuals of the data presented in Figure V.11 . . . . .	119
V.15 Residuals of the data presented in Figure V.11 . . . . .	120
V.16 M-analysis fit of the combined oxidized cytochromes <u>a</u> and <u>a<sub>3</sub></u> spectrum for the oxygenated oxidase . . . . .	122
V.17 Three eigenvectors M-analysis fit to the spectrum of reduced cytochrome <u>a</u> . . . . .	124
V.18 Three eigenvectors M-analysis fit to the spectrum of reduced cytochrome <u>a<sub>3</sub></u> . . . . .	125
V.19 Concentration-time profile for the growth of reduced cytochrome <u>a</u> , (B); reduced cytochrome <u>a<sub>3</sub></u> (C); and for the disappearance of the combined oxidized ( <u>aa<sub>3</sub></u> ) . . . . .	126
VI.1 Spectral shapes during the anaerobic reduction of 3.78 $\mu\text{M}$ cytochrome oxidase by 47 $\mu\text{M}$ sodium dithionite . . . . .	132

## CHAPTER I

### INTRODUCTION

#### A. Cytochrome c Oxidase

Cytochrome c oxidase (ferrocytochrome c: oxygen oxidoreductase, EC 1.9.3.1) is the terminal oxidase in the respiratory chain of all aerobic organisms. The enzyme, referred to as cytochrome aa<sub>3</sub> or cytochrome oxidase, is a membrane-bound heme protein which catalyzes the reduction of molecular oxygen to water by ferrocytochrome c, according to Equation I.1



The energy released is used for the synthesis of adenosine triphosphate (ATP), which, in turn, is used as the source of energy in other cell activities (see, for example, Lemberg, 1969). It is estimated that about 90% of the oxygen consumption in biological systems is achieved through cytochrome oxidase (Malmstrom, 1973). The protein is, therefore, prominent in tissues where energy requirements are high (Challoner, 1968; Tucker, 1966). Although this study will focus on the electron transport properties of the protein, the proton translocation across the mitochondrial membrane as a result of Equation I.1 has been observed and suggests that cytochrome oxidase can act as a proton pump (Wikström and Krab, 1979).

The work of Keilin (see, for historical background, Keilin, 1966) conclusively demonstrated the heme nature of the prosthetic group of the protein and its link to the cell respiratory chain. Due to the obvious importance of the protein, it was, and currently is, the subject of active investigation by every conceivable physico-chemical technique. Various comprehensive reviews have appeared in the literature which survey the state of understanding of the protein at the time of their publication. Examples are the articles by Lemberg (1969), Malstrom (1973), Wharton (1974), Nicholls and Chance (1974), Erecinska and Wilson (1978), and Malmstrom (1979).

#### A.1 Structure and Subunits

A.1.1 Metal components.--It is now agreed that all functional preparations of cytochrome oxidase contain iron and copper as essential components (Volpe and Caughey, 1974). It is also well established that the iron to copper ratio is 1 (Griffith and Wharton, 1961a,b). Caughey et al. (1976), reported that most preparations contain about 11 nanomoles of iron per mg protein. More recent procedures (Komai and Capaldi, 1973; Hartzell and Beinert, 1974) contain iron ratio as high as 14 nanomole/mg protein.

Keilin and Hartree (1938a,b; 1956) demonstrated that the iron of the oxidase is present as heme a (Figure I.1). They also showed, from reactions with CO and other inhibitors that cytochrome oxidase is actually composed of two heme a components: Cytochromes a and a<sub>3</sub> (hence the name cytochrome aa<sub>3</sub> for the oxidase). Only cytochrome a<sub>3</sub> is found to react with exogenous ligands such as cyanide, azide, CO



and oxygen. However, only one heme compound with a particular structure, heme a, (Fig. I.1), is isolated from cytochrome oxidase (Caughey et al., 1975). This classical cytochrome aa<sub>3</sub> picture was confirmed by recent investigations of the stoichiometry of the CO binding, showing that only one-half of the oxidase heme binds CO (Wharton and Gibson, 1976; Toshikawa et al., 1977). Thus, the cytochrome oxidase molecule must contain two iron and two copper ions.

Although the immediate environments of the iron of the oxidase are now accepted to be heme a, the environments of the two copper atoms are less well understood. The copper is apparently well shielded by the protein, which is evident from the fact that it is not readily extractable by common  $\text{Cu}^{2+}$  ligands. Griffith and Wharton (1961) showed that there is no exchange between added  $\text{Cu}^{2+}$  and the copper ions of the oxidase. When Cu was removed from cytochrome oxidase, the activity was irreversibly lost (Wharton and Tzagoloff, 1964). From electron paramagnetic resonance (EPR) studies, it was concluded that there exist two different functional copper ions in the oxidase (see Section A.3), only one of which is EPR detectable. The EPR detectable Cu, normally associated with cytochrome a is designated  $\text{Cu}_a$  (sometimes  $\text{Cu}_d$ ). The EPR undetectable Cu is designated  $\text{Cu}_{a_3}$  (or  $\text{Cu}_u$ ).

Based on spectroscopic properties, the copper sites in copper proteins are put into one of three major classifications (Malkin and Malmstrom, 1970). Type I or "blue" copper sites exhibit absorption bands near 450 nm ( $\epsilon = 0.3\text{-}1.0 \text{ mM}^{-1} \text{ cm}^{-1}$ ), 600 nm ( $\epsilon = 3\text{-}10 \text{ mM}^{-1} \text{ cm}^{-1}$ ), and a near infrared band at around 800 nm ( $\epsilon = 0.3\text{-}3.0 \text{ mM}^{-1} \text{ cm}^{-1}$ ).

Type I copper exhibits narrow EPR hyperfine structure (Peisach and Blumberg, 1974) and an oxidation-reduction potential of about 0.3 - 0.4 V. Type II copper sites (non-blue copper) have less well-defined optical properties, they have a weak absorption band at 600 - 700 nm ( $\epsilon = 0.3 - 0.4 \text{ mM}^{-1} \text{ cm}^{-1}$ ) and their EPR spectra are characterized by a broad hyperfine structure (Peisach and Blumberg, 1974). In proteins having both type I and type II copper sites, the blue copper is more quickly reduced, while the non-blue copper has more affinity toward anions. Type III copper sites are EPR non-detectable. They are thought to be diamagnetic and consist of either  $\text{Cu}^+$  or a spin-paired,  $\text{Cu}^{2+} - \text{Cu}^{2+}$ . Their oxidation-reduction potentials are greater than 0.5 V (Malkin and Malmström, 1970).

A.1.2 Peptide subunits.--Isolated cytochrome oxidase contains several subunits. The number and composition of these subunits, as well as their positions relative to one another and in the membrane, are still uncertain. The hypothesis that the enzyme complex consists of seven different subunits was developed on the basis of studies on microbial enzymes (Sebald et al., 1973; Poyton and Schatz, 1975) and was subsequently extended to include mammalian enzyme (Downer et al., 1976; Tracy and Chan, 1979; Hochli and Hackenbrock, 1978). These subunits are given the Roman numerals I - VII. However, several other groups have prepared bovine enzymes with only six subunits (Rubin and Tzagoloff, 1973; Briggs et al., 1975; Penttila et al., 1979). The subunits are reported to be present in 1:1 ratio (Downer et al., 1976; Yu and Yu, 1977). There is, however, substantial disagreement about

the molecular weights of the individual subunits. The hydrophobic nature of many of these peptide subunits adds another complication, since most conventional methods of determining molecular weights cannot be applied to them. Instead, gel electrophoresis was used. Recent preparations (Hartzell and Beinert, 1975) give good agreement between the molecular weight calculated on the basis of heme: protein ratio (14 nanomole/mg) and the sum of the individual molecular weights of the subunits, 140,000 Daltons.

Since the number of subunits is greater than the number of metal ions in the enzyme complex, some of the polypeptides may have a role in arranging the complex in the membrane (Steffens and Buse, 1979) and/or a proton pump function (Wikström and Krab, 1979). Phan and Mahler (1976a,b) reported experiments in which they prepared a four-subunit enzyme that retained electron transfer activity (toward cytochrome c<sup>2+</sup> oxidation). These results have been extended by Fry et al. (1978) who claim to have separated the protein into an electron transfer complex and an ion (H<sup>+</sup>) transfer portion, which contains no metal ions. The metal binding polypeptide subunits are subject to a great uncertainty. Almost all subunits have been reported to bind either copper or iron, or both (Tanaka et al., 1977; Gutteridge et al., 1977). Also, the results of experiments that have been designed to identify which subunit interacts with cytochrome c are quite variable (Briggs and Capaldi, 1978; Bisson, et al., 1978; Birchmeier et al., 1976; Seiter et al., 1979). Recently Winter et al. (1980) reported that subunit II bound most of the Cu

and that heme a was found in equal amounts in subunits I and II. They suggested that subunit II is the site for cytochrome c binding, while subunit I is the binding site for oxygen.

Isolated cytochrome oxidase has not been crystallized in a form suitable for X-ray diffraction studies, although one account of a crystalline lyophilized preparation (Yonetani, 1961) and a crystalline cytochrome c-cytochrome oxidase complex (Ozawa et al., 1980) have appeared. Two dimensional "crystals" of membranes containing cytochrome oxidase have, however, been obtained. Henderson et al. (1977) have shown that the oxidase molecule is asymmetrically placed in the membrane. The picture that emerges from these studies, though far from perfect, is that of a multi-subunit enzyme spanning the membrane with two "heads," one in the cytosolic side and the other in the matrix side.

A.1.3 Lipids.--Depending on the method of preparation, isolated cytochrome oxidase contains variable amounts of lipids. Certain amounts of lipids are essential in order to maintain electron transport activity. To solubilize the protein, the use of several non-denaturing detergents has been implemented. The importance of different phospholipid head-groups to cytochrome oxidase activity has been examined by several research groups (Awasthi et al., 1971; Yu et al., 1975). A study on the decrease in activity of the oxidase upon lipid depletion has been reported by Vanneste et al. (1974). However, the activity was restored by the addition of phospholipids or detergents.

Robinson and Capaldi (1977) found important differences in the mode of action of non-denaturing detergents. Their study on the displacement of the protein phospholipids by several ionic and non-ionic detergents showed that some phospholipids do not exchange with detergents. Their studies also suggest that the oxidase is in a dimer form (4 heme a/oxidase complex) and that the oxidase activity is greatly affected by the nature of the hydrocarbon portion of the detergent.

Rosevear et al. (1980) have examined the interaction of the detergent lauryl maltoside with cytochrome oxidase. Their results indicate that this detergent, in addition to maintaining high electron transport activity (oxidation of cytochrome c), also has the advantage that the protein solution is monodisperse (probably as the dimer).

## A.2 Physico-Chemical Properties

It is almost impossible, due to their diversity, to cover in this introduction all the physico-chemical studies which have been done on cytochrome oxidase. Hence, this section will cover only recent studies relevant to the electron transfer properties on the protein.

A.2.1 Optical absorption of cytochrome oxidase and its derivatives.--Simple and more convenient than many other physical methods, optical absorption spectroscopy provides a way to monitor changes in the oxidase induced by various chemical reactions. Indeed, spectral observations were instrumental in the pioneering experiments that characterized this important protein.

Cytochrome oxidase has several absorption peaks that characterize its redox and/or ligation state. Figure I.2 shows the spectral characteristics of the oxidized (resting) and the fully reduced protein. The electromagnetic absorption in the near UV (the "Soret" or  $\alpha$ -band) and that in the visible (the  $\alpha$ -band) is due to the porphyrin ring of the heme a moieties. The structure of heme a is shown in Figure I.1. A theoretical discussion of the origin of porphyrin spectra, based on group theoretical calculations of the  $D_{4h}$  symmetry of the polyene and allowing for configuration interaction is given by Gouterman (1959).

Assignments of wavelengths and extinction coefficients for hemes a and a<sub>3</sub> and copper (Vanneste, 1966) have been rather widely accepted (Lemberg, 1969). These assignments are summarized in Figure I.3. It is, however, risky to synthesize spectra for cytochromes a and a<sub>3</sub> on the assumption that the properties of one heme are independent of the oxidation or ligation state of the other metal component(s) (Caughey et al., 1976). This comment takes into account the fact that there is ample evidence of facile electron and magnetic exchange between the metal centers in the oxidase (Hartzell et al., 1974; Babcock, et al., 1978).

It is obvious that any absorption, or in the same sense, change in absorption, due to copper in the Soret or the  $\alpha$ -regions will be obscured by the much larger absorptions of the heme chromophores (see Section A.1.1 for the magnitudes of protein copper extinctions).

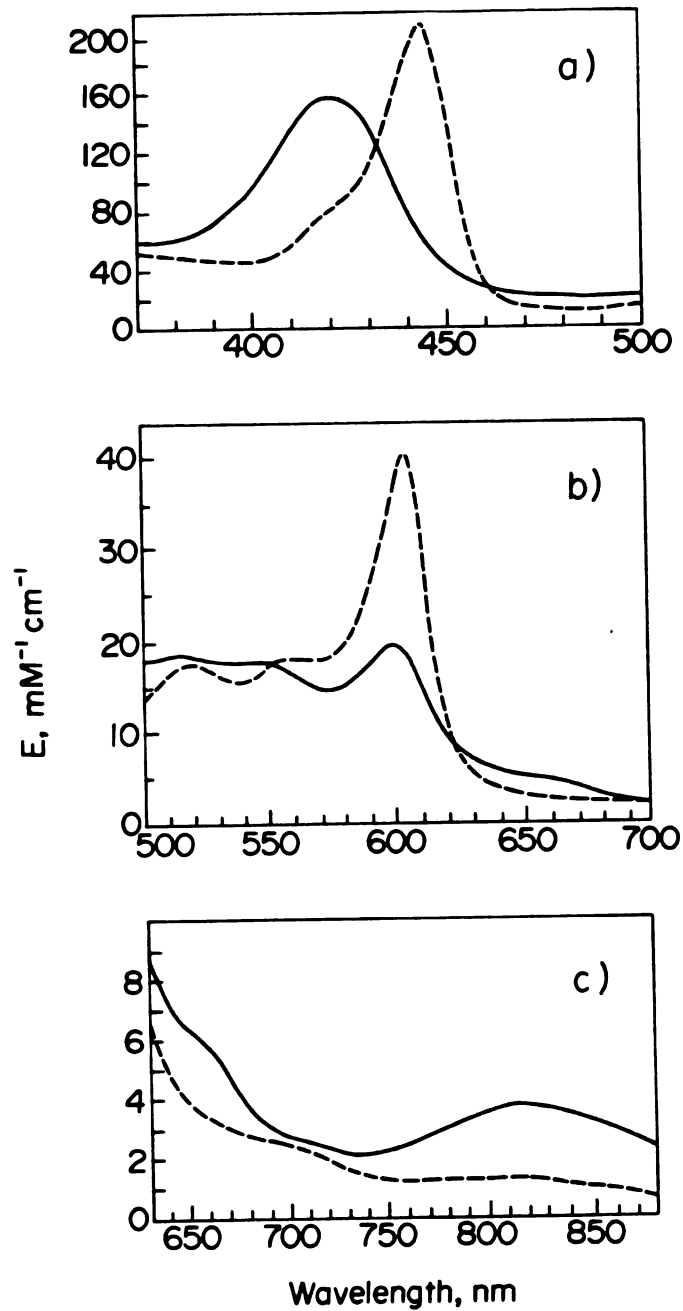


Figure I.2.--Optical absorption spectra of cytochrome oxidase: \_\_\_\_\_, oxidized, and ----, fully reduced. Molar absorptivities are expressed per unit containing two hemes and two copper ions.

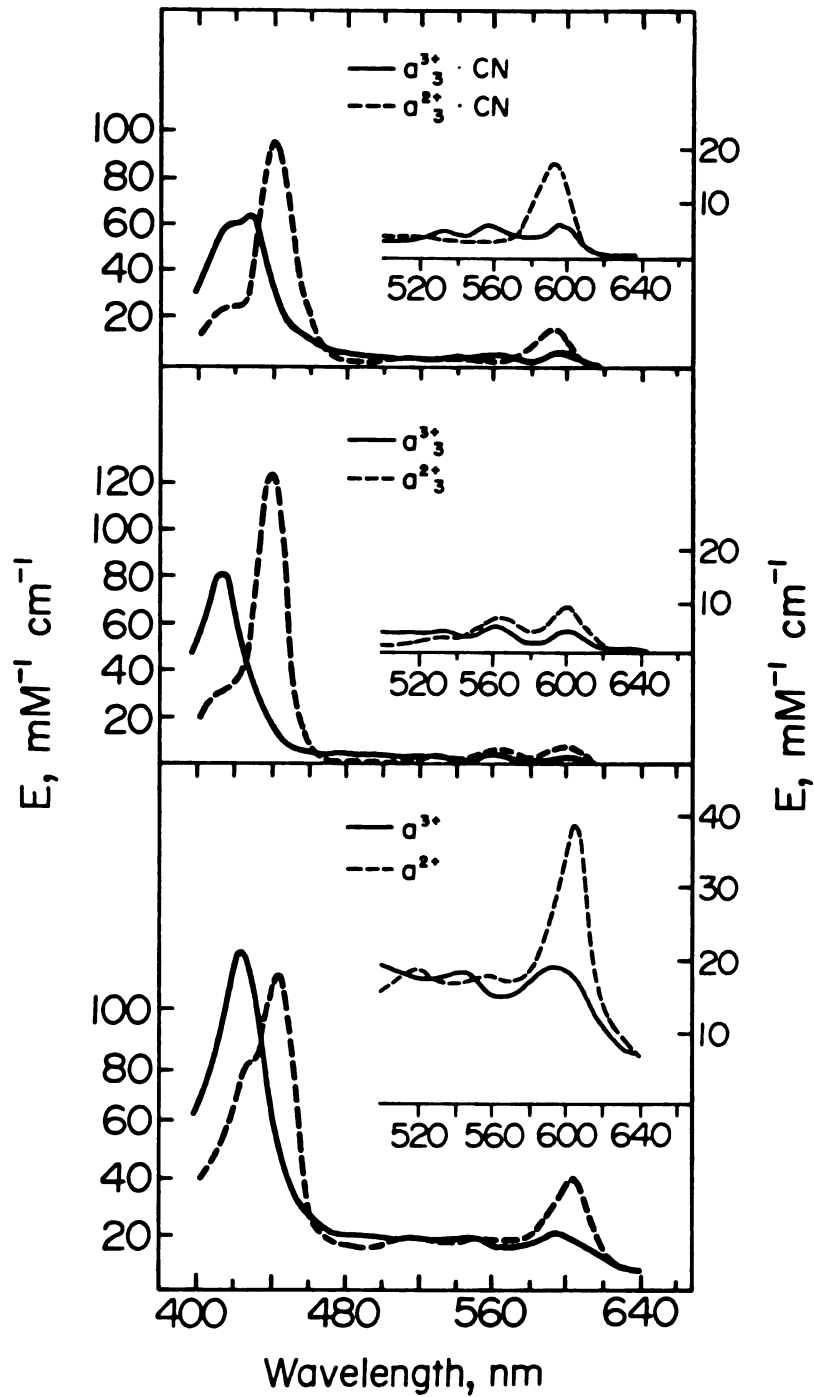


Figure I.3.--Absorption spectra of cytochromes  $a$ ,  $a_3$  and the CN-complex of cytochrome  $a_3$ ; \_\_\_\_\_, oxidized and -----, reduced; taken from Vanneste (1966).

Griffiths and Wharton (1961a) drew attention to a weak absorption band ( $\epsilon \sim 4\text{mM}^{-1} \text{cm}^{-1}$ ) in the near I.R. region (800 - 900 nm). This band was attributed mainly to copper,  $\text{Cu}_a$ , absorption (Wharton and Tzagoloff, 1963). However, it was argued that the oxidase hemes may contribute in this region (Greenwood et al., 1974). Based on extended X-ray absorption fine structure (EXAFS), Powers et al. (1979) proposed that the absorption in the near IR region is due to both  $\text{Cu}_a$  and  $\text{Cu}_{a_3}$ . However, this proposal was countered by Beinert et al. (1980) who presented a survey of data over many years (mainly EPR and optical reflectance spectra), and concluded that  $\text{Cu}_{a_3}$  does not have significant absorption in the 800 - 900 nm region, in agreement with the conclusions of Babcock et al. (1978).

A.2.2 EPR and magnetic susceptibility.--Several EPR signals have been detected for cytochrome oxidase (Hartzell and Beinert, 1974). The spectrum of the oxidized oxidase has contribution from low-spin heme (cytochrome  $\underline{a}^{3+}$ ) at g values = 3.0, 2.2, 1.5. A narrow signal at g = 2 is generally attributed to  $\text{Cu}_a^{2+}$  (see, however, Hu et al., 1977, and Peisach and Blumberg, 1974, for another interpretation of the "copper" signal). Assa et al. (1976) integrated the intensities of the various signals and showed that the low-spin heme signal corresponds to only one heme. These authors also showed, by simulation, that the signals from the low-spin heme and copper correspond to two magnetically isolated centers ( $>10\text{\AA}$  apart). The copper g = 2 signal corresponds to only about one-half of the total copper.

On partial reduction, a high spin heme signal at  $g = 6$  appears. Babcock et al. (1978) studied reductive titrations of the oxidase by sodium dithionite followed by optical absorption and EPR measurements under argon. They suggested that the high spin signal is due, at least partially, to cytochrome a. Their EPR data are summarized in Figure I.4 for the  $g = 2,3$  and 6 signals.

Magnetic susceptibility measurements provide information about the spin state of metal centers which is complementary to the EPR data. The susceptibility of the fully oxidized oxidase was measured at room temperature (Falk et al., 1977) and at 7-200°K (Tweedle et al., 1978). The data from the two groups indicate that the oxidized enzyme has two  $S = 1/2$  centers; cytochrome a<sup>3+</sup> and Cu<sup>2+</sup>, and one  $S = 2$  center, an antiferromagnetically coupled cytochrome a<sub>3</sub><sup>3+</sup> - Cu<sub>a3</sub><sup>2+</sup> pair. The reduced oxidase has an  $S = 2$  center, which is attributed to high spin cytochrome a<sub>3</sub><sup>2+</sup>, with all other centers being diamagnetic.

A.2.3 Other spectroscopic studies.--Babcock et al. (1976, 1978) studied the magnetic circular dichroism (MCD) of cytochrome oxidase during the course of reductive titration. They also studied the MCD characteristics of several inhibitor complexes of the oxidase. Comparison with the MCD spectra of model compounds led these authors to confirm that cytochrome a is low-spin, while cytochrome a<sub>3</sub> is high-spin. The authors also suggested, from MCD properties at various redox levels, that there is no interaction between cytochromes a and a<sub>3</sub> apparent in the MCD spectra.

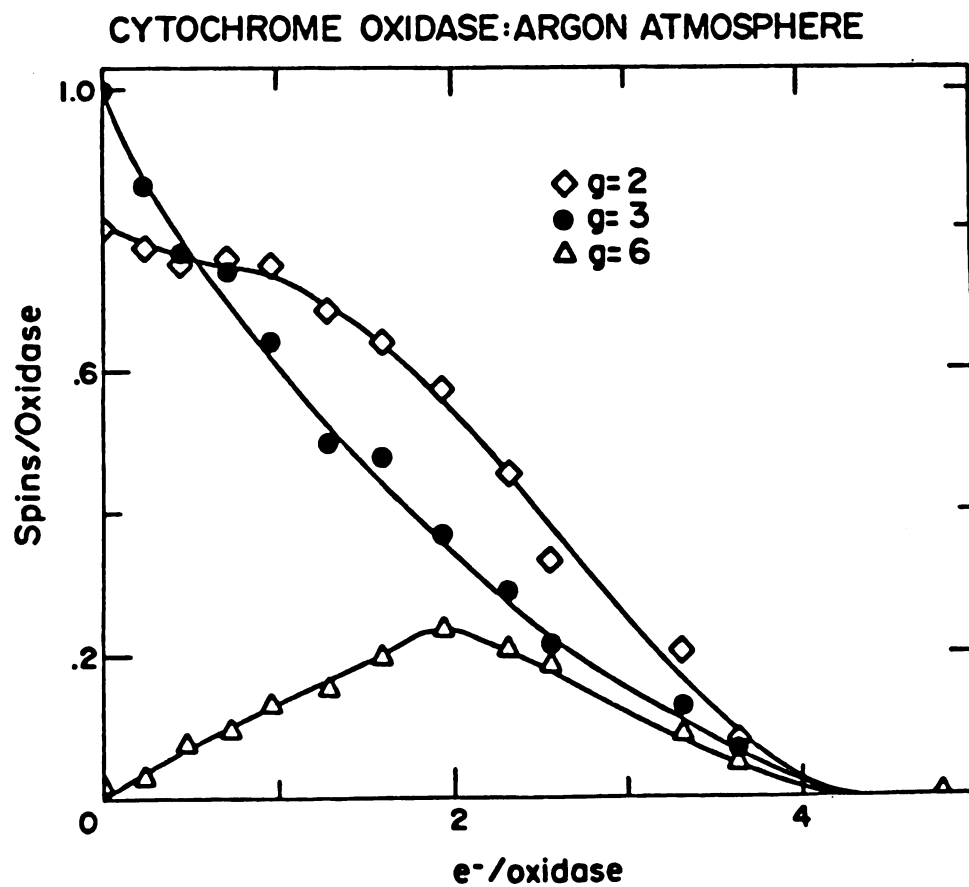


Figure I.4.--EPR reductive titration data for  $g = 2, 3,$  and  $6$  signals (from Babcock et al., 1978).

Resonance Raman (RR) spectroscopy is currently an active tool for the study of the environments of the hemes in cytochrome oxidase. In principle, RR measurements should be capable of distinguishing the two heme environments. The problem of photoreduction of the oxidized protein in the laser beam (Adar and Yonetani, 1978) has been minimized by using a flowing sample (Babcock and Salmeen, 1979). By careful choice of the excitation frequencies, Babcock et al. (1981) were able to enhance selectively and assign vibrations to a particular heme in the oxidized, reduced or inhibitor-complexed cytochrome oxidase. On the basis of comparison to RR spectra of heme a model compounds, these authors concluded that cytochrome a is six coordinate low spin in both oxidized and reduced states. Cytochrome a<sub>3</sub>, however, was shown to be six coordinate and high-spin in the oxidized, but five coordinate and high-spin in the reduced enzyme. A correlation of these results to the porphyrin core size was attempted (Babcock et al., 1981; Callahan and Babcock, 1981). The conclusions drawn from these studies agree closely with earlier deductions of the spectra of the separate components of the oxidase by Vanneste (1966). Another recent RR study on mixed valence cytochrome oxidase, compound C (Chance et al., 1975) was done at low temperatures (-70° C) (Yang et al., 1981). This study suggests that compound C has reduced cytochrome a and Cu<sub>a3</sub> while cytochrome a<sub>3</sub> - C<sub>u<sub>a3</sub></sub> are oxidized, as suggested in the original assignments of this compound.

The EXAFS method is emerging as a useful tool for the study of the environments of metal centers in metalloproteins. Recent

EXAFS studies on cytochrome oxidase (Powers et al., 1981) gave interesting insights into the structure of the oxygen reducing site, the  $\underline{a}_3$  - Cu $_{\underline{a}_3}$  pair. The results indicate the presence of a sulfur bridge in the resting enzyme, with a Cu $_{\underline{a}_3}$  - Fe ( $\underline{a}_3$ ) distance of 3.75Å. Chance and Powers (1981) suggested that as this site becomes reduced ( $\underline{a}_3^{2+}$  - Cu $_{\underline{a}_3}^+$ ), an oxygen molecule can replace the sulfur bridge to form the peroxide. To account for the high turnover number of the protein, the authors suggest that the sulfur bridge does not reform during turnover. This picture requires the bridging sulfur to be a weak ligand, since cytochrome  $\underline{a}_3$  is high-spin. The model derived from these measurements is shown in Figure I.5.

### A.3 Redox Properties

Electrochemical titrations of cytochrome oxidase monitored by optical measurements were reported by Shroedl and Hartzell (1977a, b,c). Their interpretation of the results was that there are two different potentials for the two cytochromes, referred to as high and low-potential hemes without assignment of potentials to specific hemes. They also concluded that two different copper redox potentials, similar to those of the hemes, must be present. Nicholls and Hildebrandt (1978) concluded that binding of a single HCN molecule to the oxidase prevents the reduction of both cytochrome  $\underline{a}_3$  and the copper associated with it.

It should be emphasized, however, that these measurements suffer from two major difficulties:

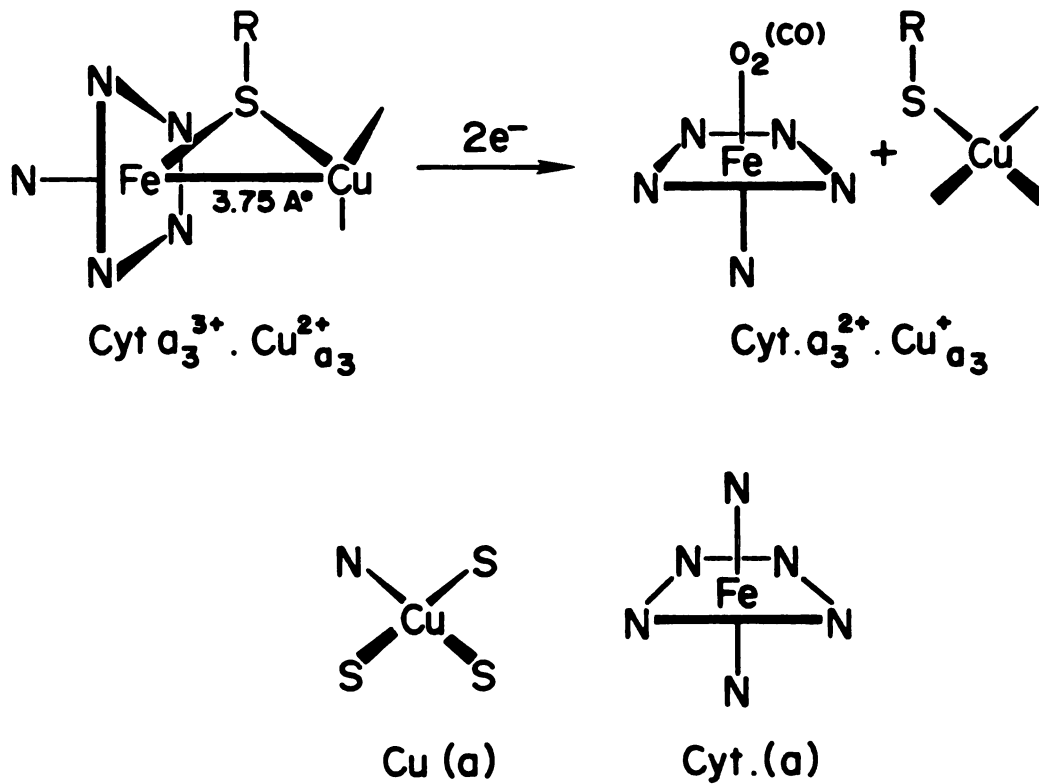


Figure I.5.--The Cu ( $a_3$ ) - Fe ( $a_3$ ) and Cu (a) - Fe (a) centers in cytochrome oxidase (from Powers et al., 1981).

1. Electrochemical titrations usually contain high concentrations of organic and inorganic redox couples and electron mediators that may interfere with the redox properties of cytochrome oxidase (Lanne et al., 1977).
2. Optical spectra cannot clearly discriminate between the isolated vs. interacting models of the metal redox centers at equilibrium.

Magnetic techniques were also applied to the study of the oxidase redox properties. In particular, EPR measurements during redox titrations were very useful in monitoring redox centers of the protein (Hartzell and Beinert, 1975). Babcock et al. (1978) studied the optical, MCD and EPR properties during redox titration of the oxidase with sodium dithionite. Their EPR data (presented in Figure I.4) and optical data indicate that the two cytochromes titrate together at all points, as seen, for example, from the  $g = 3$  signal. Their data also indicate that the EPR detectable copper,  $Cu_a$ , lags the reduction of the two cytochromes. These results are different from earlier results (van Gelder et al., 1973; Tiesjama et al., 1973) in which cytochromes  $a$  and  $a_3$  and the detectable copper were assigned equal redox potentials of 280 mV. The data of Babcock et al. (1978) provide evidence for heme-heme interaction via redox potentials, and indicate that the reduction of one cytochrome makes reduction of the other more difficult (negative cooperativity). It should be mentioned, however, that EPR measurements are usually done at low temperatures and at higher protein concentrations than are optical

measurements. The redox potentials are, of course, temperature dependent and electron redistribution may occur during freezing.

It is becoming more widely accepted, as shown by Lanne and Vanngard (1978), that a non-interacting four-redox center cannot describe the available EPR and optical data. Their analysis, on the other hand, showed that if interaction is introduced, the available data cannot discriminate between various models. In other words, assignments of equilibrium redox potentials to the four metal centers is still far from established.

#### A.4 Kinetic Studies

As is the case with other enzymatic systems, the study of the kinetics of cytochrome oxidase reactions plays an important role in understanding and characterizing its action. Studies of enzymatic reactions usually start by determining the steady state parameters in turnover experiments involving the enzyme and its natural substrate(s). Since turnover experiments are usually complex and involve the adjustment of many parameters, the study of transient state kinetics of pre- or post-steady state steps usually follows. These studies become important in determining accurate rate constants and in discriminating between mechanisms. The present study is devoted primarily to the investigation of the kinetics pathways which lead to reduction of the four redox centers of the oxidase. Hence, a summary of the literature data on the reaction of cytochrome oxidase with different substrates is presented below.

A.4.1 The reaction with cytochrome c.--The reaction of cytochrome c oxidase with its natural substrate, cytochrome c, has obviously received a great deal of attention. The kinetics of this reaction have been studied both anaerobically and in aerobic steady-state. The steady-state reaction mixtures usually contained ascorbate, cytochrome c, cytochrome oxidase and oxygen, with ascorbate serving as the electron source and oxygen as the sink.

The kinetics of the steady-state reaction have been extensively studied (Slater, 1949; Yonetani, 1962; van Buuren et al., 1971; Petersen et al., 1976; Errede and Kaman, 1979; and Petersen and Cox, 1980). Most of these studies have found that Minnaert mechanism IV, (Minnaert, 1961), equation II.2 fit the data.



More recent experiments, in which wider ranges of cytochrome c concentrations were used, have shown non-linear Lineweaver-Burk and Eadie-Hofstee plots (Ferguson-Miller et al., 1976; Errede et al., 1976). In other words, the simple hyperbolic behavior of  $k(\text{obs})$  expected from equation I.2 is not found. A rate equation of the form given by equation I.3 has been shown to describe the rate dependence on the cytochrome c concentration (Errede et al., 1976; Errede and Kamen, 1978).

$$\text{Velocity} = \frac{\alpha_1 + \alpha_2 [c]}{1 + \beta_1 [c] + \beta_2 [c]^2} [\text{Oxidase}] [\text{Ferrocytochrome } \underline{c}] \quad \text{I.3}$$

Where  $\alpha_1$ ,  $\alpha_2$ ,  $\beta_1$ ,  $\beta_2$  are constants and  $[c]$  is the total cytochrome c concentration. The quadratic term in total cytochrome c concentration indicates that under certain conditions two molecules of cytochrome c may be bound to the oxidase at the moment of electron transfer. The stoichiometry of cytochrome c binding (Ferguson-Miller et al., 1976; Erecinska, 1975) supported this mechanistic model. Errede and Kamen (1979) discussed several models that can lead to the observed rate law behavior.

Transient state kinetic studies of the reaction between cytochrome oxidase and cytochrome c have been of great importance in understanding the nature of the interaction between the two enzymes. Under anaerobic conditions, the reaction is multiphasic (Gibson et al., 1965; Antonini et al., 1973; Andreasson et al., 1972; Andreasson, 1975). Most authors report a second order rate constant for the initial phase of about  $8 \times 10^7 \text{ M}^{-1} \text{ s}^{-1}$ , depending on the ionic strength (Gibson et al., 1965; Andreasson, 1975; Wilms et al., 1981). It was also found that added ligands such as  $\text{CN}^-$  or  $\text{N}_3^-$  do not affect this fast phase (Gibson et al., 1965; Andreasson, 1975), which suggests that this phase involves the reaction of cytochrome c with the cytochrome a site of the oxidase. The slower phases are not as well defined as the initial phase. These phases, particularly the last phase, are too slow to be of significance in catalytic cycles. The presence of oxygen is thought to shift the redox potentials, such that these slow phases are much faster (Andreasson et al., 1972) to account for turnover numbers of the protein as high as  $400 \text{ s}^{-1}$  (Petersen et al., 1976). Andreasson et al. (1972), who monitored the reaction

kinetics at 830 nm and at 605 nm, observed similar kinetics at these two wavelengths. They interpreted their data by assigning about 40% of the absorbance at 830 nm to cytochrome a.

A.4.2 Reaction with oxygen.--The reaction of the reduced cytochrome oxidase with oxygen is also multiphasic (Greenwood and Gibson, 1967). The first phase is diffusion controlled ( $k = 1 \times 10^8 \text{ M}^{-1} \text{ s}^{-1}$ ) and the flash-flow technique, where the reduced form of the oxidase was generated photochemically from the reduced oxidase--CO complex, was used to measure the reaction rate (Gibson and Greenwood, 1963).

To slow the reaction with oxygen and to identify the possible intermediates leading to the reduction of molecular oxygen to water, Chance et al. (1975) used low temperature flash photolysis technique. Chance and co-workers (Chance et al., 1975; 1978; Chance and Leigh, 1977) have identified several intermediates in this reaction pathway. Their results have been confirmed by Clore and E. M. Chance (Clore and Chance, 1978a,b,c; 1979).

It appears that the proximity of  $\text{Cu}_{a_3}$  and  $\text{Fe}(a_3)$  plays an important role in the reduction of molecular oxygen. The high redox potential of the oxidase (Malmstrom, 1973) in addition to the unfavorably high energy for the formation of superoxide radical lend support to the idea that both  $\text{Cu}_{a_3}$  and  $\text{Fe}(a_3)$  must be reduced before forming the peroxide. The bound peroxide intermediate could then be reduced via two one-electron steps. The intermediates formed are thought to be stabilized by electron delocalization within the  $\text{Cu}_{a_3} - \text{Cyt } a_3 - \text{O}_2$  unit.

A.4.3 The "oxygenated" and the "oxygen-pulsed" forms.--When reduced cytochrome oxidase is reoxidized by oxygen, a new form of the protein, which is spectrally and functionally different from the resting enzyme, is produced (Okunuki et al., 1958). This form is called the "oxygenated" cytochrome oxidase, to distinguish it from the resting protein (the enzyme as prepared). The terminology originated from the belief that this form contains an enzyme-oxygen complex (Sekuzu et al., 1959).

Subsequent studies have shown, however, that this form does not contain oxygen bound to its metal centers, but instead, it represents a conformational variant of the enzyme (Tiesjema et al., 1972; Nicholls and Petersen, 1974; Brittain and Greenwood, 1976). The "oxygenated" oxidase is characterized by an absorption maximum at 425 nm compared to 418 nm in the Soret region of the resting protein.

Antonini et al. (1977) introduced the term oxygen-pulsed oxidase, which is formed by exposing the reduced protein to a "pulse" of oxygen. This form was shown to be more active in reaction with cytochrome c and during turnover experiments (Antonini et al., 1977; Petersen and Cox, 1980), which led these authors to suggest that this conformation is the catalytically significant form of the oxidized protein. However, the claim that this catalytically active species can form only after fully reducing the protein (Antonini, 1977) should be taken with caution, since the natural reducing agent, cytochrome c, cannot fully reduce the oxidase (4 electron) anaerobically (unpublished results; see also Andreasson, 1975). This is also disproved

by the fact that turnover is achieved after the addition of about two electrons to the oxidase.

### B. Scanning Stopped-Flow Technique for the Study of Multicentered Enzyme Reactions

Stopped-flow spectrophotometry has been extensively used in the study of the kinetics of enzymatic reactions. The method most commonly used is to monitor changes in the absorbance at a certain wavelength as a function of time (for historical background, see Sturtevant, 1964).

Advances in computer-controlled data acquisition made scanning wavelength experiments practical for many enzymatic reactions (Papadakis et al., 1975; Coolen et al., 1975; Suelter et al., 1975; June et al., 1979; Cox and Holloway, 1977; Halaka et al., 1981a). In a scanning wavelength experiment, a spectral region is repeatedly scanned and the absorbance (or other spectrophotometric response) is measured for every scan. The data are stored as a function of time for every wavelength "channel." If the time of scan is short compared to the half-time of the reaction(s) studied, these data can be considered as a matrix  $\underline{A}$  composed of  $N$  consecutive spectra (each essentially instantaneous at time  $t$ ), measured at  $p$  wavelength channels. The element  $A_{ij}$  of this matrix is the absorbance measured at wavelength channel  $i$  at the time of scan  $j$ .

The advantages obtained by collecting this time-wavelength-absorbance surface for a spectral region are important when studying enzymes with two or more interacting chromophores. The power of this

method becomes apparent from the consideration that one can have information about the kinetics of each chromophore at many wavelength channels in the same experiment. This, of course, eliminates long time base-line drift problems and minimizes problems which result from lack of reproducibility from one experiment to another.

As can be seen from the discussion on cytochrome oxidase, rapid-scanning stopped-flow methods seem ideal for the study of the kinetics of this enzyme. The results promise to provide information about possible pathways of electron transfer and sites of interaction with substrates.

### C. Treatment of Scanning Stopped-Flow Data

Scanning stopped-flow experiments produce massive amounts of data for every reaction studied. A general procedure for treating these data is discussed below.

#### C.1 Rate Equations--Program KINFIT4

The first step in studying the kinetics of a certain reaction is to find the equation(s) that fit the time course at the wavelength channels of interest. This, in itself, can lead to important information about the interactions between chromophores in multicentered reactions and the mechanism of their reactions with certain reagents (e.g., sequence of steps and cooperativity).

The computer program that is used to extract the rate and equilibrium constants is the program KINFIT4, which is a modified version of program KINFIT (Dye and Nicely, 1971). This program

utilizes a simultaneous fit of the equations to a number of data sets and computes estimates of the marginal standard deviations. These uncertainties include the effect of coupling among rate constants and other adjustable parameters. If the model proposed for the reaction is correct, these statistics can give reasonable confidence in the rate and equilibrium constants which result.

### C.2 Weighted Principal Component Analysis

One of the ultimate goals of studying chemical kinetics is to propose and understand a mechanism that accounts for the known facts about a certain reaction. An essential step toward this goal is to know the number of interacting species in the reaction mixture. Enzyme reactions usually involve transient intermediates whose spectra are unknown. In fact, binding to proteins modifies the spectra of many substrates.

To determine the number of light-absorbing species in a chemical reaction, the method of weighted principal component analysis, PCA, was developed (Cochran and Horne, 1977, 1980; Cochran et al., 1980). The method and its history are discussed in detail in the Ph.D. dissertation of R. Cochran (1977). The PCA starting point is the matrix model mentioned in the previous section. No mechanistic assumptions are needed to apply PCA; the only assumption required is that the absorbances of species in the reaction mixture are linear functions of their concentrations (Beer's law).

Two kinds of PCA, the second moment matrix principal component analysis (called M analysis) and the sample covariance matrix

principal component analysis (S analysis) are useful for kinetics experiments. Each requires only the matrix A (with the proper weights; see Chapter V) and each gives an estimate of the minimum value of q, the number of independent chromophores in the reaction. M analysis gives for q a lower bounds estimate that is sensitive to any linear dependences of the concentrations of the various detectable species. S analysis gives an estimate that is sensitive to the linear dependence of the time rates of change of the concentrations. The two estimates of q are not necessarily the same, and the application of both analyses enables one to discriminate between alternate stoichiometries during reaction (Cochran and Horne, 1977).

#### D. Reducing Agents for the Study of Electron Transfer Reactions of Cytochrome Oxidase

Scanning stopped-flow experiments provide information not only about the kinetics of a chemical reaction, but also about the spectral properties of the intermediates. Therefore, a reducing agent with characteristic spectral shape that does not interfere strongly with those of the oxidase, is preferred for these studies. Such a reducing agent will also have the advantage of providing estimates of the number of reducing equivalents which have been added to the oxidase at any extent of reaction.

Cytochrome  $c^{2+}$ , the natural reductant, was discussed in Section C.3.1. There are two difficulties involved in reduction by cytochrome c:

1. The large Soret absorption of cytochrome c obscures changes in the cytochrome oxidase spectrum in this region.

2. As shown by anaerobic equilibrium titrations (this study), only two electrons can be transferred from cytochrome c to cytochrome oxidase, in agreement with previous observations by stopped-flow (Andreasson, 1975; this study).

Sodium dithionite is widely used as a reductant in biological systems (Lambeth and Palmer, 1973; Mayhew, 1978). This reductant has also been used to study reduction of the oxidase (Lemberg and Mansley, 1965; Orii, 1979). Sodium dithionite was used in the present study in scanning experiments and was valuable in providing information and in discriminating between the two hemes of the oxidase, since it is the only negatively charged reductant known to reduce the oxidase which does not require another electron mediator. The implication of this property will be discussed throughout this study. However, because of the complex redox chemistry of dithionite and the apparently variable (and small) molar absorptivity ( $6.2 \text{ mM}^{-1} \text{ cm}^{-1}$  at 320 nm [Mayhew, 1978]), it is difficult to use the dithionite absorption band to quantify the electron transfer.

Metal ion redox couples have also been used for the study of the oxidase reduction. Greenwood et al. (1977) have used hexaaquochromium (II) as the reductant. Scott and Gray (1980) used ruthenium (II) hexamine. Both of these studies showed that these positively charged reductants preferentially reduce cytochrome a of the oxidase in the first phase followed by slow electron redistribution.

Reduced nucleotide adenine dinucleotide (NADH) coupled to N-methyl phenazinium methyl sulfate (MPMS) is also widely used. When

mixed anaerobically, these compounds form 5, 10-dihydro 5-methyl phenazine (MPH), which is the reducing species. (See Chapter III). The difficulty with using this couple with excess NADH to cycle MPMS between the oxidized and reduced forms is that the reaction between NADH and MPMS is, itself, rather slow (Halaka, Babcock and Dye, 1981b) so that fast reduction processes involving MPH and the oxidized oxidase are obscured.

MPH is the reductant used most extensively in this study. It was pre-formed by the anaerobic titration of MPMS by NADH. A sharp absorption band of MPMS at 388 nm (not present in MPH) (Halaka et al., 1981b) can be used to monitor the number of electrons transferred (see Chapter III).

## CHAPTER II

### EXPERIMENTAL METHODS

#### A. Materials

Beef hearts were obtained fresh from Michigan State University Meat Lab. Sodium dithionite was a Virginia Smelting Co. product. Cytochrome c (Type III or Type VI), NADH, MPMS, EPES (see Chapter III), N-2-hydroxy ethyl piperazine N-2-ethanesulfonic acid (HEPES), and the detergents: octyl phenoxy polyethoxy ethanol (Triton X-100), polyethoxy ethylene sorbitan monolaureate (Tween 20), and cholic acid were purchased from Sigma Chemical Co. The detergents Triton X-114 and Tween 20 were kept refrigerated as 20% (v/v) solutions in water. Cholic acid was purified by recrystallizing from 95% ethanol. The crystals were mixed with equivalent amounts of potassium hydroxide to give 20% (w/v) solution in cholate ion. The pH was then adjusted by the addition of 6N hydrochloric acid to give pH=8. Purification of cholic acid was required for successful preparations of cytochrome oxidase. Argon gas was purified by passing through a one-meter BASF catalyst column (at 100° C). Water was double distilled in glass. All other reagents were of analytical grade and, unless otherwise mentioned, were used without further purification.

## B. Methods

### B.1 Preparation of Cytochrome Oxidase

Cytochrome oxidase was prepared by the method of Hartzell and Beinert (1975). During the preparation, all steps were carried out at 0-5° C. Centrifugations were done in a Sorvall RC or RCB centrifuge with a rotor SS-34 or GSA. Whenever ammonium sulfate was added during the preparation, the drop in the pH from 7.4 was compensated for by the addition of small increments of 6N KOH. The protein concentration before the TX-114 or the cholate extractions was determined by the biuret method after solubilizing with deoxy cholate (Jacob et al., 1956). Small volumes (1-1.5 ml) of concentrated oxidase solutions (0.5 - 1.0 mM in heme a) in 50 mM HEPES buffer (pH = 7.4) containing 0.5% Tween 20 (v/v) were kept frozen in liquid nitrogen and were thawed prior to use. Freezing of the protein for long periods (more than one year in some cases) did not seem to affect its properties. The spectral properties of the solubilized protein were in agreement with those reported in the literature (Lemberg, 1969). In all the experiments reported in this text, the ratio of the absorbance of the reduced oxidase at 444 nm to that at 420 nm was at least equal to 2.4. This ratio has been noted to be a sensitive measure of the protein integrity (Gibson et al., 1965). Also, the spectra of the reduced oxidase did not show any peaks at 520 or 550 nm indicating the absence of bc<sub>1</sub> contamination.

Although keeping the oxidase solutions at room temperature for as long as one day did not seem to affect its properties, the protein

solutions prepared for stopped-flow experiments were kept in ice-cold water and were mounted onto the stopped-flow apparatus not more than one hour before being pushed against reactants. This was a necessary precaution since it usually took several hours to degas and calibrate the stopped-flow system (see Section C).

### B.2 Activity Assays of Cytochrome c Oxidase

The activity of the oxidase was measured spectrophotometrically (Smith et al., 1955). The assays were carried out in 50 mM HEPES buffer containing 0.5% Tween 80, pH = 6.5. The assay mixture typically contained about 15  $\mu$ M ferrous cytochrome c and 15 nM oxidase in a 3 ml cuvette. The molecular activity (see, for example, van Buuren et al., 1972; Vanneste et al., 1974), which is the number of moles of ferrocyanochrome c oxidized per mole of cytochrome c oxidase per second, is given by Equation II.1.

$$MA = k \times [\text{ferrocyanochrome } \underline{c}] / [\text{cytochrome } \underline{aa}_3] \quad \text{II.1}$$

where k is the observed pseudo first-order rate constant of the oxidation of ferrocyanochrome c, monitored at 550 nm. MA for the oxidase had values between 130 and 170. The activity is, however, highly dependent on the detergent present. In the presence of 0.5% cholate as the detergent the activity was almost lost.

### B.3 Preparation of Anaerobic Solutions

Solutions were made anaerobic by a series of successive evacuations followed by filling with purified argon (at least six times with

intervals of about 4 min.). The solutions were kept under about 3 psig argon pressure. The glass solution bottles were connected to the vacuum line or mounted onto the stopped-flow system via Fischer-Porter 5 mm Solv-Seal joints (Figure II.1a). Check of the anaerobicity of these solutions, which were prepared by the use of the anaerobic train in Dr. Babcock's laboratory, was done periodically by either titrating lumoflavin-3-acetate with sodium dithionite or MPMS with NADH. Anaerobicity was achieved when the first increment of the titrant produced as much change in the absorbance (460 nm in the case of lumoflavine-3-acetate or 388 nm in the case of MPMS) as later additions.

#### B.4 Anaerobic Titrations

Anaerobic titrations and the preparation of MPH and other reductants were carried out by using the cell shown in Figure II.1b. The reductant was delivered anaerobically by using a calibrated syringe. The advantage of using the cell shown in Figure II.1b is that one can monitor the spectra as reductant is added, hence, one can know, with confidence, the concentration of the reducing agent. MPH was thus prepared by anaerobically titrating MPMS with NADH and monitoring the decay of the MPMS peak at 388 nm. This was an important factor in the study of the reduction of cytochrome oxidase by MPH, since excess NADH causes complications of the kinetics by reacting with the resulting MPMS.

Equilibrium spectra were taken with a Cary 17 spectrophotometer. A rectangular aluminum box was mounted on the cell compartment of the

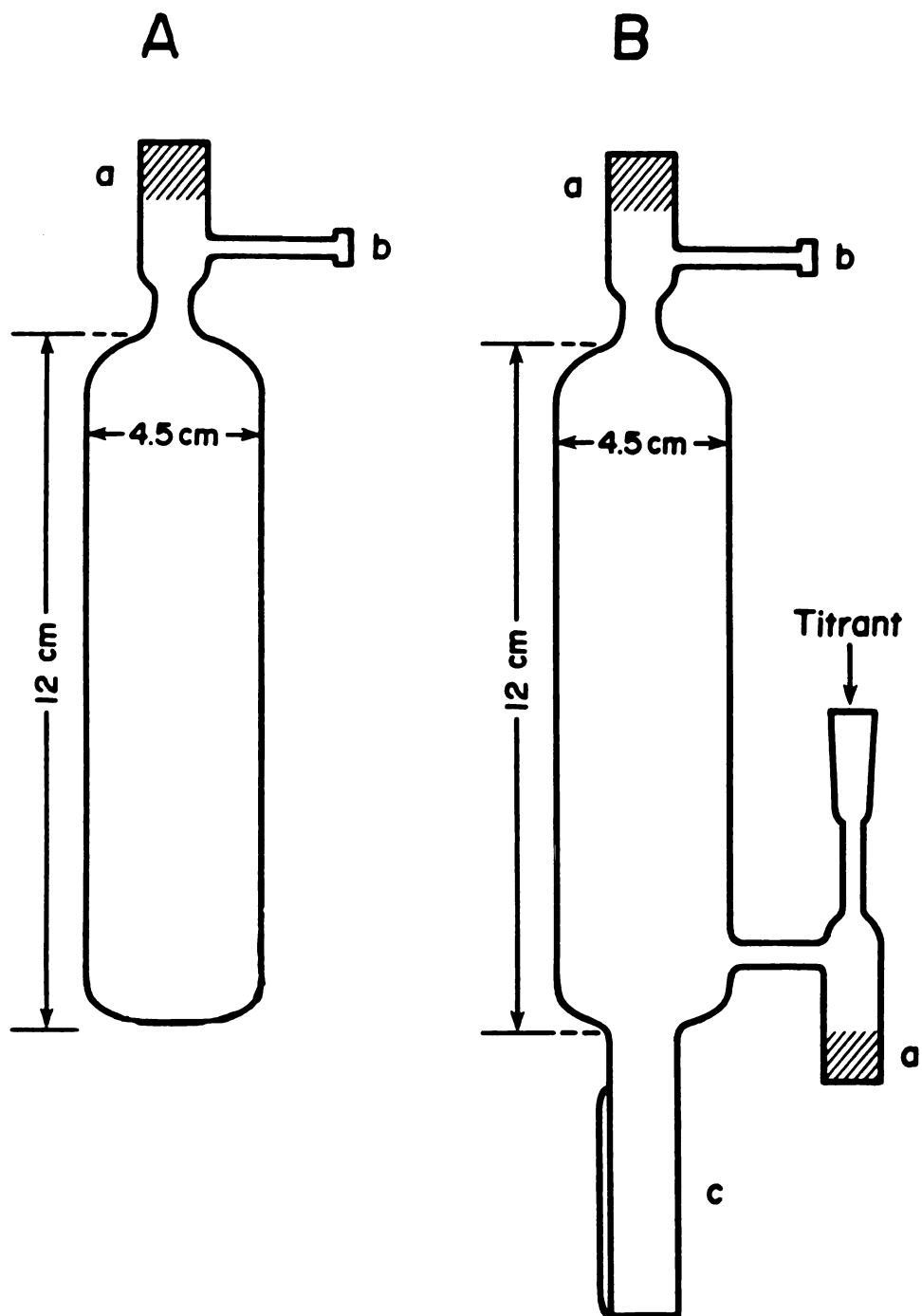


Figure II.1.--Cells used for preparing anaerobic solution (A) and for anaerobic titrations and preparation of air-sensitive reductants, (B). (a) Kontes high-vacuum valves, (b) Fischer-Porter joint, used to connect cell to vacuum line, argon gas, or to mount cell onto the stopped-flow apparatus, (c) quartz 1-cm path-length optical cell.

spectrophotometer to cover the cell shown in Figure II.1b during titrations. Spectra of MPH prepared by the above method were checked before mounting onto the stopped-flow system. No changes in these spectra were detected for periods as long as 24 hours. Whenever MPMS or MPH were used, the container was wrapped in aluminum foil, as was the stopped-flow buret which conveyed the MPMS or MPH solutions to the pushing syringes (see Chapter III).

### C. The Stopped-Flow System

A double-bema, vacuum-tight, rapid-scanning stopped-flow apparatus was used throughout this study (Papadakis et al., 1975; Coolen et al., 1975; Suelter et al., 1975). Detailed descriptions of this system are given in the Ph.D. dissertations of N. Papadakis (description of the flow system, glassware, and mechanics of the system) and R. B. Coolen (computer interfacing, synchronization of scans, and signal averaging schemes in both scanning and fixed-wavelength modes).

The system was operated under positive pressure (~1 psig) of purified argon gas instead of under vacuum (vapor pressure of solutions). This was a necessary modification for two reasons:

1. Protein solutions are not stable under reduced pressures, and in the presence of detergents, as most of the solutions in this study contained detergents, solutions foam and create bubbles
2. Operating under positive pressure has the advantage that, if there is a slow leak, air will not enter the

apparatus. This is particularly important for experiments requiring long times.

### C.1 Handling and Performance of the Stopped-Flow System

Since the system is all-glass, it always required special care in handling and operation. Solution handling and mounting of reagents were carried out under argon. After all solutions (except protein) had been mounted, the system was evacuated to  $< 0.001$  mm Hg and flushed with argon. This cycle was repeated at least four times. After the last cycle, while the apparatus was still under vacuum, water was delivered to the observation cell (to avoid bubbles). Argon was then introduced to 1 psig positive pressure throughout the entire run. When the protein was ready to be pushed, the protein solution was mounted onto the system. The buret delivering the protein solution, which can be isolated from the rest of apparatus by Kontes valves, was evacuated and flushed with argon separately several time to insure anaerobicity.

The performance of the stopped-flow system was checked periodically by various tests, some of which will be discussed below.

C.1.1 Flow velocity and flow profile.--In stopped-flow experiments, the flow of solutions should be fast enough to cause turbulence for efficient mixing. However, pushing the solution too fast may cause cavitation. Cavitation occurs when the external pressure on the liquid is less than its vapor pressure. An important parameter,

which gives information about the kind of flow is the Reynolds Number, R:

$$R = d v \rho / \zeta \quad \text{II.2}$$

Where  $d$  is the diameter of the tube,  $v$  is the average velocity of the liquid,  $\rho$  is the density, and  $\zeta$  is the viscosity. Empirically, it has been found that turbulent flow occurs at  $r = 2000 - 3000$  for fully regular tubes. However, it can be as low as 10 for jet-type mixers (see Wiskind and Berger, 1964). The mixer used in this study is a four-jet one (Papadakis et al., 1975).

Figure II.2 shows the velocity profile of the solution flow. With Equation II.2, the critical velocity to get turbulent flow for water at 20° C is given by  $v = 200/d$ , where  $d$  is the mm. Since 2 mm diameter tubes were used for constructing the mixing and observation cell, the critical velocity is about 100 cm/s. The velocities shown in Figure II.2 are then high enough to insure turbulent flow. By using an equation given in the reference mentioned in this section, cavitation should be expected at velocity around 1000 cm/s for a 2 mm tube. Experimentally, cavitation should be easy to detect from the response of the photomultiplier tubes.

C.1.2 Mixing efficiency.--Besides using a four-jet mixer and measuring the flow velocity, the mixing efficiency was tested by a specifically-designed reaction. A non-buffered acid solution of the acid-base indicator methyl orange was pushed against a base to give a final pH = 4.5, which is enough to give the color of the basic form

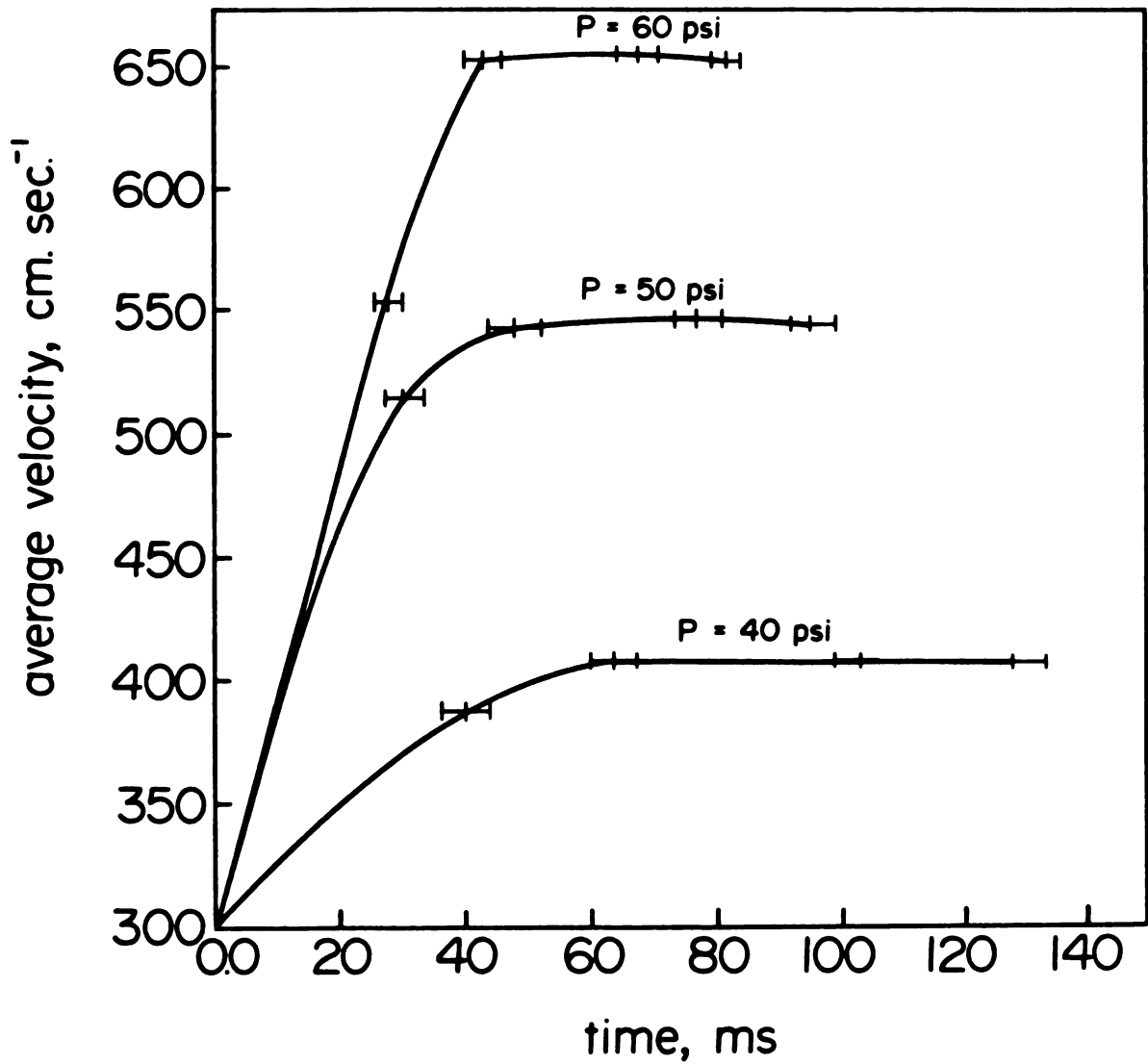


Figure II.2.--Flow-velocity profile as a function of pressure. The plateau region of uniform velocity indicates that data could be collected at any point in this plateau.

of the indicator. A non-buffered solution is used in this test because if the final solution were strongly buffered, it might give the final color change even if the solutions were not efficiently mixed.

Since protonation reactions of acid-base indicators are diffusion-controlled, the acid form in that experiment should go to the basic form during the dead time of the instrument (~7 ms), and slow changes should not be observed if the mixing were complete. Figure II.3 presents a fixed-wavelength push of such a test (at 465 nm). The absorbance change at this wavelength, as measured on a Cary 17 spectrophotometer, was 0.62. Since no significant change in the absorption was observed, it was concluded that mixing was complete before the solution reached the observation point.

C.1.3 Anaerobicity tests.--The anaerobicity of the stopped-flow apparatus was tested by several reactions that are air-sensitive. One such test was pushing MPH against buffer and collecting spectra as a function of time. In the presence of oxygen, the oxidized form, MPMS, which has a sharp peak at 388 nm, is produced (see Chapter III). This test proved to be useful and economical, since MPH was the reductant in most of the reactions mentioned in this text. Another test that had been used earlier, when sodium dithionite was used as the reductant, was pushing reduced lumoflavin-3-acetate against buffer. The reduced form of the reagent is colorless, while the oxidized form is yellow (peak at 460 nm). In each case, the system showed anaerobicity for periods as long as 36 hours.

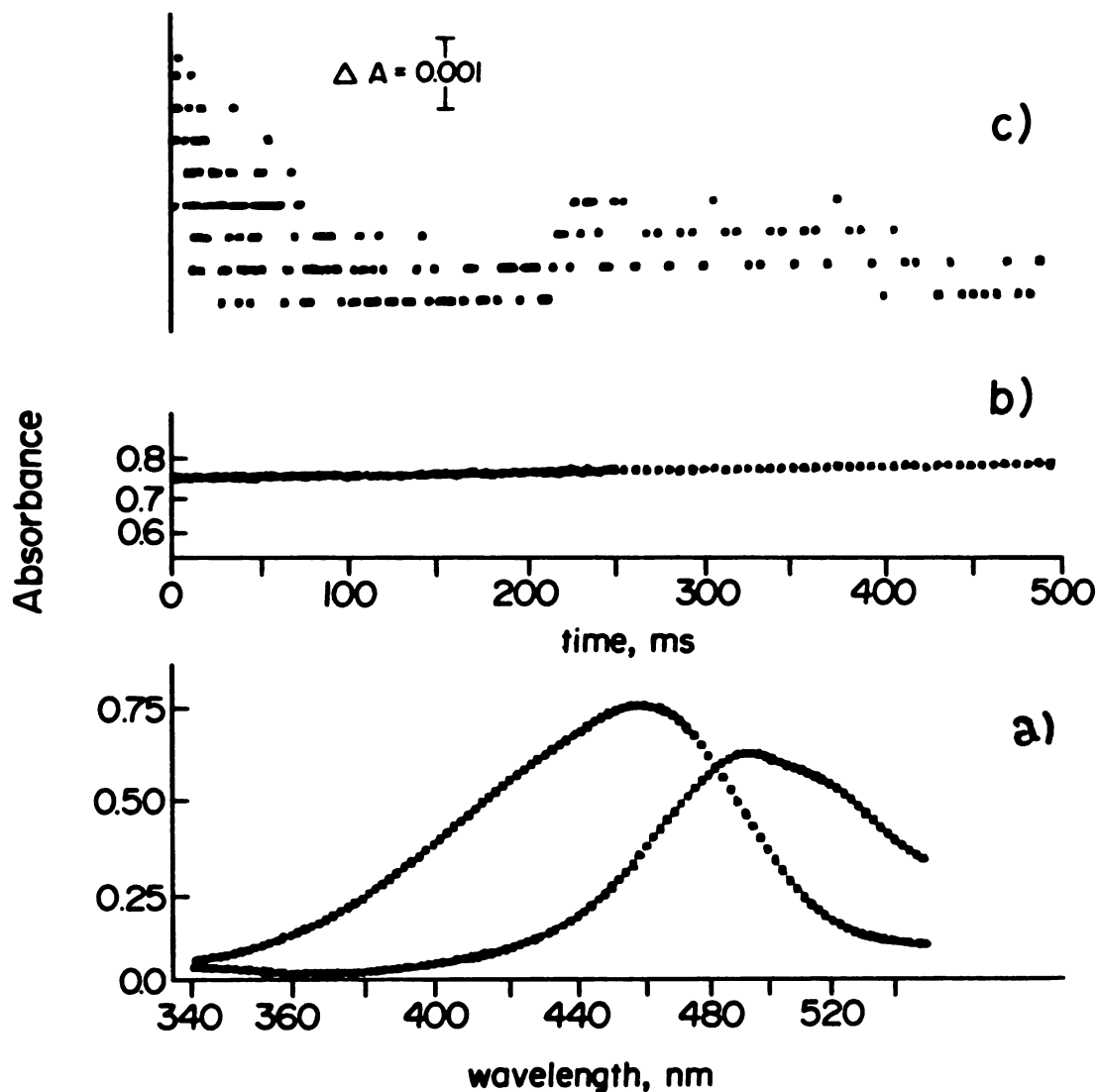


Figure II.3.--Test of mixing efficiency in the stopped-flow apparatus. (a) Spectral changes that occurred upon mixing of the acid-base indicator methyl orange (at pH = 2.5) with base to give final pH of 4.2, (b) time progress curve of the absorbance at 465 nm collected in fixed-wavelength mode, (c) same as in b, but enlarged 200 times.

The anaerobic reduction of cytochrome oxidase, in addition, is a very sensitive measure of any oxygen present. Concentrations of oxygen as low as a fraction of micromolar cause a steady state to be observed in the reduction. The steady state portion of the curve becomes more pronounced at higher oxygen concentrations.

#### D. Data Handling, Computations and Computer Graphics

Data acquisition was done by a PDP8/I computer interfaced to the stopped-flow system. The stored data were displayed on a Tektronix model 610 storage-display scope connected to a Tektronix model 4601 hard-copy unit, which was used for preliminary examination and production of figures, such as that presented in Figure II.3.

Data were transferred to Michigan State University CDC 750 computer, where kinetic and principal component analyses were performed. Correction for finite scan times and conversion of channel numbers to wavelength were also performed as described in Appendix E of the Ph.D. dissertation of R. Cochran.

Computer graphics of the type shown throughout this work were accomplished by using program MULPLT, written by Dr. T. Atkinson at Michigan State University for the Chemistry Department PDP-11 Computer. Computer programs to transfer calibrated stopped-flow data to be used for MULPLT from the CDC 750 computer to the PDP-11 were written in collaboration with Dr. T. H. Pierce. Data representing wavelength vs. absorbance (see, for example, Figure III.5) were subjected to a smoothing spline. However, the original data were displayed along with the "smoothed" data to assure that the spline smoothing did

not affect the shapes of the curves (see Figure VI.8). Three dimensional plots were constructed by program GEOSYS from the Michigan State University HAL routines.

## CHAPTER III

### PROPERTIES OF 5-METHYL PHENAZINIUM METHYLSULFATE:

#### REACTION OF THE OXIDIZED FORM WITH NADH

#### AND OF THE REDUCED FORM WITH OXYGEN

##### A. Introduction

5-methyl phenazinium methyl sulfate (MPMS), often referred to as "phenazine methosulfate," is widely used as an electron-transfer catalyst in a variety of biological reactions and as a redox buffer in potentiometric titrations of protein-bound, oxidation-reduction cofactors. For example, MPMS has been used in the study of photophosphorylation (Zaugg et al., 1964; Vernon et al., 1963), and in redox reactions involving the mitochondrial electron transport chain (Kearney and Singer, 1956; Low and Vallin, 1963; Singer and Kearney, 1957; Dutton and Wilson, 1974) and with other biological systems (Dearman et al., 1974; Nishikimi et al., 1972; Ohno et al., 1975).

The spectral and redox properties of MPMS are, however, fairly complex in that both protonation reactions and semiquinone formation can occur and that these processes are often significant in the physiological pH range. Zaugg (1964) studied the spectral properties of the 5-methyl phenazinium ion,  $MP^+$ , of the two-electron reduced species, MPH, and of the intermediate semiquinonoid forms,  $MPH^+$  and  $MP^\cdot$  (see Figure III.1) as a function of pH. While  $MPH^+$

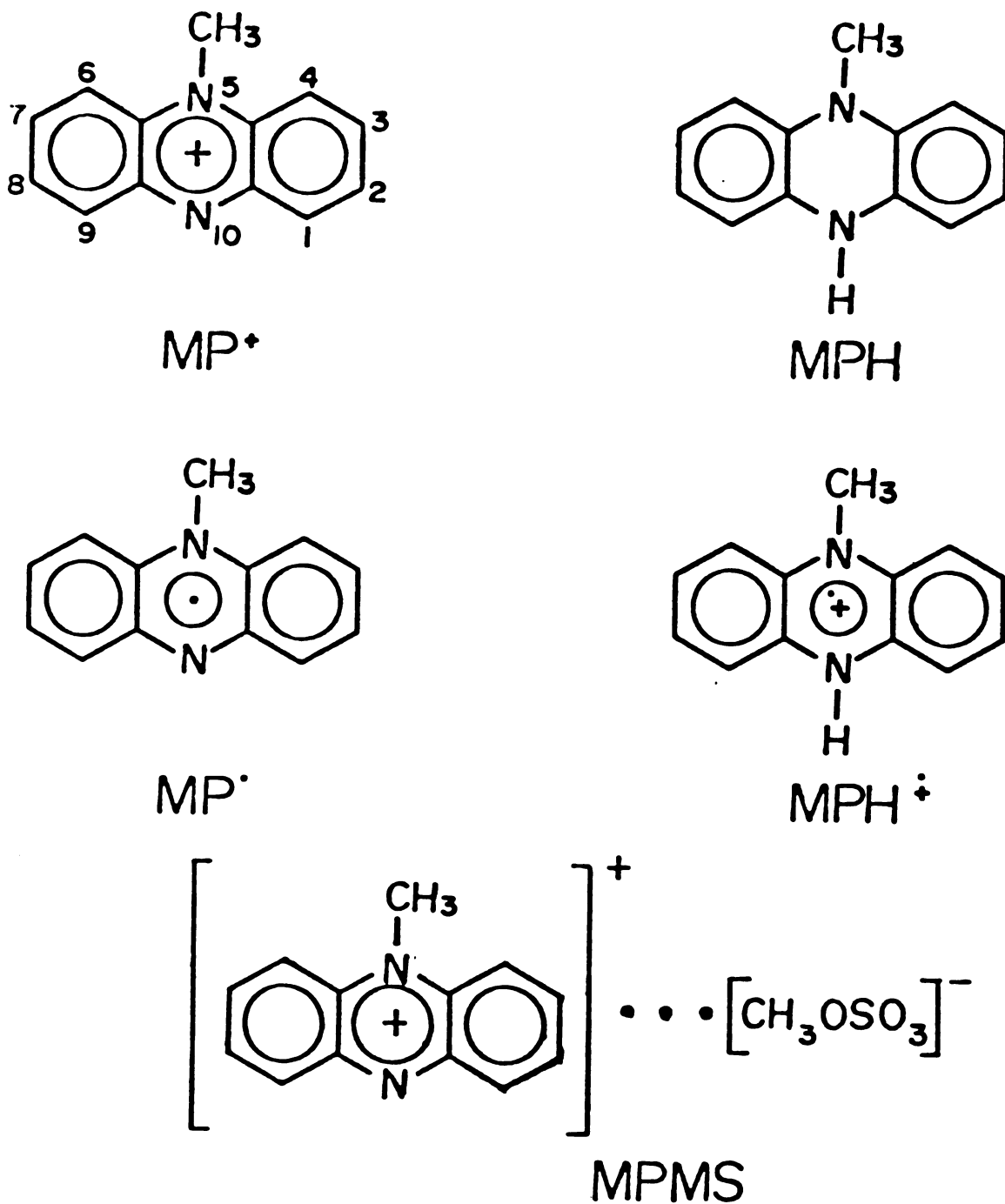


Figure III.1.--Structure of N-methyl phenzaine at different protonation and oxidation levels.

is stable below pH = 3.5,  $MP^{\cdot}$  and  $MPH^{\cdot+}$  apparently disproportionate to  $MP^+$  and MPH at neutral and higher pH values. For the deprotonation of  $MPH^{\cdot+}$ , pKa values of 6.8 (Rao and Hayon, 1976) and 5.7 (Rubaszewska and Grabowski, 1975) have been reported. However, these are apparent pKa values since both deprotonation and disproportionation could be involved.

It is well known that MPMS is photosensitive (McIlwain, 1937; Marzotko et al., 1973; Rubaszewska and Grabowski, 1975). In recent comprehensive photochemical studies (Chew and Bolton, 1980; Chew et al., 1980), electron paramagnetic resonance (EPR) and optical methods were used to determine a number of rate and equilibrium constants. They showed that irradiation at pH below 7 with excitation wavelength below 500 nm yields two products: the 5-methyl 10-hydrophenazine cation radical ( $MPH^{\cdot+}$ ) and 1-hydroxy-5-methyl phenazinium cation, pyocyanine ( $PYH^+$ ) in a stoichiometric ratio 2:1. At higher pH values which favor disproportionation, photolysis would thus ultimately lead to the formation of equimolar amounts of  $PYH^+$  and MPH. Because of problems with photolability of MPMS in enzyme assays, Ghosh and Quayle (1979), suggested the use of 5-ethyl phenazinium ethylsulfate (EPES) as the electron mediator. They based their conclusion on the non-enzymatic reaction of MPMS and EPES with 2,6-dichloro indophenol and on EPR measurements. Other authors (Hisada and Yagi, 1979; Nakamura et al., 1980) have suggested the use of 1-methoxy-5-methyl phenazinium methyl sulfate.

The reduced nicotinamide adenine dinucleotide (NADH)/MPMS couple is often used as the reducing substrate in the study of

biological redox reactions. Generally, NADH is present in substrate amounts and MPMS serves to mediate electron transfer between NADH and the oxidizing cofactor (Nakano et al., 1975; Bergmeyer and Bernt, 1974). In two independent recent studies (Farrington et al., 1980; Anderson, 1980) NADH was shown to be essentially a two-electron donor, and that the one-electron transfer from NADH will only occur with oxidants for which  $E^{0'}$  is more positive than about 300 mV. Thus MPMS with a reduction potential of 80 mV at neutral pH (Jagendorf and Margulies, 1960), is likely to serve as a two electron shuttle in most assay systems.

Our interest in the NADH-MPMS system involved its use as the reductant couple in the study of aerobic (steady state) and anaerobic reduction of cytochrome c oxidase (Halaka et al, 1981). In order to understand the mechanism of this reaction and other reactions in which the NADH-MPMS couple are used, we studied the reaction of NADH with MPMS both anaerobically and in the presence of oxygen as well as the reaction of MPH with oxygen. These studies made use of scanning and fixed-wavelength stopped-flow spectrophotometry. We also report the spectral changes which follow anaerobic and aerobic photolysis of MPMS and EPES.

### B. Experimental Section

MPMS, EPES and NADH were from Sigma Chemical Co. Unless otherwise mentioned, all solutions were prepared in 0.05 M N-2-hydroxy ethyl piperazine N-2-ethane sulfonic acid (HEPES) buffer, pH = 7.4, using glass-distilled water. Argon gas was purified by

passing it through a one meter BASF catalyst column heated to 115°C. Time-independent spectra and spectrophotometric equilibrium titrations were measured with a Cary 17 spectrophotometer equipped with a temperature controller. Equilibrium anaerobic titrations were performed in the cell shown in Figure II.1b. The same cell was also used for the preparation of MPH for stopped-flow studies. During anaerobic titrations the cell was wrapped with aluminum foil to prevent light-induced decomposition and the solution was kept under a positive argon pressure of ~3 psig. Photochemical decomposition of MPMS or EPES during stopped-flow experiments was prevented by turning off the room lights and wrapping the MPMS (or EPES) burets and containers with aluminum foil.

An anaerobic rapid-scanning double-beam computerized stopped-flow spectrophotometer (Coolen et al., 1975; Papadakis et al., 1975; Suelter et al., 1975) was used to collect up to 150 spectra/s over the desired wavelength region. Alternatively, it could be used in a fixed-wavelength mode if desired. Anaerobicity of the stopped-flow apparatus was achieved by at least three evacuations (<0.001 torr) followed by filling with purified argon. The system was kept under positive argon pressure (~1 psig) during the anaerobic experiments. The anaerobicity was checked by mixing MPH with anaerobic buffer in the stopped-flow system. Since MPH reacts with oxygen to give MPMS, which has a characteristic sharp peak at 388 nm (extinction coefficient =  $26.3 \text{ mM}^{-1} \cdot \text{cm}^{-1}$ , Zaugg, 1964), the presence of oxygen could have been easily detected. Since no change in absorbance at 388 nm

after mixing MPH solution with buffer was detected over a time span of many minutes, we conclude that the oxygen concentration in the buffer was less than 0.3  $\mu\text{M}$ .

### C. Results and Discussion

#### C.1 Anaerobic Titration and Transient Kinetics of the Reduction of MPMS by NADH

Figure III.2 shows the spectral changes which occurred in a 7 ml solution of 15.9  $\mu\text{M}$  MPMS following the addition of 0.026 ml increments of 0.527 mM NADH. The isosbestic point at 358 nm and the uniformity of the relative absorbance changes at all wavelengths suggest that there are no detectable intermediates formed when  $\text{MP}^+$  is reduced to MPH (Equation III.1).



A detailed examination of the spectra shows that even at the midpoint of the equilibrium titration, one-electron intermediates account for less than about 7% of the total starting concentration at this pH (7.4). The absence of such intermediates was further supported by studying the kinetics of the reaction represented by Equation III.1.

Figure III.3 displays the spectral changes which resulted when MPMS was rapidly mixed with NADH anaerobically at pH 7.4 to give final concentrations of 31.9 and 39  $\mu\text{M}$  respectively. The change in absorbance at 388 nm with time (data from the same experiment) is shown in the inset to Figure III.3. A generalized non-linear

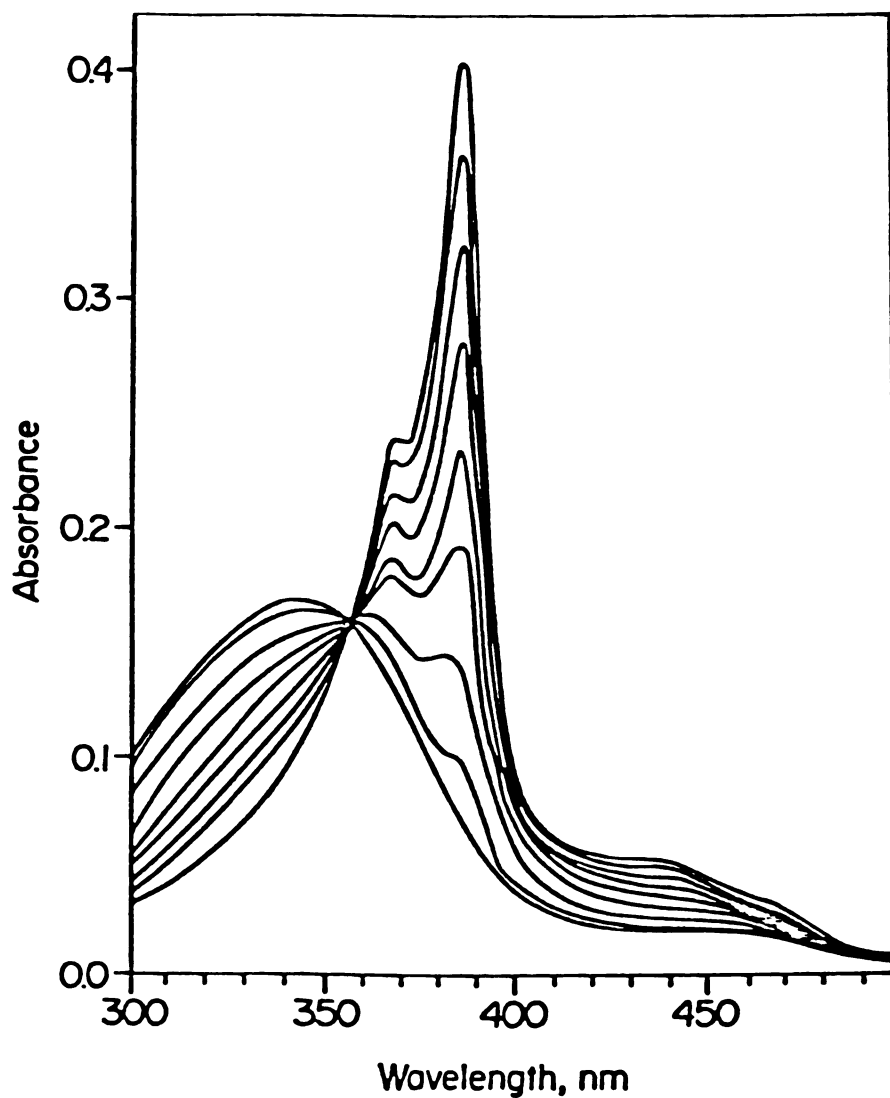


Figure III.2.--Anaerobic titration of 7 ml of 15.9  $\mu\text{M}$  MPMS by successive additions of 0.026 ml increments of 0.527 mM NADH in 50 mM HEPES buffer, pH = 7.4. The cell (Figure II.1) was wrapped with aluminum foil to prevent photodecomposition of MPMS and was kept under 1 psig argon pressure throughout the titration. Temperature =  $21 \pm 1^\circ \text{C}$ .

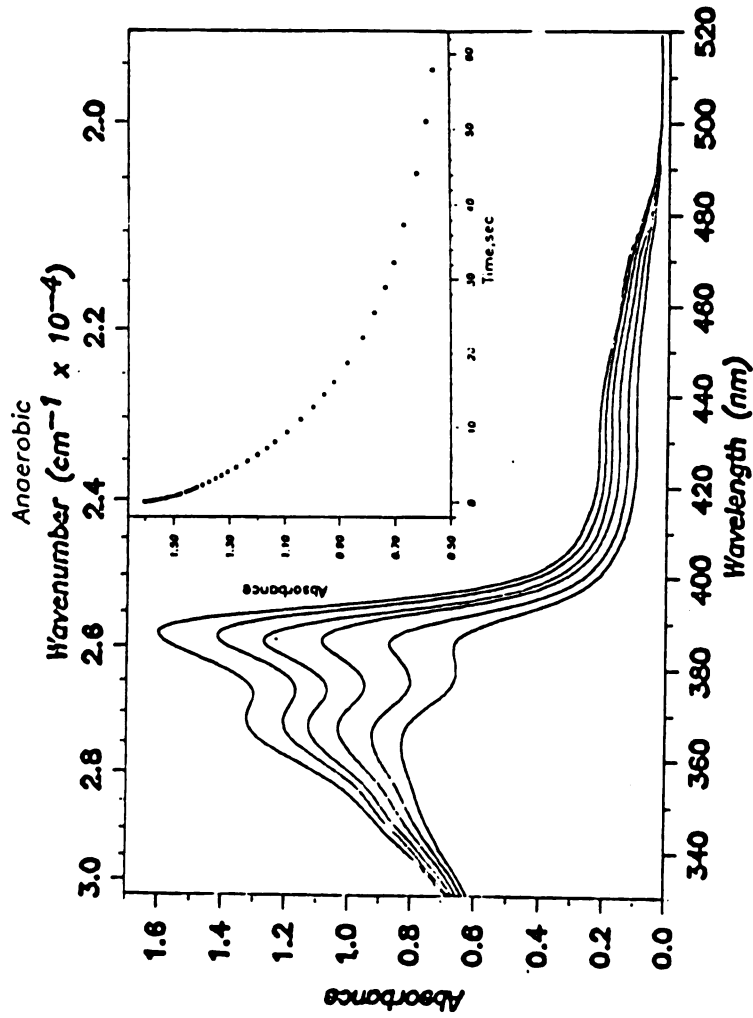
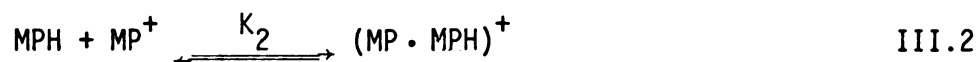


Figure III.3.--Spectral changes during the anaerobic reduction of 31.9  $\mu\text{M}$  MPMS by 39  $\mu\text{M}$  NADH (after mixing). Spectra were collected by the stopped-flow system described in the experimental section. Times, in seconds for the selected spectra are, from the top: 0.014, 1.96, 4.63, 9.32, 18.7, 37.5. Cell path length = 1.85 cm. Inset shows the changes in absorbance at 388 nm with time, taken from the same data. Conditions are the same as in Figure III.2.

least-squares program (Dye and Nicely, 1971) was used to analyze the rate data. When a second order rate equation was fitted to these data, it gave a fairly well-determined second order rate constant. However, the residuals (calculated-observed absorbances) varied systematically. Recalling that  $MP^+$  forms a complex with MPH (Zaugg, 1964) a rate equation was derived from the following scheme:



The fit of these equations to the data gave random residuals. It was assumed that the equilibrium step (Equation III.2) is fast, that the spectrum of  $(MPH MP)^+$  is the sum of the spectra of  $MP^+$  and MPH and that the complex does not react at an appreciable rate with NADH. This analysis gave  $k_1 = (3.8 \pm 0.5) \times 10^3 \text{ M}^{-1} \text{ s}^{-1}$  and  $K_2 = (1.3 \pm 0.2) \times 10^4 \text{ M}^{-1}$ . The constants reported here were averaged from the analysis of rate data of several experiments at 388 and 340 nm. The value of  $K_2$  represents only about 14% bound complex at  $[MPH] = [MP^+] = 15 \mu\text{M}$ . This accounts for the fairly good fit with only a simple second-order process.

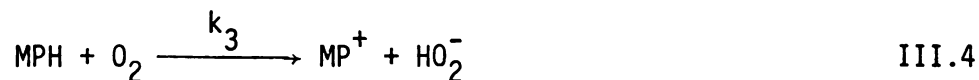
An alternative explanation is the removal of up to 14% of the  $MP^+$  concentration by the formation of semiquinoid intermediates according to:



The data would be equally well fit by this scheme provided that neither  $MP^\bullet$  nor  $MPH^{\bullet+}$  react at an appreciable rate with NADH. The difficulty with this scheme is that it is known that the spectra of  $MP^\bullet$  and  $MPH^{\bullet+}$  are different from those of  $MP^+$  and MPH (Zaugg, 1964), so that 14% of the material bound as the semiquinoid form should have been detectable.

### C.2 Reaction of MPH with Oxygen

The reaction of MPH with oxygen, Equation III.4, appears to be second order (first order in each reactant)



The spectral changes, as expected, are the opposite of those shown in Figure III.2. A pseudo first-order rate equation gave very small and random residuals when fitted to the data collected for this reaction. Under atmospheric conditions the solubility of oxygen in water is 0.25 mM (Wilhelm et al., 1977) so that the mixture with anaerobic MPH solution had half this concentration. The second-order rate constant for the oxidation of MPH by oxygen was then calculated to be  $180 \text{ M}^{-1} \text{ s}^{-1}$ . This is only an approximate value, since it is based upon the solubility of oxygen in pure water rather than in the buffer solution.

### C.3 The Reaction of MPMS with NADH in the Presence of Oxygen

In the presence of oxygen,  $MP^+$  acts as a catalyst for the oxidation of NADH by oxygen. This should be kept in mind when studying

biological reactions that use the MPMS-NADH couple under aerobic conditions. By using the rate constants derived above for the reduction of MPMS by NADH and the oxidation of MPH by oxygen, one can predict the behavior of the  $\text{NADH-MP}^+-\text{O}_2$  system. The scheme represented by Equations III.1, III.2, (or III.3) and III.4 can be used to describe this system.

In a scanning experiment, digitized data are stored for the entire wavelength region spanned as a function of time. These data describe the kinetics of absorbance changes for every wavelength channel, at essentially the same time. This enables one to check the validity of a certain kinetic scheme at more than one wavelength.

Figure III.4 represents the spectral changes in an experiment in which  $125 \mu\text{M}$  NADH solution reacted with  $22 \mu\text{M}$  MPMS in the presence of atmospheric oxygen. The simultaneous changes at 388 nm and at 340 nm obtained from these spectra could be completely described by the scheme mentioned above. The resulting two coupled differential equations which represent the rate of change of  $[\text{MPMS}]$  and  $[\text{NADH}]$  with time, were solved numerically by using the program KINFIT4 (Dye and Nicely, 1971) for the full time course shown. In this case, since all solutions were aerobic, the concentration of oxygen was taken to be  $0.25 \text{ mM}$ . The rate constants for the reduction of MPMS by NADH and for the oxidation of MPH by oxygen were adjusted. This analysis gave values for the rate constants,  $k_1$ ,  $k_4$ , (in Equations III.1 and III.4) of  $3.6 \times 10^3 \text{ M}^{-1} \text{ s}^{-1}$  and  $160 \text{ M}^{-1} \text{ s}^{-1}$ , respectively, which are in satisfactory agreement with the values obtained for the separate reactions.

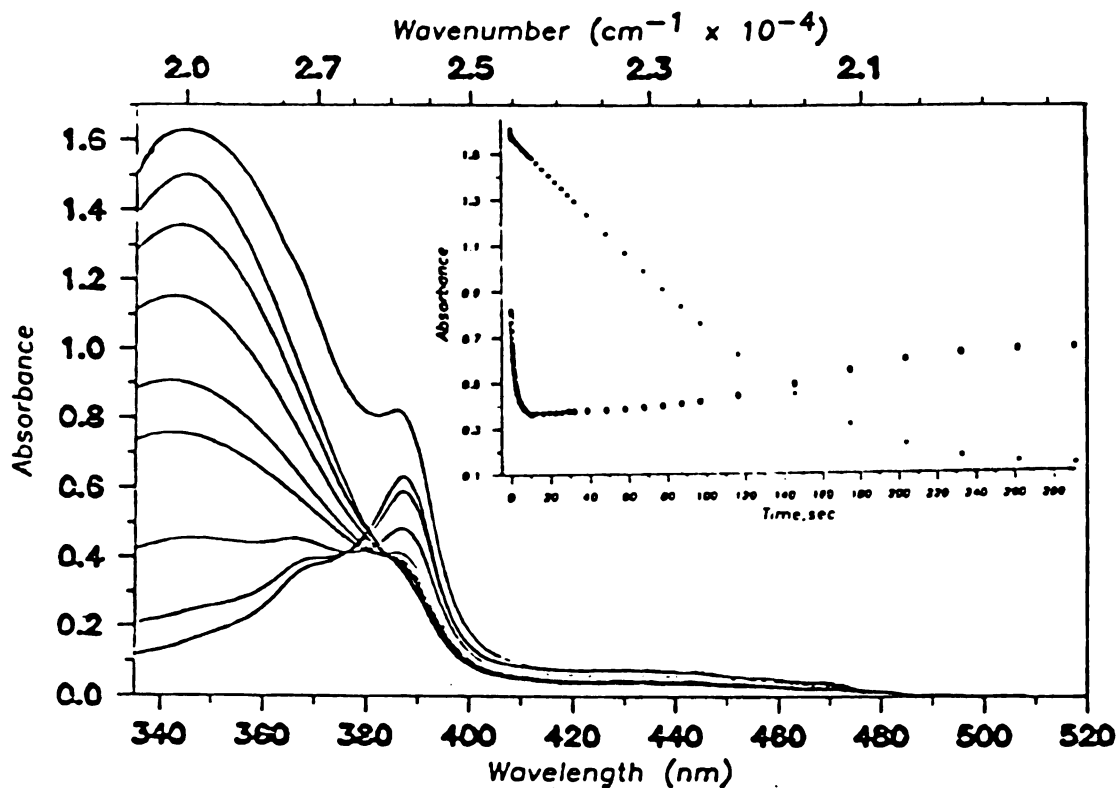


Figure III.4.--Spectral changes which result from mixing NADH with MPMS in the presence of atmospheric oxygen. Concentrations after mixing were 125 and  $22 \mu\text{M}$ , respectively. Times, in seconds (from top to bottom at 340 nm) are: 0.015, 1.47, 25.9, 48.6, 77.7, 97.1, 146, 204, 292. Inset shows the changes in absorbance at 388 (dots) and 340 nm (circles) with time from the same data. Medium is the same as in Figure III.2.

#### C.4 Effect of Room Light on the Spectra of MPMS

Figure III.5 shows the spectral changes which occur when a solution of 31.2  $\mu\text{M}$  aerobic MPMS solution at  $\text{pH} = 7.4$  is exposed to room (fluorescent) light. From these spectral changes and the isosbestic point at 345 nm, we conclude that the main, and apparently the only, product of the photodecomposition of MPMS in the presence of oxygen at this pH is pyocyanine (absorption maximum at 310 nm). This was also observed by McIlwain (1937) and by Chew and Bolton (1980) to be a major product of the irradiation of MPMS by light at  $\text{pH} = 7$ .

It is worth mentioning in this context that EPES, the ethyl analog of MPMS gave nearly identical results. Not only was EPES found to be similar to MPMS in photosensitivity, but also in all the other reactions mentioned in this text. Thus the conclusion by Ghosh and Quayle (1979) that EPES is less photolabile than MPMS at  $\text{pH} = 9.7$  cannot be extended to lower pH values ( $\text{pH} = 7.4$  in these experiments).

When anaerobic solutions of MPMS were exposed to room light, the spectral changes were different from those shown in Figure III.5. The photodecomposition apparently produced MPH as well as  $\text{PHY}^+$ . The two products were formed in nearly equal amounts since upon exposure of the final products to atmospheric oxygen, the absorbance of MPMS at 388 nm rose to about half its starting value. In addition, the absorbance of pyocyanin at 310 nm reaches only about half the value anaerobically that it attains aerobically. These observations are consistent with the scheme proposed by Chew et al. (1980) for high pH

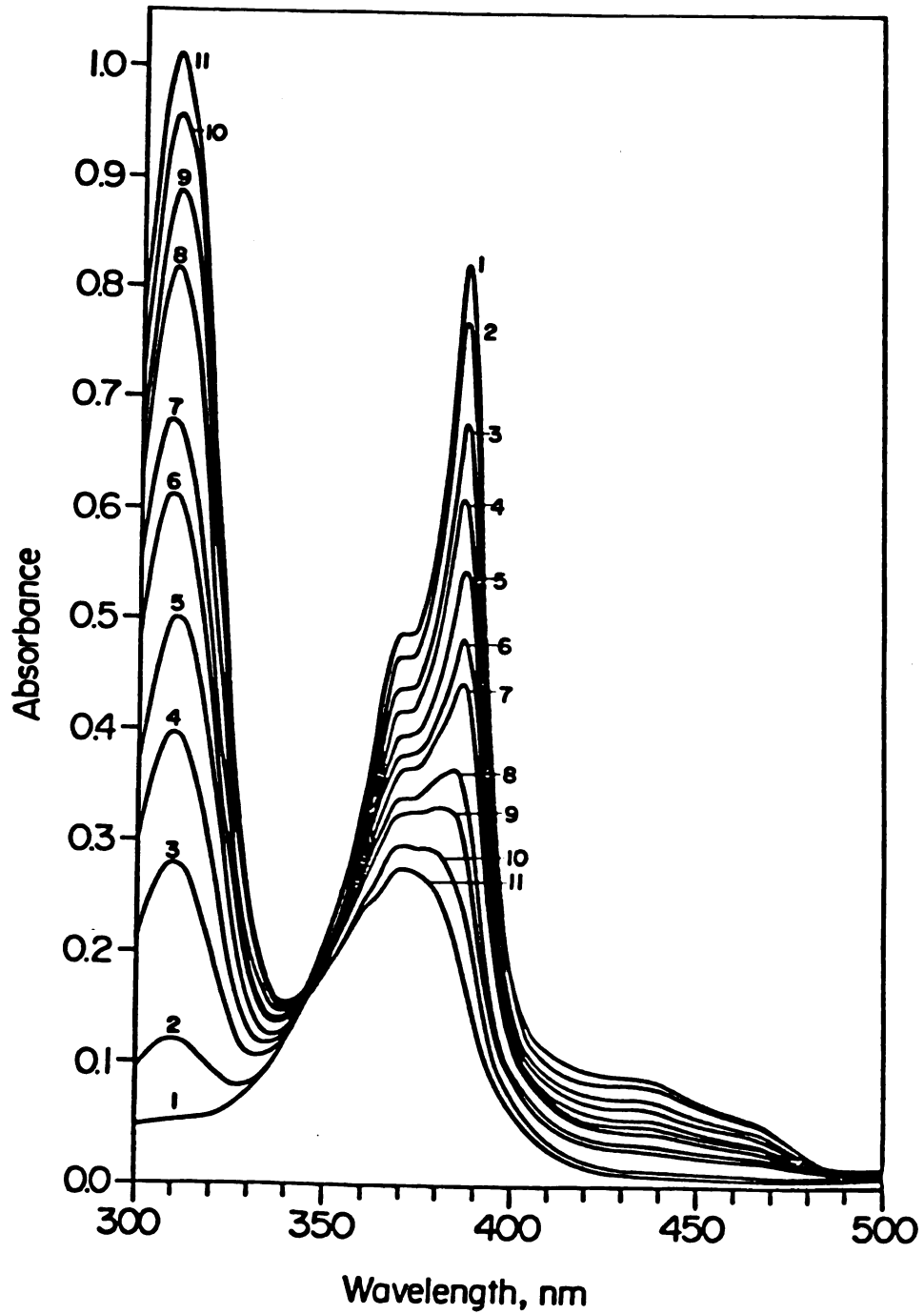
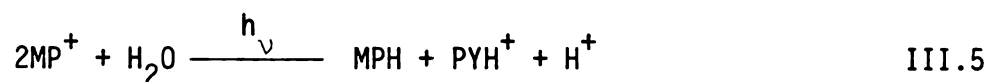


Figure III.5.--Effect of room fluorescent light on the spectra of 21.2  $\mu\text{M}$  aerobic MPMS. Time between successive spectra was about 10 minutes. Buffer was the same as in Figure 3.

values as well as with the observation by Zaugg (1964) that most of the semiquinonoid (one-electron) form undergoes disproportionation at pH values between 7 and 8 in aqueous solutions.

Thus the stoichiometry of the anaerobic photodecomposition of  $MP^+$  at pH = 7.4 may be represented by Equation III.5



In the presence of oxygen, the reaction represented by Equation 4 will take place, and the photoreaction of  $MP^+$  will produce only pyocyanine, as suggested by the spectra shown in Figure III.5.

The results described here would appear to eliminate one of the possible mechanisms presented by Chew et al. (1980). Their value for the disproportionation constants of  $MPH^+$  and  $MP^+$  (Equations 11 and 12 of the mechanism proposed in their paper) are  $2.5 \times 10^{-8}$  and  $6.3 \times 10^5$ ; respectively. If these values were correct, then at the midpoint of the reduction of  $20 \mu\text{M}$   $MP^+$  by NADH, at pH = 7, the concentrations of  $MP^+$  and  $MPH^+$  would be  $5 \mu\text{M}$  and  $10 \mu\text{M}$ , respectively. This would lead to  $[MP^+] = [MPH] = 2.5 \mu\text{M}$ , a drop of 75% from the radical-free case.  $MP^+$  and  $MPH^+$  are known to have different spectra (Zaugg, 1964; and Chew et al., 1980) so that conversion of one of these forms to another would result in an appreciable change in the absorbance at 450 nm (where  $MPH^+$  absorbs with an extinction coefficient of  $10 \text{ mM}^{-1} \text{ cm}^{-1}$ ) and at 388 nm. This would lead to different rate profiles at 450 nm ( $MPH^+$  peak), 388 nm ( $MP^+$  peak) and 340 nm (NADH peak) during reduction by NADH. In fact, the rate profiles

showed no detectable deviation from clean stoichiometry. Therefore, the equilibrium constants for the disproportionation mechanism, presented as one of several possibilities by Chew et al. (1980) cannot be correct.

#### D. Conclusions

The data presented here should be useful for those who use the MPMS-NADH couple in enzyme assays, particularly in the presence of oxygen. The reduction of MPMS by NADH is slow compared to the rate of many enzymatic reactions. Thus, the former reaction could be rate limiting and add complications to the enzymatic reaction being studied. The reaction of MPH with oxygen is also slow, and for many practical purposes can be ignored compared to the much higher rate of the reduction of oxygen by biological systems (for example, the rate of reaction of oxygen with reduced cytochrome c oxidase is about  $10^8 \text{ M}^{-1} \text{ s}^{-1}$  (Greenwood and Gibson, 1967)).

## CHAPTER IV

### REDUCTION OF CYTOCHROME OXIDASE BY MPH

Redox reactions of cytochrome c oxidase are of central importance to the understanding of the catalytic activity of this protein in electron transport. The reduction of the protein, either under anaerobic conditions or during turnover in the presence of oxygen, has been studied extensively, particularly by using its natural substrate, cytochrome c (see, for example, Gibson et al., 1965; Andréasson et al., 1972; Andréasson, 1975; Wilms et al., 1981). The reduction of the oxidase has also been carried out under anaerobic conditions with the positively charged metal ion complexes hexa-aquochromium (II) (Greenwood et al., 1977) and hexamine ruthenium (II) (Scott and Gray, 1980). It was concluded from those studies that the charge type of the reductant plays an important role in the kinetics of the reduction as well as in the site of the interaction with the oxidase.

The reductant, 5, 10- dyhydro-5-methyl phenazine (MPH) was used in the present work to study the anaerobic four-electron reduction of the oxidase by rapid scanning stopped-flow spectrophotometry (see Experimental). MPH was chosen because of its spectral properties (see Chapter III), because it is a neutral molecule, and because it has a low reduction potential at neutral pH (80 mV, Jagendorf and

Margulies, 1960), which is sufficiently negative to drive the four electron reduction of the oxidase. The implications of each of the properties mentioned above are discussed in the text.

#### A. Spectral Shape Analysis

The visible and near ultraviolet electronic absorption properties of the MPH/MP<sup>+</sup> couple are discussed in Chapter III. Figure IV.1 displays a three dimensional plot of the overall spectral changes from 330 to 530 nm which occur when oxidized cytochrome oxidase is mixed anaerobically with excess MPH. This wavelength region was chosen to insure the simultaneous observation of the spectral changes due to MPH, MP<sup>+</sup> and reduced and oxidized cytochrome oxidase in the Soret region, without significant loss of wavelength resolution. When the  $\alpha$ -band of the oxidase was studied, another wavelength region, usually ranging from 400 to 650 nm, was scanned. Owing to the fact that neither MP<sup>+</sup> nor MPH absorb appreciably in this region, the three dimensional surface of such an experiment (Figure IV.2) has spectral contributions only from the oxidase chromophores.

The principal changes of absorbance in Figure IV.1 are the decay of the oxidized cytochromes  $\underline{a}$  and  $\underline{a}_3$ , with maximum total absorbance at 418 nm, and the growth of the reduced heme band with a narrower peak at 444 nm. In addition, the peak of MP<sup>+</sup> grows in at 388 nm. Comparison of the initial and final spectra with those of MP<sup>+</sup>, MPH and oxidized and reduced cytochrome oxidase shows that the reaction follows the overall stoichiometry:

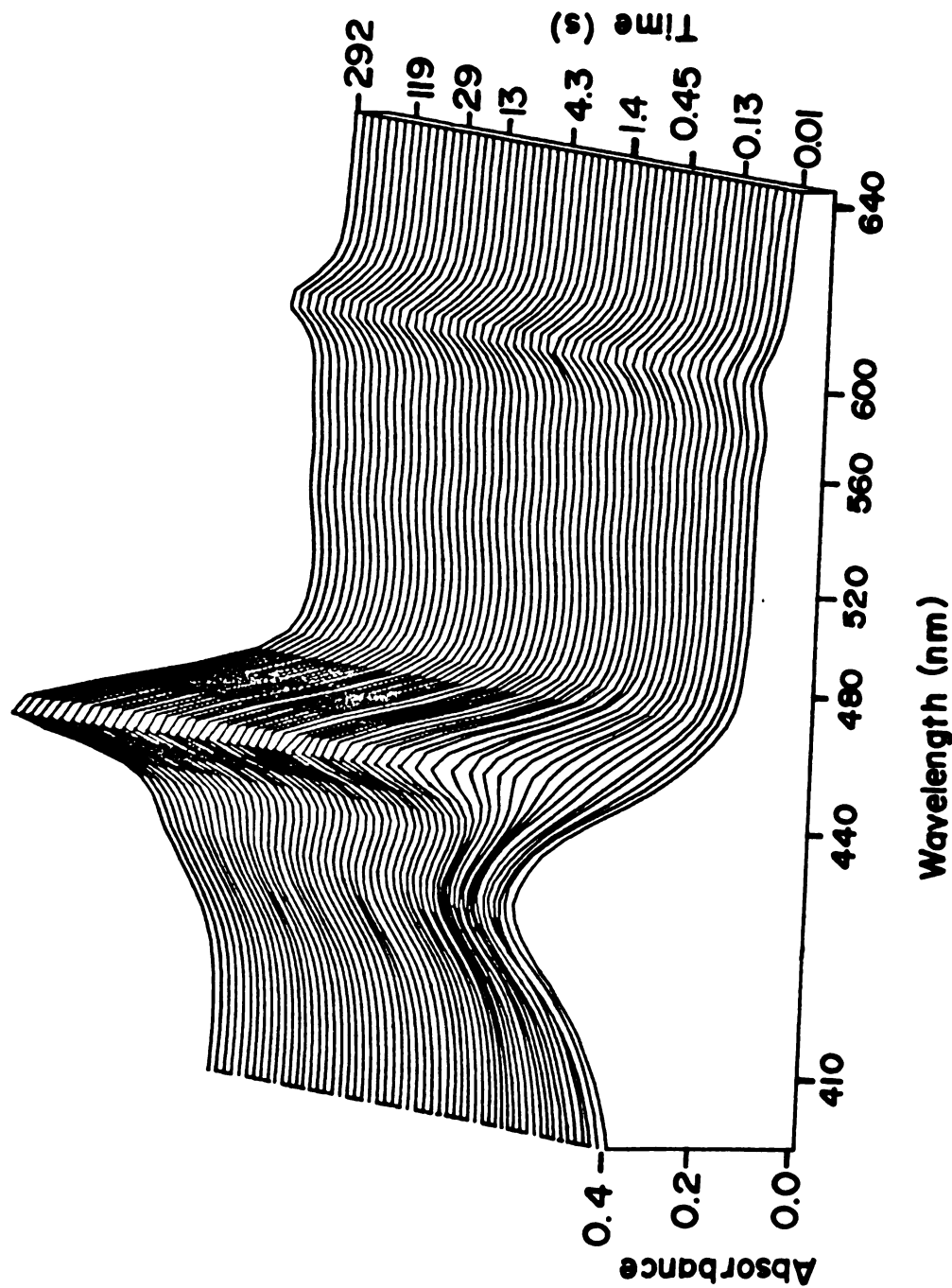


Figure IV.2.--Absorbance-time wavelength surface for the anaerobic reduction of cytochrome oxidase by MPH in the 400 - 630 nm region. Concentrations after mixing were: Oxidase, 3.32  $\mu\text{M}$ ; MPH, 26  $\mu\text{M}$ . Other conditions are the same as in Figure IV.1.

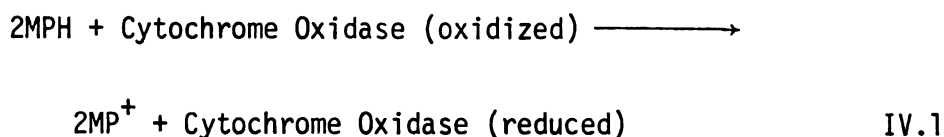


Figure IV.3 displays, in two dimensions, spectra selected from Figure IV.1 as a function of time, as well as the spectrum of the oxidized cytochrome oxidase (against buffer, same conditions). When the spectrum of the oxidized oxidase was subtracted from the spectra shown in Figure IV.1, the resulting "kinetic difference" spectra (Figure IV.4) show a striking feature of this reaction. Two minima in the difference spectra are observed at around 410 and 430 nm and suggest that the Soret region of the oxidized oxidase consists of two bands that decay at different rates upon reduction. Furthermore, these spectra suggest that during the early stages of the reduction, the absorbance change at around 430 nm, where cytochrome a has its absorbance maximum (Vanneste, 1966; Babcock et al., 1981; Halaka et al., 1981a), is greater than that at 410 nm, where cytochrome a<sub>3</sub> has its absorbance maximum. In the initial fast process, the difference spectra also indicate that there may be a shift (~5 nm) of the cytochrome a<sub>3</sub> band to a longer wavelength (or of the cytochrome a band to a shorter wavelength). The last phase of the reaction shows a greater change on the short wavelength (a<sub>3</sub>) side of the Soret band. The latter effect is large enough to halt the growth in absorbance at 388 nm due to  $\text{MP}^+$  formation, as expected by comparison of the  $\Delta\epsilon$  values for  $\text{MP}^+$  and cytochrome a<sub>3</sub>, which are approximately equal at this wavelength. The shift in the isosbestic point from 437 to 428 nm as the reaction proceeds supports this observation. Examination of

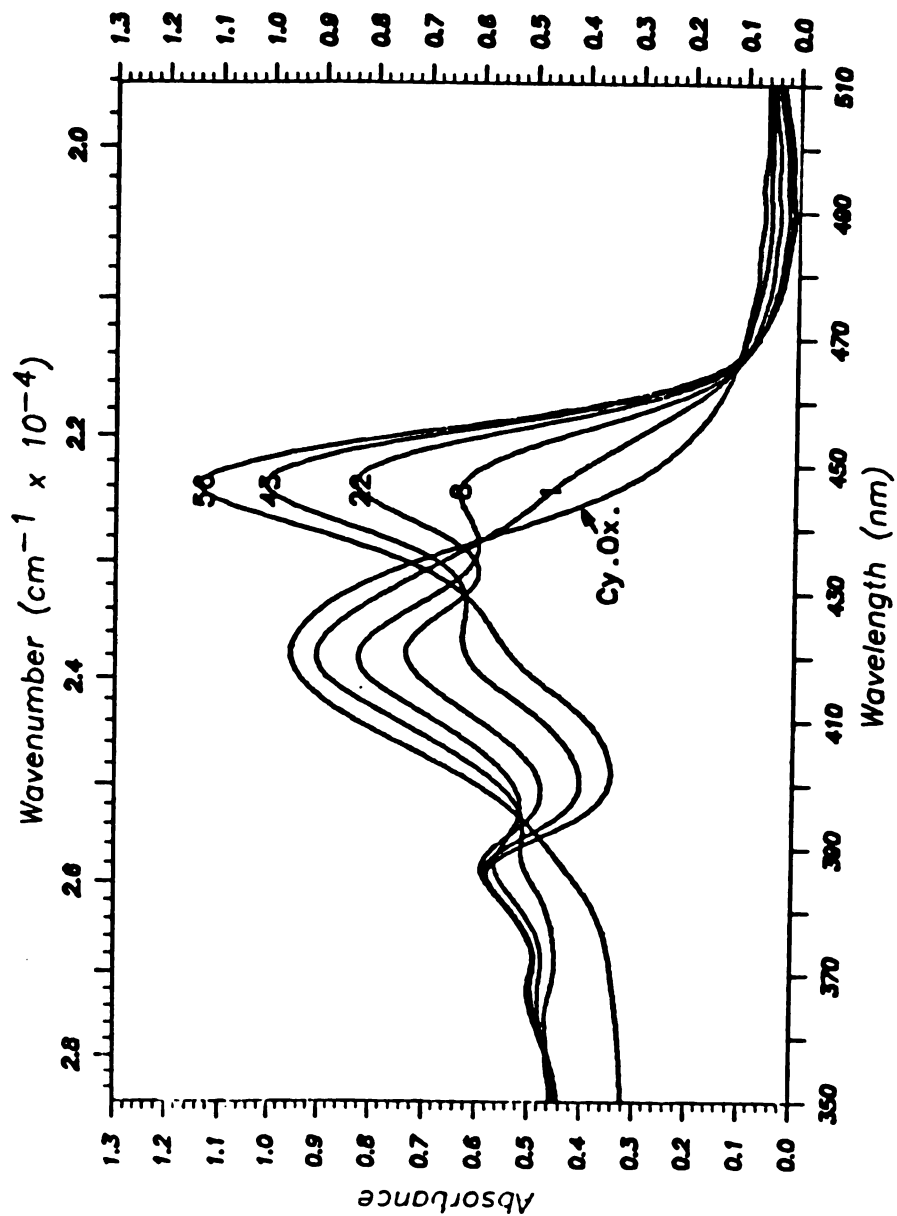


Figure IV.3.--Selected spectra from Figure IV.1. The spectrum labeled cy. ox. is that of the oxidized cytochrome oxidase (same concentration) with no reaction. Times for various spectra are: 1, 13.5 ms; 8, 110 ms; 22, 1.39 s; 43, 38.8 s; 56, 292 s.

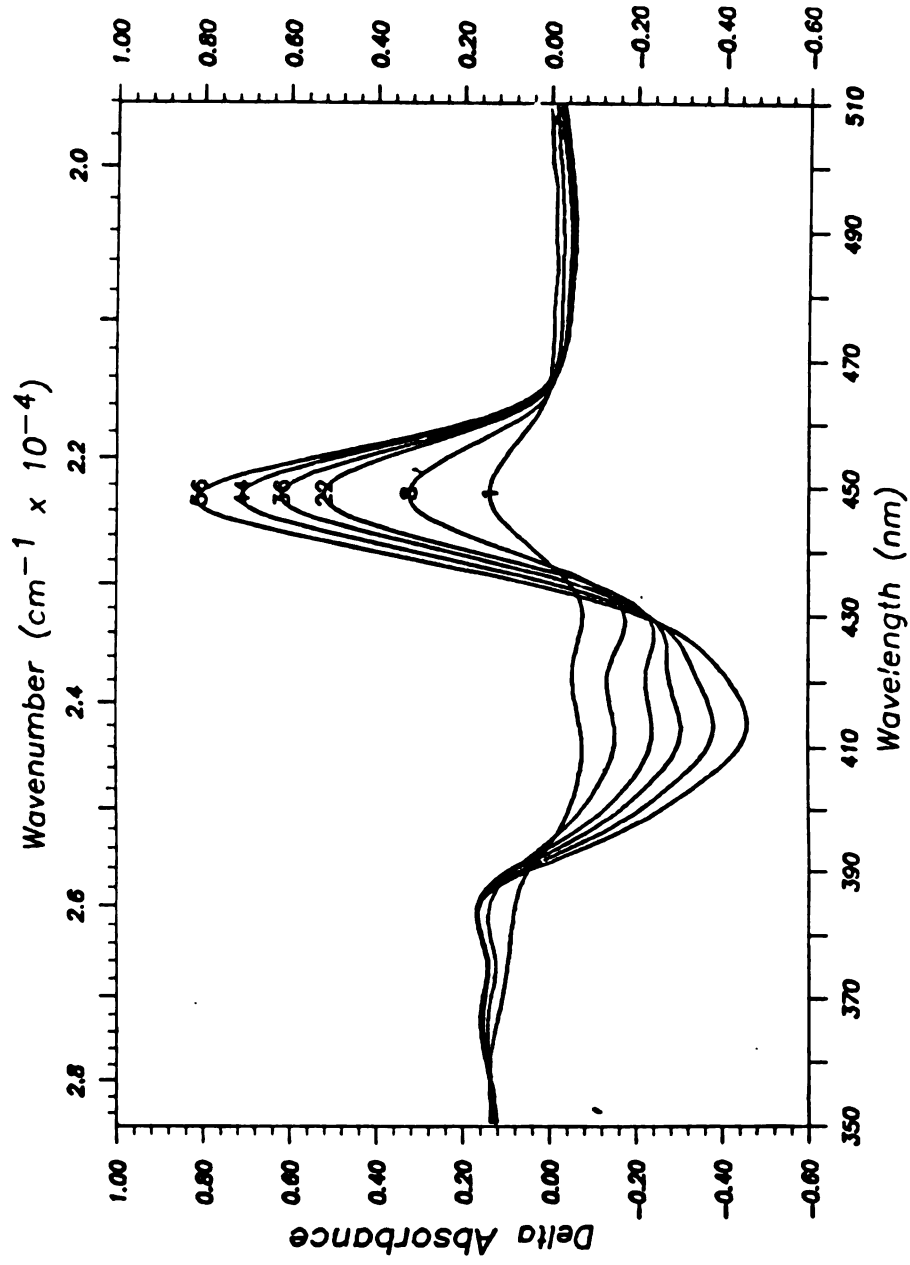


Figure IV.4.--Selected difference spectra constructed from Figure IV.1 by subtracting the oxidized oxidase spectrum (labeled cy ox in Figure IV.3). Times are: 1, 13.5 ms; 8, 110 ms; 22, 1.39 s; 36, 13 s; 44, 39 s; 56, 292.

time courses at several wavelengths (Figure IV.5) also shows the different kinetic profiles of cytochromes a and a<sub>3</sub> (see below).

Other features of this reaction are apparent in Figure IV.6 which displays spectra in both the Soret and the  $\alpha$ -bands. Inspection of the difference spectra in the  $\alpha$ -band region shows that most of the changes here are completed in the early stages of the reduction (see below for quantitative estimates). It is also important to note the shift in the peak position to shorter wavelength in the final spectrum, a phenomenon which, although small, is reproducible. This implies that the component that is reduced in the last stage of the reduction (cytochrome a<sub>3</sub>) has its peak around 595 nm compared to 604 nm for cytochrome a. This observation is further confirmed by the study, to be discussed in Chapter VI, of the reduction of the oxidase by sodium dithionite.

#### B. Kinetics of the Reduction of Cytochrome Oxidase by MPH

The kinetics of the anaerobic reduction of cytochrome oxidase by MPH were studied by stopped-flow spectrophotometry in scanning and fixed-wavelength modes. Although scanning experiments performed with the stopped-flow apparatus described in Chapter II produce data with high signal to noise ratio and could be used to obtain rate parameters, kinetic analyses were usually done on data collected in a fixed-wavelength mode. This is due to the fact that, in a fixed-wavelength experiment, it is possible to collect more data points for the particular wavelength under study, which owing to computer memory limitations, cannot be obtained in scanning experiments.

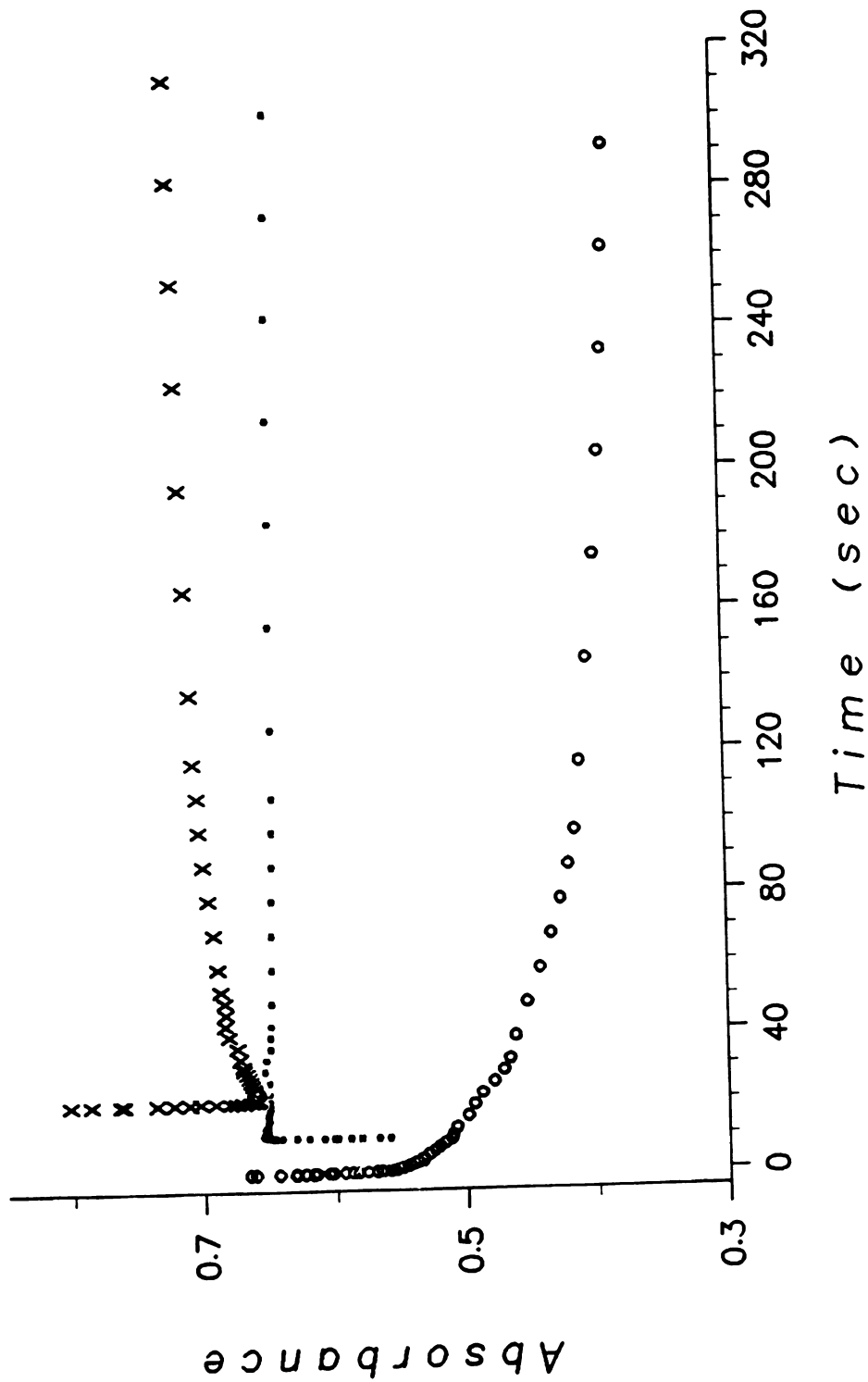


Figure IV.5.--Time dependence of absorbance at 430 nm (x), 412 nm (o) and 388 nm (\*), taken from the spectra shown in Figure IV.1. The time scales for \* and x are shifted by 10 and 20 s, respectively.

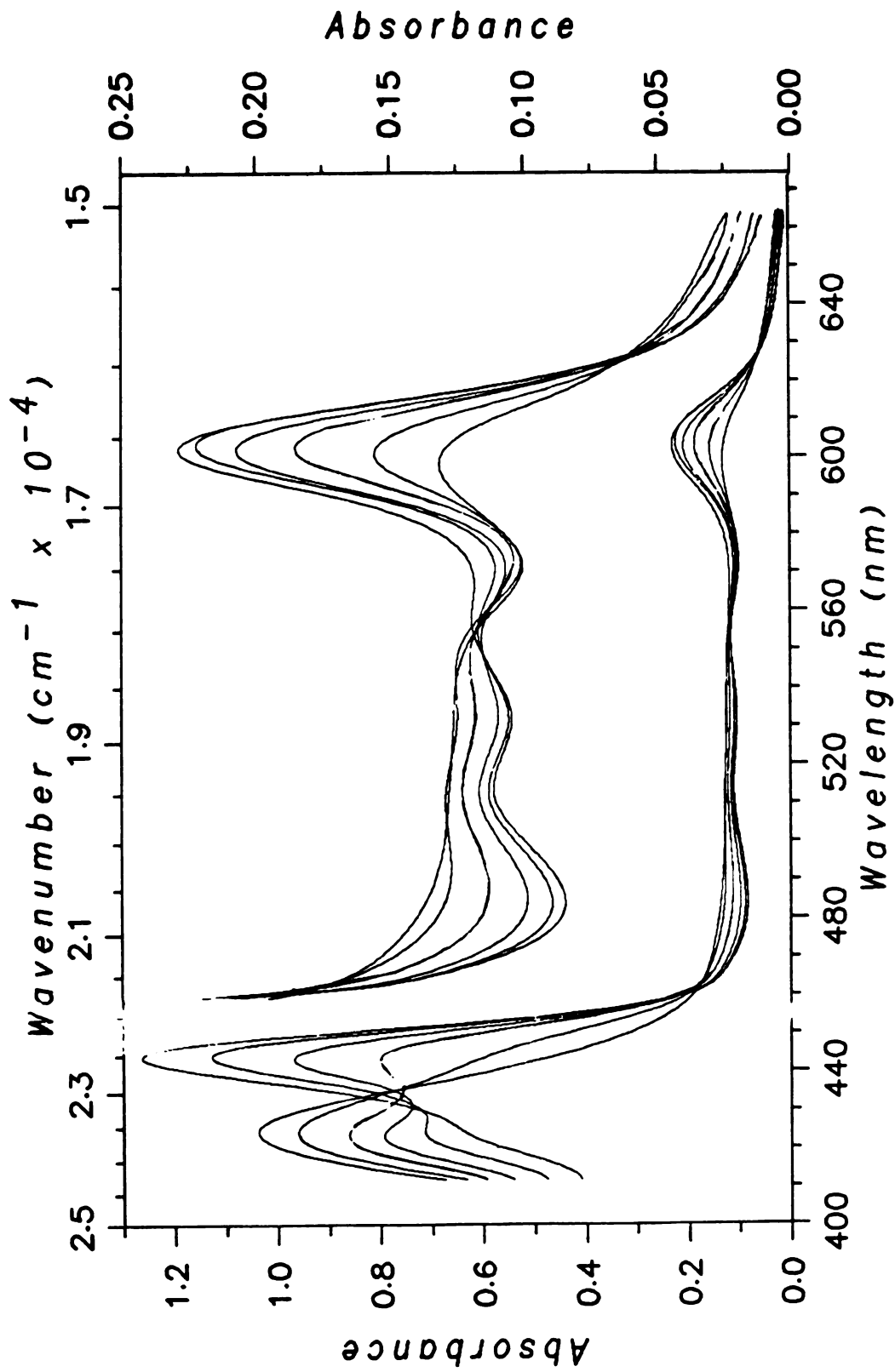


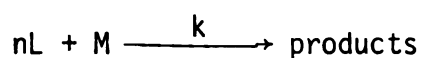
Figure IV.6.--Selected spectra in the reaction of MPH with cytochrome oxidase, taken from the data shown in Figure IV.2. Note the shift of the  $\alpha$ -peak in the last spectrum to a shorter wavelength. Times of spectra in seconds from bottom to top at 600 nm, are: 0.014, 0.110, 0.354, 0.914, 25.87, 292.

Scanning experiments, besides providing rate information, are used in spectral shape and principal component analyses. The reproducibility in fixed-wavelength experiments was such that the same rate constants to within 1% could be obtained in different experiments.

Non-linear least squares fitting was carried out by using program KINFIT4 (a modified version of program KINFIT, Dye and Nicely, 1971) and showed that the anaerobic reduction of the oxidase by MPH is triphasic. This was concluded from analysis of absorbances at 444 nm as well as several other wavelengths. The initial phase is best described by a second order reaction between MPH and the oxidase. This is followed by two first order processes, as discussed below.

### B.1 Analysis of the Fast Phase

A generalized second order rate equation (Equation IV.6) was used to fit second order processes, and is derived by considering that any second order reaction can be represented by



where  $n$  is a stoichiometric ratio. If  $[L_0]$  and  $[M_0]$  are the initial concentrations of  $L$  and  $M$ , respectively, then the rate of this reaction can be represented as

$$\frac{dx}{dt} = k[M_0] (R-nx)(1-x) \quad \text{IV.2}$$

where  $x$  is the extent of the reaction,  $k$  is the rate constant and  $R$  is given by

$$R = \frac{[L_0]}{[M_0]}$$

Integrating Equation IV.2, leads, for  $R \neq n$ , to

$$\ln \frac{R-nx}{1-x} = (R-n)k[M_0]t + \ln R \quad \text{IV.3}$$

Solved for  $x$  equation IV.3 becomes

$$x = \frac{e^{-k't} - 1}{\frac{n}{R} e^{-k't} - 1} \quad \text{IV.4}$$

where  $k' = k (R-n) [M_0]$ . Recall that for a stoichiometric reaction,  $x$ , in absorbance form is given by

$$x = \frac{A_t - A_0}{A_\infty - A_0} \quad \text{IV.5}$$

where  $A_t$ ,  $A_0$ , and  $A_\infty$  are the absorbances at time  $t$ , zero, and infinity, respectively. Substituting  $x$  from Equation IV.5 into Equation IV.4 gives

$$A = A_0 + (A_\infty - A_0) \frac{1 - e^{-k't}}{1 - \frac{n}{R} e^{-k't}} \quad \text{IV.6}$$

The term  $(A_\infty - A_0)$  corresponds to the absorbance changes for a particular phase and can be adjusted as a parameter to give the extent of that phase.

Figure IV.7 displays a typical fit of the second order equation to the initial phase of the reduction (in a fixed-wavelength

$$R = \frac{[L_0]}{[M_0]}$$

Integrating Equation IV.2, leads, for  $R \neq n$ , to

$$\ln \frac{R-nx}{1-x} = (R-n)k[M_0]t + \ln R \quad \text{IV.3}$$

Solved for  $x$  equation IV.3 becomes

$$x = \frac{e^{-k't} - 1}{\frac{n}{R} e^{-k't} - 1} \quad \text{IV.4}$$

where  $k' = k (R-n) [M_0]$ . Recall that for a stoichiometric reaction,  $x$ , in absorbance form is given by

$$x = \frac{A_t - A_0}{A_\infty - A_0} \quad \text{IV.5}$$

where  $A_t$ ,  $A_0$ , and  $A_\infty$  are the absorbances at time  $t$ , zero, and infinity, respectively. Substituting  $x$  from Equation IV.5 into Equation IV.4 gives

$$A = A_0 + (A_\infty - A_0) \frac{1 - e^{-k't}}{1 - \frac{n}{R} e^{-k't}} \quad \text{IV.6}$$

The term  $(A_\infty - A_0)$  corresponds to the absorbance changes for a particular phase and can be adjusted as a parameter to give the extent of that phase.

Figure IV.7 displays a typical fit of the second order equation to the initial phase of the reduction (in a fixed-wavelength

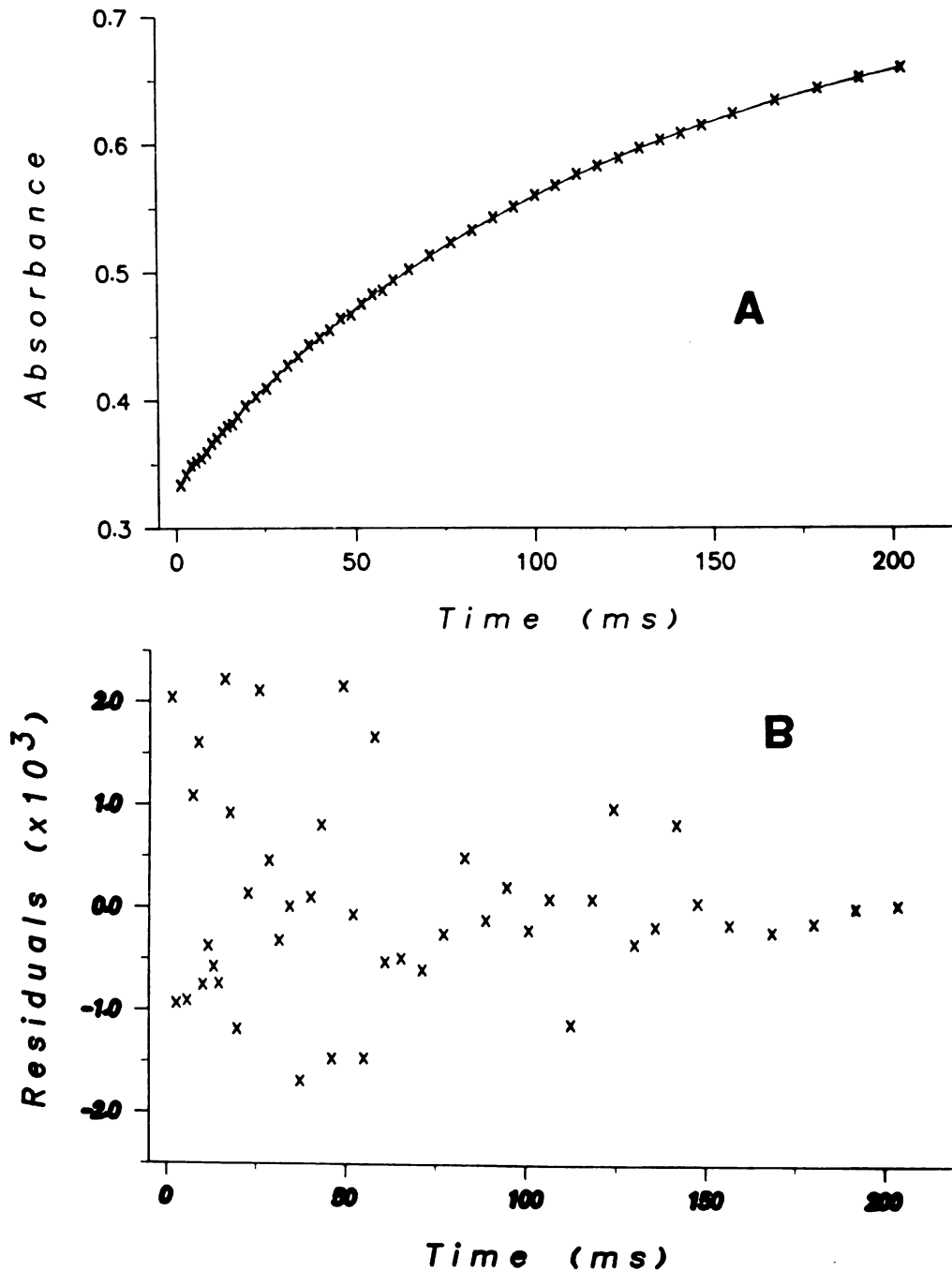


Figure IV.7.--(A) Fit of the fast phase for the reduction of cytochrome oxidase by MPH. X's are the experimental data points and the solid line is the calculated curve. Data collected in a fixed-wavelength mode. Concentrations after mixing were: Oxidase,  $3.1 \mu\text{M}$  and MPH,  $19 \mu\text{M}$ . (B) residuals of the fit shown in (A). Residuals are defined as  $A(\text{calculated}) - A(\text{observed})$ . Other conditions are the same as in Figure IV.1.

experiment at 444 nm). This phase was easily analyzed by simply choosing data points covering about the first 200 ms of the reaction, although analysis of the full time course, consisting of a second order phase followed by two first order processes was also done. Analysis of the full-time course becomes easier when MPH concentration is high compared to that of the oxidase (pseudo-first order conditions), where a three exponential equation representing the three processes was used. The rates of the three processes are sufficiently different so as to allow their easy separation. Note that the residuals in Figure IV.7b are small and random which is an indication that the equation used describes the data. Table IV.1 summarizes results of the analysis of the fast phase of the reduction.

It is worth mentioning here that the analysis gave, for absorbance changes at 444 nm, a delta absorbance equal to about 50% of the total change, while at 605 nm, the contribution of the fast phase was about 80% at this wavelength, in agreement with Scott and Gray (1980) on stopped-flow results obtained on the reduction of the oxidase by hexamine ruthenium (II). This implies that cytochrome a contributes a major portion of the overall enzyme absorbance in the 605 nm region.

B.1.1 Kinetics of the fast phase at 830 nm.--The kinetics of the reduction of the oxidase by MPH in the near I.R. region were studied by an experiment that was designed to follow the anaerobic absorbance changes at 830 and 605 nm. The kinetics of the growth at 605 nm showed the expected second order behavior in the fast phase,

TABLE IV.1 -- Analysis of the fast phase of the reduction of cytochrome oxidase by MPH in HEPES buffer containing 0.5% Tween 20, pH = 7.4 at  $21 \pm 1^\circ\text{C}$ .  $k_1$  is the second order rate constant for the process.

$[\text{aa}_3], \mu\text{M}$	$[\text{MPH}], \mu\text{M}$	$k_1^f \times 10^{-5}, \text{M}^{-1} \text{s}^{-1}$
11.2	30.0	$2.8 \pm 0.3^{a,c}$
3.7	23.0	$3.6 \pm 0.3^{a,d}$
3.3	23.0	$4.1 \pm 0.4^{b,d}$
2.59	23.0	$3.2 \pm 0.4^{a,d}$
1.1	8.4	$2.9 \pm 0.4^{b,d}$
		Avg = $3.2 \pm 0.5$

<sup>a</sup>Analysis done on a fixed-wavelength experiment.

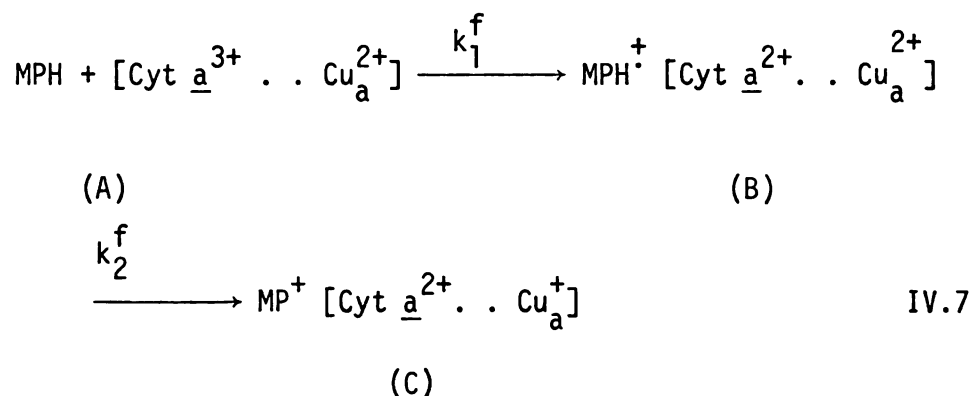
<sup>b</sup>Scanning experiment.

<sup>c</sup>Wavelength of analysis, 605 nm.

<sup>d</sup>Analysis at 444 nm.

with essentially the same second order rate constant as that determined at 444 nm (see Table IV.1). However, the rate of the 830 nm band decay, under identical conditions, showed a detectable lag (Figure IV.8). Although only one set of concentrations was used, this lag was reproducible.

A simple scheme that accounts for the observed lag at 830 nm and agrees with the kinetic measurements at 605 nm is presented below



The observed rate at 605 nm would be proportional to the formation of species B and C (defined in Equation IV.7) since both of them have reduced cytochrome a. Also this rate is second order, as discussed above. We here make the assumption that MPH<sup>+</sup> would transfer an electron fast so that, in effect, it will keep the heme reduced while the latter transfers electrons to its associated copper. The concentration of B + C at time t (measured at 605 nm) would then be given by

$$([B] + [C])_t = \frac{[L_0](1 - e^{-k't})}{1 - ([L_0] - [M_0])e^{-k't}} \quad \text{IV.8}$$

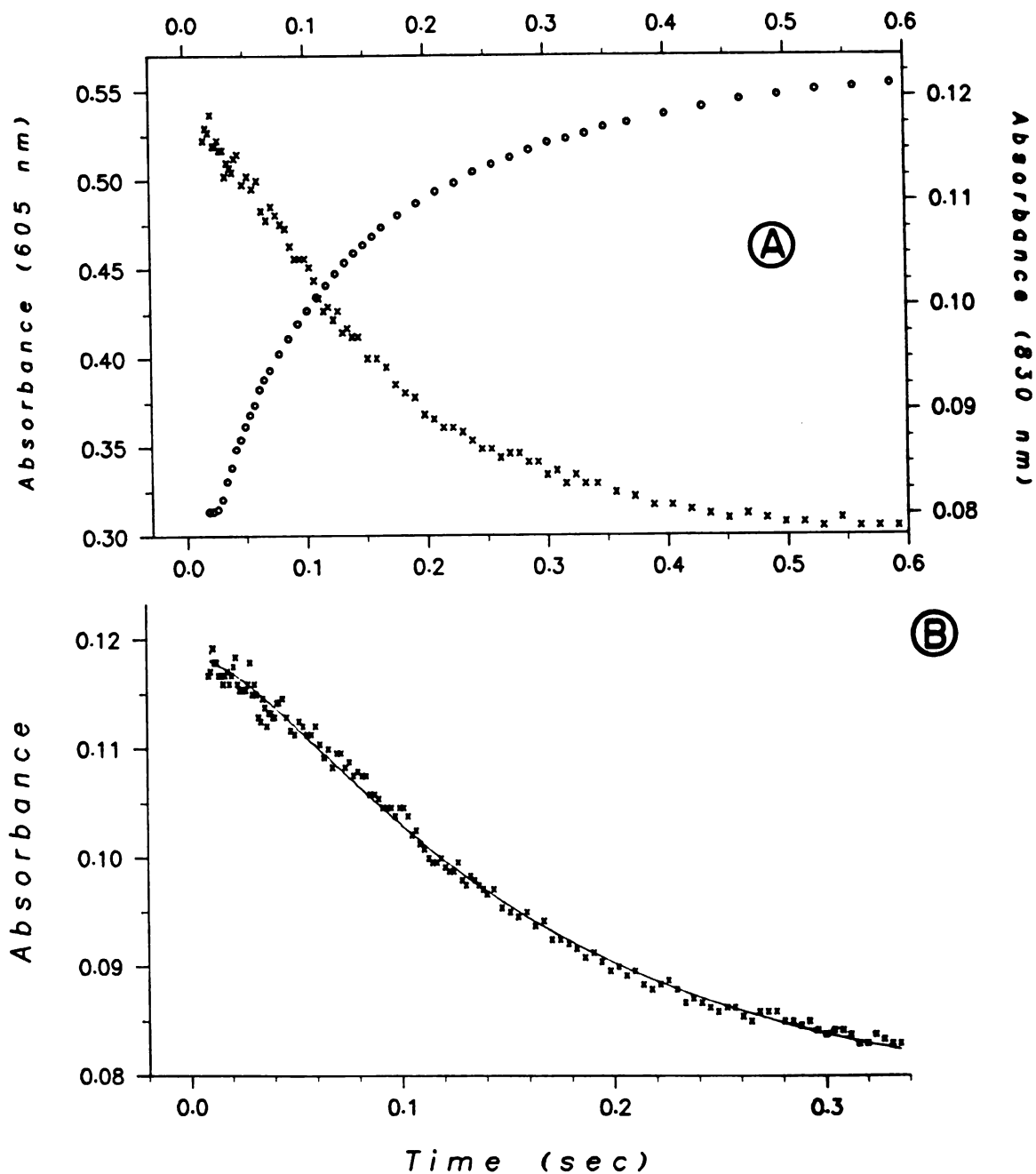


Figure IV.8.--(A) The decay at 830 nm and 605 nm during the reduction of  $10.8 \mu\text{M}$  cytochrome  $aa_3$  by  $27 \mu\text{M}$  MPH. (B) Fit of Equation IV.8 to the data at 830 nm; x's are experimental points and the solid line is the calculated curve. Other conditions are the same as in Figure IV.1

where  $[L_0]$  and  $[M_0]$  are the initial concentrations of MPH and oxidase, respectively, and  $k' = k_1^f ([L_0] - [M_0])$ . At 830 nm, the rate of change of absorbance is proportional to the production of species C, whose rate is given by

$$\frac{d[C]}{dt} = k_2^f (([B] + [c]) - [c]) \quad \text{IV.9}$$

We then substitute the term  $([B] + [c])$  by its value from Equation IV.8. Equation IV.9 was solved numerically and  $k_2^f$  was adjusted. The fit (see Figure IV.8) gave  $k_2^f$  a value of  $17.8 \pm 0.5 \text{ s}^{-1}$ .

## B.2 Kinetics of the Slow Processes

The slow phase of the reduction is best fitted by two first order processes which are independent of MPH concentration (Halaka et al., 1981a). This is not in agreement with the suggestion of Scott and Gray (1980) that the slow phase is described by a single second order process (in enzyme). Their interpretation came about because of the better fit of their data for this phase to a second order equation than to a single first-order process. It is not surprising that two first order processes can be better fitted by a second order process than by a single exponential. A fit of the second order equation to the slow phase gave slightly less systematic residuals (Figure IV.9a, 10a) than a fit by a single exponential (Figure IV.9b, 10b). However, a fit of the same data by two first order processes gave the smallest and most random residuals (Figure IV.9c, 10c).

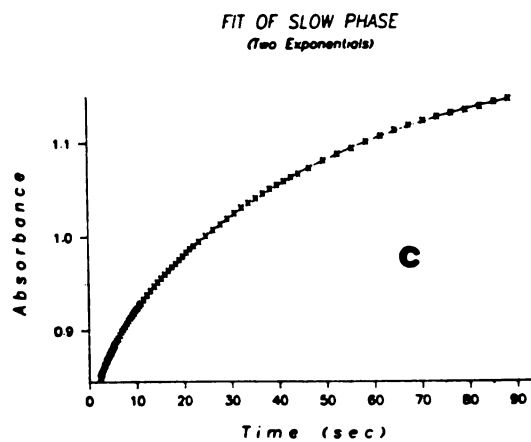
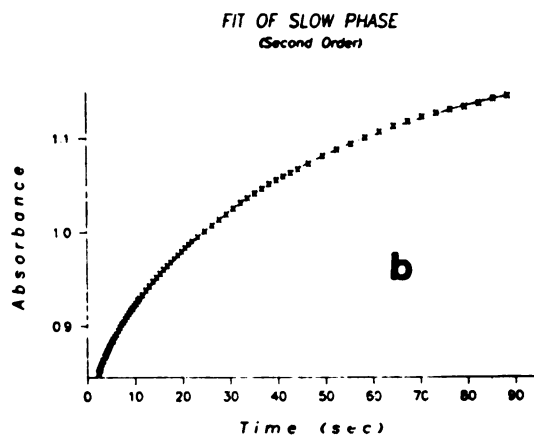
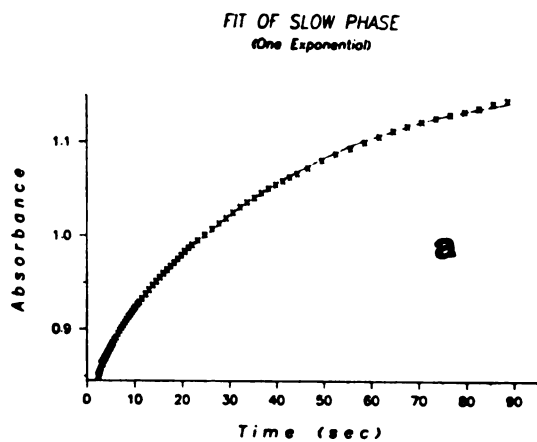
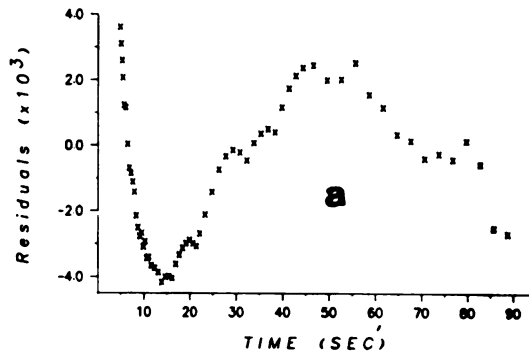
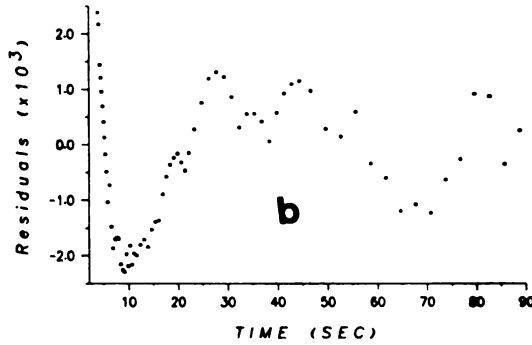


Figure IV.9.--Fit of the "slow phase" to one exponential (a); To a second order process,(b); and to two exponentials (c). Conditions are the same as in Figure IV.7.

RESIDUAL PLOT OF SLOW PHASE  
(One Exponential)



RESIDUAL PLOT OF SLOW PHASE  
(Second Order Equation)



RESIDUAL PLOT OF SLOW PHASE  
(Two Exponentials)

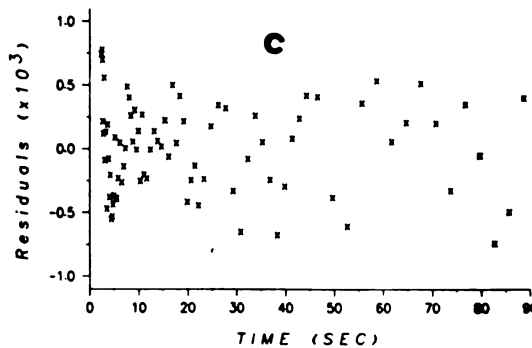


Figure IV.10.--Residual plots for the fit to the data in Figure IV.9.  
(a) One exponential, (b) Second order, and (c) Three exponentials.

In addition to inspecting the randomness of the residuals, the distinction between intermolecular (second order) and intramolecular (first order) electron transfer in the slow phase was tested by varying the enzyme concentration. Over more than a 4-fold range of protein concentration, a fit of the slow phase by a second order equation did not show the expected dependence of the rate on the protein concentration, whereas a two-exponential fit gave essentially the same first order rate constants over that range. Table IV.2 summarizes results of this study of the kinetics of the slow phase.

### C. Reduction of the Cyanide-Bound Cytochrome Oxidase

As mentioned in Chapter I, ligands such as HCN react with cytochrome  $a_3$  of the oxidase (and possibly with the copper associated with it; (Van Gelder and Muijsers, 1966). When bound to cyanide, the peak of the oxidized cytochrome  $a_3$  shifts from 414 to 428 nm in the Soret region, the result is a narrower absorption band for the oxidized CN- oxidase which peaks at 429 nm with an extinction coefficient greater than that of the native oxidized protein ( $180 \text{ mM}^{-1} \text{ cm}^{-1}$  for the CN- bound oxidase at 429 nm compared to  $160 \text{ mM}^{-1} \text{ cm}^{-1}$  at 420 nm for the native protein).

#### C.1 Spectral Shape Analysis

Figure IV.11 displays the spectral changes on mixing  $2.4 \mu\text{M}$  CN- oxidase with  $6.5 \mu\text{M}$  MPH (concentration after mixing). Note that the reaction is fast and that the reduced Soret peak of the oxidase does not grow to the same absorbance as in the case with the native protein, which is due to the fact that when complexed with HCN,

TABLE IV.2 -- Summary of kinetic studies on the "slow phase" of the reduction of cytochrome oxidase by MPH in HEPES buffer containing 0.5% Tween 20, pH = 7.4, T = 21 ± 1°C.

<u>aa<sub>3</sub></u>	-----Concentration, μM-----		-----Two Exponentials-----		---Second-Order---
	MPH	$k_1^s, s^{-1} \pm \sigma$	$k_2^s, s^{-1} \pm \sigma$	$k \times 10^{-4} M^{-1} s^{-1}$	
3.70	23.0	0.182 ± 0.009	0.0213 ± 0.0002	2.5	
3.34	8.4	0.13 ± 0.1	.0180 ± .0004	3.2	
2.00	23.0	.176 ± .005	.0208 ± .0002	5.8	
1.10	23.0	.209 ± .002	.0206 ± .0002	11.0	

## REDUCTION OF CN-OXIDASE BY MPH

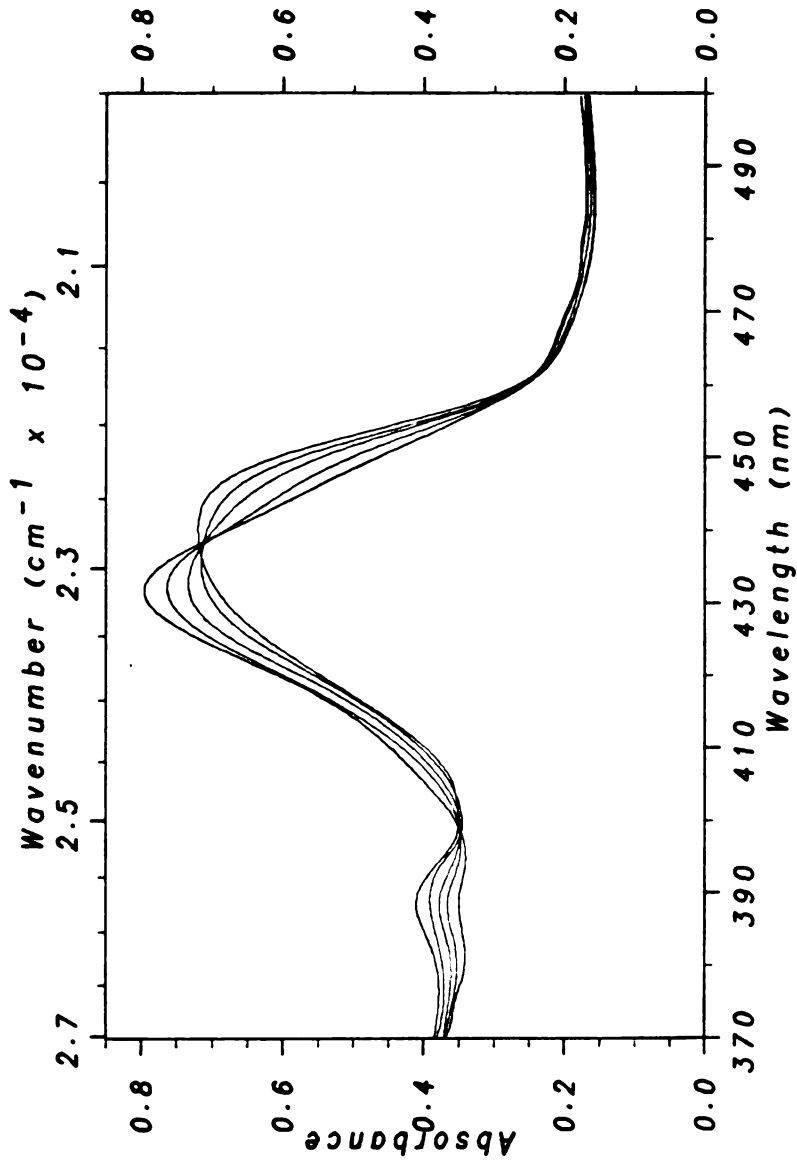
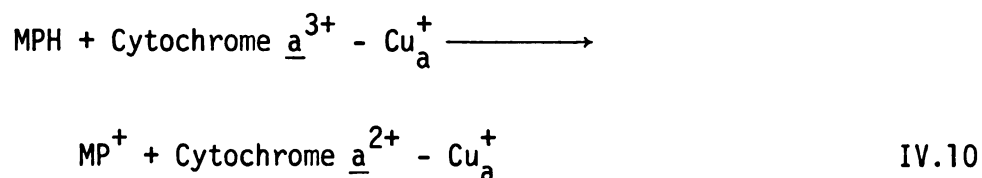


Figure IV.11.--Spectral changes that resulted on the reduction of 2.4  $\mu\text{M}$  CN-oxidase by 6.5  $\mu\text{M}$  MPH (concentrations after mixing). Times, in seconds, from top to bottom at 430 nm are: 0.018, 0.31, 0.71, 1.51, 22.9. Other conditions are the same as in Figure IV.1.

cytochrome  $\underline{a}_3^{3+}$  is not reducible. The spectra also show, by comparison of absorbance changes at 388 nm and 444 nm, that the stoichiometry of the reduction in the case is



The reduction of  $\text{Cu}_a$  ion is deduced because two electrons are provided to the oxidase - CN molecule from MPH, while only one electron is detected in the reduced heme band at 444 nm.

### C.2 Kinetics

The reduction of the CN-bound oxidase by MPH appears to be monophasic. Analysis of kinetic data obtained by fixed wavelength experiments at 430 nm (Figure IV.12a), 444 nm (Figure IV.12b) and 605 nm (Figure IV.12c) shows that the reaction is second order (first order in both reactants). Note that the rate of decay at 430 nm matches the rate of growth at 444 nm and 605 nm which is indicative that these changes are due only to the reduction of cytochrome  $\underline{a}$  of the oxidase. The residuals for the fits shown in Figures IV.12a to IV.12c are small and random and indicate that a second order process describes these data. Table IV.3 summarizes the results obtained for this reaction. The rate of this reduction is essentially identical to that of the initial phase of the reduction of the native oxidase by MPH, which implies that MPH reduces cytochrome  $\underline{a}$  (and its associated copper) in the initial phase.

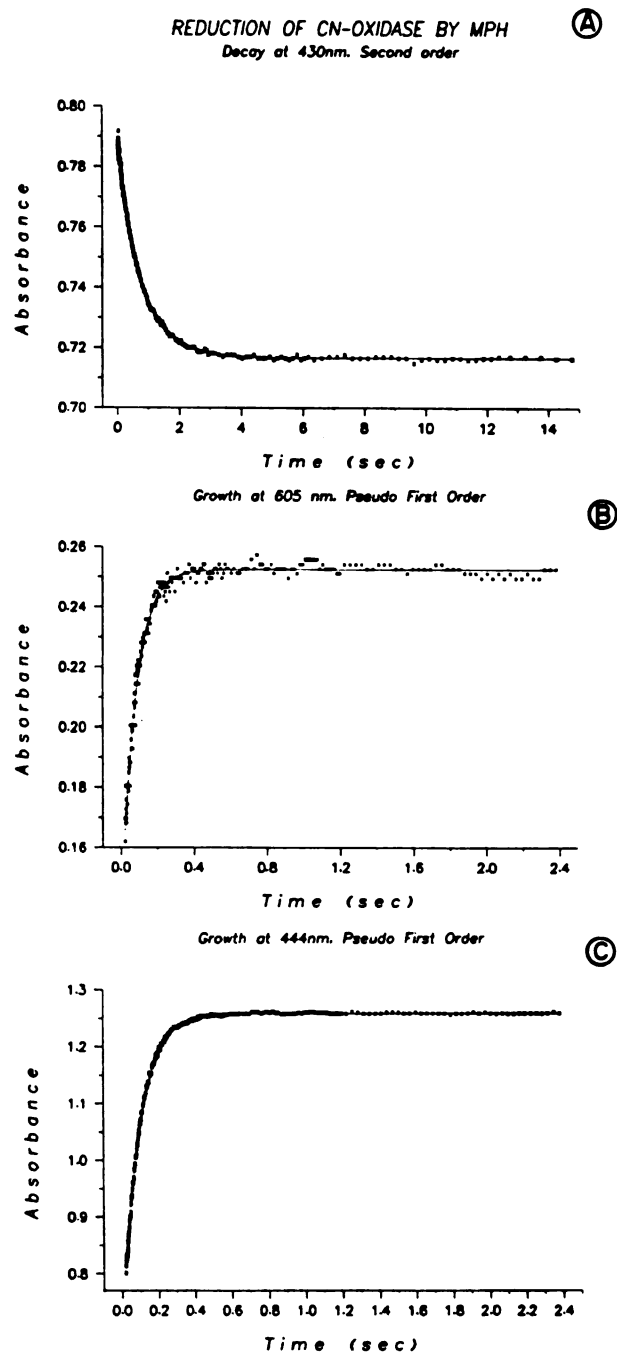


Figure IV.12.--Time courses for the reduction of the CN-oxidase by MPH followed at 430 nm (A), 605 nm (B) and at 444 nm (C). Concentrations of CN-oxidase and MPH in  $\mu\text{M}$  are: (A) 2.4 and 6.5, (B) and (C) 4.8 and 42.5. respectively. Data are collected in fixed-wavelength mode. X's are experimental points and solid lines are the calculated curves.

TABLE IV.3 -- Rate constant for the reduction of the cyanide-bound cytochrome oxidase by MPH in 0.05 M HEPES buffer, pH = 7.4 at  $21 \pm 1^\circ\text{C}$ . Data are collected in fixed-wavelength experiments.

wavelength, nm	[aa <sub>3</sub> ], μM	[MPH], μM	k' ± σ <sup>a</sup>	k (×10 <sup>-5</sup> ), M <sup>-1</sup> s <sup>-1</sup>
430	2.4	6.5	1.16 ± 0.03 <sup>b</sup>	2.8
444	4.8	42.5	10.45 ± 0.05 <sup>c</sup>	2.4
605	4.8	42.5	12.6 ± .2 <sup>c</sup>	3.0
				Average = 2.7 ± .3

<sup>a</sup>Marginal standard deviation.

<sup>b</sup>k' from Equation IV.7.

<sup>c</sup>Pseudo first order rate constant k' = k[MPH].

The data presented here are distinct from those reported by Scott and Gray (1980) on reduction of the CN-oxidase complex by ruthenium (II) hexaamine, in which they observed biphasic kinetics. A possible resolution of this apparent discrepancy may lie in the fact that  $[\text{Ru}(\text{NH}_3)_6]^{2+}$  is a positively charged one-electron donor, so that addition of two electrons to the CN-bound oxidase may require the dissociation of an electrostatically formed complex between  $[\text{Ru}(\text{NH}_3)_6]^{3+}$  and the negatively charged cytochrome a site. Such a situation could lead to biphasic kinetics. An alternative explanation for the observed biphasicity would be the outer sphere electron transfer from  $[\text{Ru}(\text{NH}_3)_6]^{2+}$  to the "bound"  $[\text{Ru}(\text{NH}_3)_6]^{3+}$ . MPH, on the other hand, is a two electron donor (See Chapter III), and even in the case of a one-electron radical formation, it probably remains bound to the cytochrome a site for a second electron addition after the redox equilibration between cytochrome a and its associated copper; alternatively the free radical may donate directly to the  $\text{Cu}_a$ .

#### D. Conclusions

MPH, a neutral molecule, as well as positively charged metal ion complexes such as  $[\text{Cr}(\text{H}_2\text{O})_6]^{2+}$  (Greenwood et al., 1977) and  $[\text{Ru}(\text{NH}_3)_6]^{2+}$  (Scott and Gray, 1980), reduce preferentially the cytochrome a site of the oxidase. These reductants can thus be used as artificial donors that imitate the biological substrate, cytochrome c. For kinetic studies, particularly for those in which the scanning stopped-flow technique is used, MPH has an advantage over the above mentioned metal ion complexes. As MPH oxidizes,  $\text{MP}^+$  forms with a

characteristic peak at 388 nm, which has a suitable extinction coefficient, so that absorbance changes at this wavelength can be used to monitor the extent of the reduction as well as to measure the concentration of oxygen, if present. The ability of MPH to react with oxygen is important in testing for anaerobicity and in studying turnover experiments, where one can quantitatively measure the number of turnovers.

Our data on kinetics at the near I.R. region (830 nm) show that the Cu component lags in the anaerobic reduction with respect to the cytochrome a iron. These data agree with observations by Wilson et al. (1975) who showed that, during the reduction of the oxidase by cytochrome c in the presence of oxygen, the bleaching of the 830 nm band either lagged or coincided with the growth at 605 nm, depending on the reductant concentration. Our data are also in agreement with rapid-freeze EPR experiments (Hartzell et al., 1975) which show rapid equilibration between cytochrome a and its associated copper, Cu.

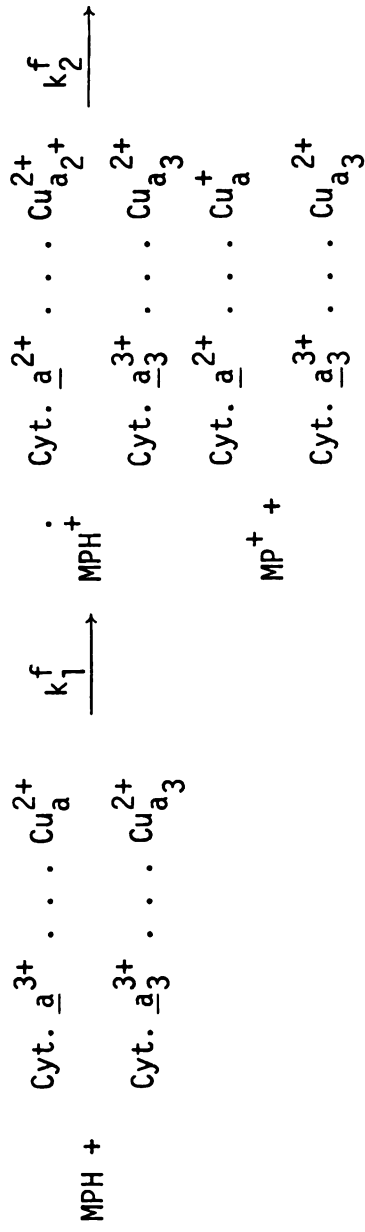
The present work, however, appears to be in disagreement with experiments on the anaerobic reduction of the oxidase by cytochrome c (Andreasson et al., 1972), in which the 830 nm decay did not show a detectable lag relative to the 605 nm growth. Since the second order rate constant for the reduction of the oxidase (cytochrome a) by cytochrome c ( $\sim 10^8 \text{ M}^{-1} \text{ s}^{-1}$ , Gibson et al., 1965) is much faster than that by MPH ( $3 \times 10^5 \text{ M}^{-1} \text{ s}^{-1}$ , present work), it appears likely that approximately one-half of the cytochrome a had been reduced during the

dead time in the reduction by cytochrome c (~5 ms under the conditions described by Andreasson et al., 1972). This is comparable to the dead time in a typical stopped-flow apparatus. Extrapolating the absorbance at 830 nm to zero-time would then obscure any lag which could have occurred, and one would observe a "parallel" reduction of the copper and iron of cytochrome a. Incidentally, these authors interpreted the absence of a lag at 830 nm by proposing that cytochrome a must contribute to the absorbance at this region. This latter conclusion is at odds not only with our own stopped-flow results, but also with a number of equilibrium titration experiments which have been carried out subsequent to the Andreasson et al. (1972) stopped-flow work. The consensus opinion from these experiments is that  $Cu_a$  is the principal absorber at 830 nm and that there is negligible contribution to this feature from either cytochrome a or a<sub>3</sub>.

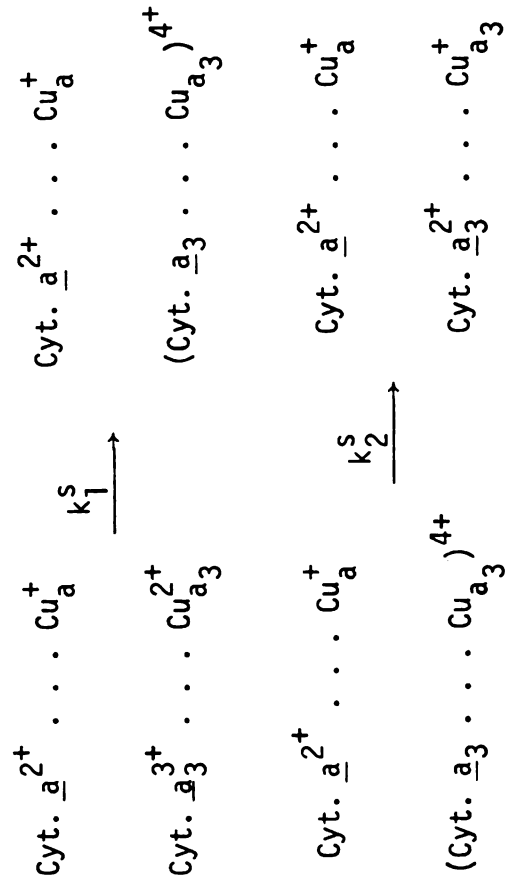
The presence of three distinct phases in the anaerobic reduction of the oxidase by MPH can be interpreted in more than one way. The fast initial phase, which is a second order process, accounts for about 50% of the total absorbance changes at 444 nm and 80% of the change at 605 nm. These observations, along with the fact that on binding to cyanide, the rate constant of the fast phase remains essentially unchanged, suggest that the fast phase monitored at 444 or 605 nm can be assigned to the reduction of the cytochrome a site and its associated copper by MPH. The second phase, a first order process with a rate constant of about  $0.2 \text{ s}^{-1}$  contributed only about 10% of the total changes at 444 nm, with the third phase accounting

for the rest of the changes. One way to interpret these observations is by the scheme represented below (Equations IV.11 - IV.13), which takes into account the negative cooperativity between the two iron centers of the oxidase (Leigh et al., 1974; Babcock et al., 1978).

Another explanation of the observed multiphasic kinetics is that it may be due to heterogeneity in the enzyme preparation. In a recent study, Brudvig et al. (1981) have shown that the oxidized oxidase can exist in at least three conformations, depending on the method of preparation used and whether the protein was subjected to any catalytic cycles.



IV.11



IV.12



IV.13

## CHAPTER V

### PRINCIPAL COMPONENT ANALYSIS OF THE REDUCTION OF CYTOCHROME c OXIDASE BY MPH

#### A. Introduction

Optical absorption spectroscopy has been of fundamental importance in the characterization of cytochrome c oxidase (see Lemberg, 1969). The protein spectrum has peaks in the near UV, visible, and near IR regions that are sensitive to the oxidation and ligation states of its four metal centers. The absorption spectra of cytochromes a and a<sub>3</sub> of the oxidase overlap strongly in the Soret and  $\alpha$ -bands. Also, in these two regions absorbance changes due to the oxidase copper centers may be obscured owing to the relatively small extinction coefficient expected for copper complexes compared to those of the heme moieties (Malmstrom, 1970). The classical a a<sub>3</sub> picture of the oxidase, including assignments of wavelength and extinction coefficients for the two hemes (Vanneste, 1966) has been rather widely accepted. It was argued (Caughey et al., 1976), however, that it is unwise to synthesize spectra of cytochromes a and a<sub>3</sub> on the assumption that the properties of one heme are not affected by changes in the oxidation or ligation states of the other metal components, since there is strong evidence for electron and magnetic interactions between the metal components of the oxidase (Hartzell et al., 1973; Babcock et al., 1978).

We have used data obtained by rapid scanning stopped-flow spectrophotometry to resolve the individual spectra of cytochromes  $a$  and  $a_3$  by the method of principal component analysis (PCA). In the scanning wavelength experiments described here, a selected wavelength region is rapidly and repeatedly scanned as a function of the time after mixing of the "scan." The result is a  $p \times N$  data matrix  $A$  composed of  $N$  consecutive spectra (essentially instantaneous if the time of scan is short compared to the half-time of the reactions studied), measured at  $p$  wavelength channels. There are good reasons for sampling this three dimensional space of absorbance-wavelength-time in the study of the kinetics of cytochrome oxidase instead of the two-dimensional space obtained in fixed-wavelength experiments; they are the need to characterize the kinetics of the strongly interacting components of the oxidase and to separate the contributions to the spectra of species with overlapping absorption bands.

#### B. The Method of Principal Component Analysis (PCA)

Data in the form of the matrix  $A$ , described above, are suitable for the application of principal component analysis (PCA), also known as principal factor analysis (PFA) (see, for example, Malinowski and Howery, 1980). Although PCA is used for a wide range of physical techniques (Sylvestre et al., 1974; Bulmer and Shurvell, 1975; Valasdi, 1974; Ritter et al., 1976), only its application to scanning stopped-flow data is briefly discussed here. The method is discussed in detail in the Ph.D. dissertation of R. Cochran (1977, MSU; see also Cochran and Horne, 1977; 1980; Cochran et al., 1980). A block diagram

of the main steps in factor analysis is shown in Figure V.1. PCA, if applied to suitably weighted data, can give the number of components (absorbers) in the system and, in favorable cases, can provide complete resolution of the absorbers' spectra and their time courses. The weighting scheme is discussed in Section B.1.1. PCA does not require any mechanistic assumptions. The only assumption required is that the absorbance at every wavelength channel be a linear function of the concentration of the absorbing species (Beer's law). In other words, the element  $A_{ij}$  (absorbance at wavelength channel  $i$  at time of scan  $j$ ) of the matrix  $\underline{A}$  is represented as

$$A_{ij} = \sum_{k=1}^q f_{ik} c_{kj} \quad \text{V.1}$$

where  $f_{ik}$  is the molar absorptivity (times the path length of the absorbance cell) of absorber  $k$  at wavelength channel  $i$ ,  $c_{kj}$  is the molarity of  $k$  at time of scan  $j$ , and  $q$  is the number of absorbers. Accordingly, the matrix  $\underline{A}$  can be "factored out" into two matrices, one of which describes the spectral shapes of the absorbers ( $\underline{F}$  matrix), while the other contains information on the concentration as a function of time, ( $\underline{C}$  matrix); Equation V.2

$$\underline{A} = \underline{F} \underline{C}^T = \sum_{k=1}^q \underline{f}_k \underline{c}_k^T \quad \text{V.2}$$

where  $\underline{F}$  is a  $(p \times q)$  matrix defined by  $\underline{F} = (\underline{f}_1, \underline{f}_2, \dots, \underline{f}_q)$ . The vector  $\underline{f}_j$ , called the static spectrum of absorber  $j$ , is a  $p$

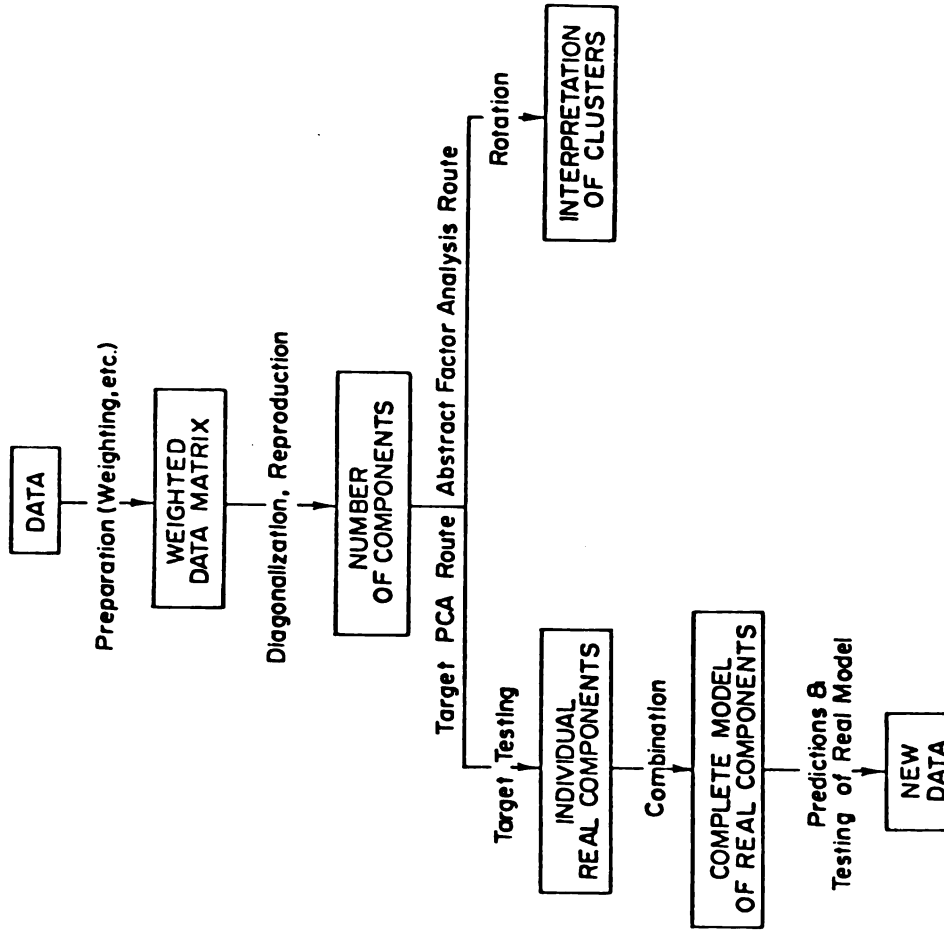


Figure V.1.--Block diagram for main steps in factor analysis (from Malinowski and Howery, 1980; with modifications).

component column vector whose ith element is the product of the cell path length and the molar absorptivity of absorber j at wavelength channel i.  $\underline{C}$  is defined by  $\underline{C} = (\underline{c}_1, \underline{c}_2, \dots, \underline{c}_q)$ , where  $\underline{c}_j$ , the concentration vector of absorber j, is an N-component column vector whose ith element is the molarity of absorber j at the time of scan i.

### B.1 Preparation Steps

The preparation steps for PCA involve, as the major part, the proper weighting of the matrix  $\underline{A}$ . The ultimate success or failure of PCA may depend on these steps.

B.1.1 Weights for principal component analysis.--In an errorless experiment, the weights are not needed and the matrix  $\underline{A}$  could be used as is for M and/or S analysis. Errors in laboratory experiments, however, must be considered in order for PCA to give correct results. Improper weights can lead to erroneous estimates of the number of absorbing species (Cochran and Horne, 1977). Equation V.2 thus becomes

$$\underline{A} = \underline{F} \underline{C}^T + \underline{\epsilon} \quad \text{V.3}$$

Noise in absorbance measurements obtained by the scanning stopped-flow apparatus used in this study can be traced to two factors: (1) A time dependent factor which is minimized by signal averaging, and (2) A position dependent component which depends on the position of a channel in the spectrum and its nominal absorbance.

Thus, the element  $i, j$  of  $\underline{\epsilon}$ ,  $\text{var}(e_{ij})$  which is assumed to have an expected value of zero, can be written in the form of Equation V.4 (Cochran and Horne, 1977).

$$\text{Var}(e_{ij}) = X_i Z_j \quad \text{V.4}$$

where  $Z_j$  is a function of the spectrum (group) number and  $X_i$  is a function of the wavelength channel number. This model for variance leads to a statistically weighted matrix  $\underline{A}$ , defined as

$$\underline{A}_w = \underline{L} \underline{A} \underline{T} \quad \text{V.5}$$

where  $\underline{L} = \text{diag}(l_1, l_2, \dots, l_p)$  and  $\underline{T} = \text{diag}(t_1, t_2, \dots, t_p)$ . As pointed out by Cochran and Horne (1977), the elements of  $\underline{L}$  and  $\underline{T}$  are given by:

$$\underline{L} = \underline{X}^{-\frac{1}{2}} a^{-\frac{1}{2}} \quad \text{V.7}$$

$$\underline{T} = \underline{Z}^{-\frac{1}{2}} b^{-\frac{1}{2}} \quad \text{V.8}$$

where  $a$  and  $b$  are arbitrary constants (set = 1) and  $X$ 's and  $Z$ 's are defined by Equation V.4.

As discussed thoroughly by Coolen (1975),  $Z_j$  depends on the nature of any on-line averaging procedure and becomes smaller at longer times of data collection when averaging is performed. In terms fully defined by Coolen et al. (1975),  $Z_j$  is given by Equation V.9.

$$Z_j = g^{(1-n_j)} \quad \text{V.9}$$

where  $g$  is the grouping factor (modulus for increasing the averaging) and  $n_j$  is the stored group number.

The  $X_i$  contribution, however, needs more consideration. The correct  $X_i$  should account for three major noise contributions to the absorbance at channel  $i$ : (1) The wavelength corresponding to this channel (this is mainly a photomultiplier tube noise); (2) the actual value of the absorbance, and (3) the rate of change of absorbance with wavelength at the particular channel being considered. The third contribution originates from errors in the precise wavelength reproducibility at each channel caused by mechanical vibrations of the mirror system used.

A method to calculate the values of  $X_i$  for each channel uses two scanning experiments which represent the major reactant chromophore(s) and those of the final products (with no reactions occurring in either experiment). These two "weight" experiments must be collected with the same scanning parameters used for the reaction under study (i.e., same wavelength region and number of points per spectrum), but without averaging. An average weight is then calculated from the standard deviations in each weight experiment for every wavelength channel.

The reason for adopting this method instead of using a flat absorber (e.g., a neutral density filter) originates from a consideration of the characteristics of the scanning monochromator used in this study. If a chromophore has a sharp peak, the "sides" of the peak are found to have the highest measurement errors since they are most sensitive to irreproducibility in the scan synchronization and to scanning

mirror mechanical artifacts. The method for calculating weights discussed here should be a good approximation for reactions that do not produce intermediates with spectral peaks which are greatly different from those of the reactants or products.

B.1.2 M and S analyses.--Cochran and Horne (1977) have shown that two kinds of PCA are useful for kinetic experiments; each requires only the matrix  $\underline{A}$  (or  $\underline{A}_w$ ) and each gives a lower bounds estimate of  $q$ . Second moment matrix PCA, called M analysis, gives for  $q$  a lower bounds estimate that is required to interpret the experiment.  $\underline{M}$  (and  $\underline{M}_w$ , which is used for statistically weighted PCA) are defined by

$$\underline{M} = \frac{1}{N} \underline{A} \underline{A}^T \quad \text{V.10}$$

and

$$\underline{M}_w = \frac{1}{N} \underline{A}_w \underline{A}_w^T \quad \text{V.11}$$

Sample covariance matrix PCA, or S analysis, gives the number of independent absorbers whose concentrations change during the experiment.  $\underline{S}$  and  $\underline{S}_w$  are defined by

$$\underline{S} = \frac{1}{N-1} (\underline{A} - \bar{\underline{A}}) (\underline{A} - \bar{\underline{A}})^T \quad \text{V.12}$$

$$\underline{S}_w = \frac{1}{N-1} (\underline{A}_w - \bar{\underline{A}}_w) (\underline{A}_w - \bar{\underline{A}}_w)^T \quad \text{V.13}$$

where  $\bar{A}_{jk} = \frac{1}{N} \sum_{j=1}^N A_{jk}$  V.14

The  $\underline{M}$  and  $\underline{S}$  analyses estimates of  $q$  are not necessarily the same. The rank of  $\underline{M}$ ,  $m$ , is the same as that of  $\underline{A}$ . Also, the rank of  $\underline{S}$  is the same as  $(\underline{A} - \overline{\underline{A}})$ , (Bellman, 1970). Details and rules for the ranks of  $\underline{M}$  and  $\underline{S}$  are discussed by Cochran and Horne (1977).

## B.2 Number of Components

As mentioned earlier, the rank of  $\underline{M}$  gives a lower bound estimate of the number of detectable components,  $m \leq q$ .  $m$  is determined by diagonalizing  $\underline{M}$ , which is done by solving the eigenvalue problem.

$$\underline{M}\phi = \phi\underline{\Delta} \quad \text{V.15}$$

where  $\underline{\Delta}$  is the eigenvalue matrix,

$$\underline{\Delta} = \text{diag} (\delta_1, \delta_2, \dots, \delta_p) \quad \text{V.16}$$

and  $\phi$  is a  $(p \times p)$  matrix whose columns are the orthonormal eigenvectors:

$$\underline{\phi}_i \underline{\phi}_j = 1 \quad \text{if } i = j$$

$$\underline{\phi}_i \underline{\phi}_j = 0 \quad \text{if } i \neq j$$

The essential rank,  $m$ , can be determined in two ways:

1.  $m$  is equal to the number of non-zero eigenvalues in Equation V.16;  $\delta_1, \delta_2, \dots, \delta_m$ . In an errorless experiment, this criterion is exact. The effect of random measurement errors, however, makes  $\underline{M}$  (and  $\underline{S}$ ) of full rank ( $p$  or  $N$ , depending on which is smaller). In other words, the eigenvalues in Equation V.16 become all

non-zero. For statistically weighted PCA, the weighted sum of the squares of the residuals, defined by Equation V.17 gives the condition for the value of  $r$  that equals  $m$ .

$$Q_r = \sum_{i=1}^p \sum_{j=1}^N L_i T_j (\hat{A}_{ij}(r) - A_{ij})^2 \quad \text{V.17}$$

where  $\hat{A}(r)$  is defined in Equation V.18.

When  $r = m$ , the value of the function  $Q_r/(N-r)(p-r)$ , should be approximately unity (Cochran and Horne, 1977).

2. The second method is to reconstruct a matrix  $\hat{A}(r)$ , which is a reproduction of the experimental data matrix  $A$ . For an errorless experiment,  $m$  is the lowest value of  $r$  for which

$$\hat{A}(r) = \Phi(r) \Phi^T(r) A \quad \text{V.18}$$

is exactly equal to  $A$ , where  $\Phi(r)$  is the  $(p \times r)$  matrix whose columns are the first  $r$  eigenvectors of  $M$ . For an actual experiment  $m$  is determined by finding the lowest value of  $r$  for which  $\hat{A}(r)$ , now defined by Equation V.19 (Cochran, 1977), fits the experimental matrix  $A$  to within its random errors

$$\hat{A}(r) = L^{-1} \Phi(r) \Omega(r) \Psi^T(r) T^{-1} \quad \text{V.19}$$

where

$$\begin{aligned} \Omega(r) &= \text{diag} (w_1, w_2, \dots, w_r) \\ w_j &= (N \delta_j)^{\frac{1}{2}} \end{aligned} \quad \text{V.20}$$

and

$$\underline{\Psi}(r) = (\underline{\psi}_1, \underline{\psi}_2, \dots, \underline{\psi}_r) = \underline{\Omega}(r)^{-1} \underline{A}_w^T \underline{\Phi}(r) \quad \text{V.21}$$

where the columns of  $\underline{\Psi}(r)$  contain the first  $r$  eigenvectors of  $\underline{M}'_w$ , defined by

$$\underline{M}'_w = \frac{1}{P} \underline{A}_w^T \underline{A}_w.$$

When  $r$  in equation V.19 (which is now the least squares estimate of  $m$ ) is equal to  $m$ , one can examine the residual surface  $\hat{\underline{A}}(r) - \underline{A}$ , which should be random (see below).

### B.3 PCA Determination of Real Components

PCA provides a means by which to test whether a proposed spectral shape (or a concentration profile) fits as one of the columns vectors of the  $\underline{F}$  and  $\underline{C}$  matrices (Equation V.2). This is called "Target Testing" (Malinowski and Howery, 1980). From Equation V.2 and V.19

$$\hat{\underline{A}}(m) = \hat{\underline{F}} \hat{\underline{C}}^T = \underline{L}^{-1} \underline{\Phi}(m) \underline{\Omega}(m) \underline{\Psi}(m)^T \underline{T}^{-1} \quad \text{V.22}$$

solving for  $\hat{\underline{F}}$

$$\hat{\underline{F}} = (\underline{L} \underline{\Phi}(m)) \underline{U} \quad \text{V.23}$$

where  $\underline{U}$  is an  $(m \times m)$  matrix defined by

$$\underline{U} = \underline{\Omega}_{(m)} \underline{\Psi}_{(m)}^T \underline{T}^{-1} \underline{\hat{C}} (\underline{\hat{C}}^T \underline{\hat{C}})^{-1} \quad \text{V.24}$$

similarly from V.19

$$\underline{\hat{C}} = (\underline{T}^{-1} \underline{\Psi}_{(m)}) \underline{V} \quad \text{V.25}$$

where  $\underline{V}$  is an  $(m \times m)$  matrix defined by

$$\underline{V} = \underline{\Omega}_{(m)} \underline{\Phi}_{(m)}^T \underline{L}^{-1} \underline{\hat{F}} (\underline{\hat{F}}^T \underline{F})^{-1} \quad \text{V.26}$$

From V.19, 23, 25

$$\underline{U} \underline{V}^T = \underline{\Omega}_{(m)} \quad \text{V.27}$$

It follows from Equations V.23 - 27 that if  $m$  elements of either  $\underline{U}$  or  $\underline{V}$  are known, then both  $\underline{\hat{F}}$  and  $\underline{\hat{C}}$  can be determined. Furthermore, by partitioning  $\underline{U}$  and  $\underline{V}$ :

$$\underline{U} = (\underline{u}_1, \underline{u}_2, \dots, \underline{u}_m) \quad \underline{V} = (\underline{v}_1, \underline{v}_2, \dots, \underline{v}_3) \quad \text{V.28}$$

where  $\underline{u}_j$  and  $\underline{v}_j$  are  $m$  component column vectors.

Equations V.23 and V.25 become respectively

$$\underline{\hat{f}}_j = (\underline{L}^{-1} \underline{\Phi}_{(m)}) \underline{u}_j \quad j = 1, 2, \dots, m \quad \text{V.29}$$

$$\underline{\hat{c}}_j = (\underline{T}^{-1} \underline{\Psi}_{(m)}) \underline{v}_j \quad j = 1, 2, \dots, m \quad \text{V.30}$$

In Equation V.29, we see that every spectral shape (or concentration profile) that fits, within the least squares conditions, as one of the components provides  $m$  elements of  $\underline{U}$  or  $\underline{V}$ .

Equations V.29 and V.30 can then be used as models against which suspected static spectra or kinetic profiles can be tested. Cochran and Horne (1980) presented the least squares criterion for determining whether a suspected absorber fits as one of the  $m$  linearly independent absorbers. Finding all the  $m$  absorbers (or their  $m$  concentration profiles) thus completely resolves the problem. The application of the steps summarized above on the reduction of cytochrome oxidase by MPH is discussed below.

### C. Principal Component Analysis of the Reaction of Cytochrome Oxidase by MPH

The characteristics of this reaction are discussed in Chapter IV. PCA was performed on data collected in two overlapping wavelength regions and with two forms of the oxidized protein; the resting enzyme (absorption maximum at 418 nm) and the so-called oxygenated enzyme (absorption maximum at 424 nm in the oxidized protein). The two wavelength regions were chosen for reasons of optimum resolutions of spectral peaks.

#### C.1 PCA on the Reduction of the Resting Enzyme by MPH (Wavelength Region 330-520 nm)

In the wavelength region from 330 - 520 nm, the data should contain information on the spectral shapes and kinetic profiles of the reduced and oxidized cytochromes  $a$  and  $a_3$  of the oxidase in the Soret region as well as those of the MPMS/MPH couple (see Chapters III and IV). We here describe the steps taken to resolve the independent components in this region.

C.1.1 Number of absorbers.--It should first be emphasized here that the term absorber may in fact refer to several species that are not independent in their concentration-time profiles (in M analysis), rates (S analysis), or spectral shapes (in M and S analyses). Figure V.2 presents the three dimensional wavelength-time-absorbance experimental surface obtained on mixing 3.78  $\mu\text{M}$  cytochrome oxidase anaerobically with 8.4  $\mu\text{M}$  MPH. Principal component analysis surfaces were reconstructed (Equation V.19) for  $r$  values from 1 to 5. Visual comparisons of the reconstructed surfaces with the experimental data showed that the surface was quantitatively reproduced by three absorbers. Figure V.3 shows the reconstructed surface for  $r = 3$  (this is to be compared with Figure V.2). For the sake of comparison, the reconstructed surface with two eigenvectors ( $r = 2$ ) is displayed in Figure V.4. The latter does not reproduce the experimental surface.

The residual surface ( $\hat{A}_r - A$ ) which should be random at  $r = m$  confirms the assignment of  $r = 3$ . In Figure V.5, the residual surface is shown for  $r = 3$ . The residuals constructed by using two eigenvectors are shown in Figure V.6. Note that the residuals in Figure V.5 are small and fluctuate around zero; i.e., random. Another piece of evidence for the assignment of  $r = 3$  is that the values of the function  $Q_r / (N-r)(p-r)$  were 722,12 and 2.1 for  $r = 1, 2,$  and 3, respectively. The results mentioned above were obtained for two experiments (pushes) for this wavelength region.

There are six predicted chromophores that are light absorbing in this wavelength region. These are the cytochromes  $\underline{a}^{3+}$ ,  $\underline{a}^{2+}$ ,

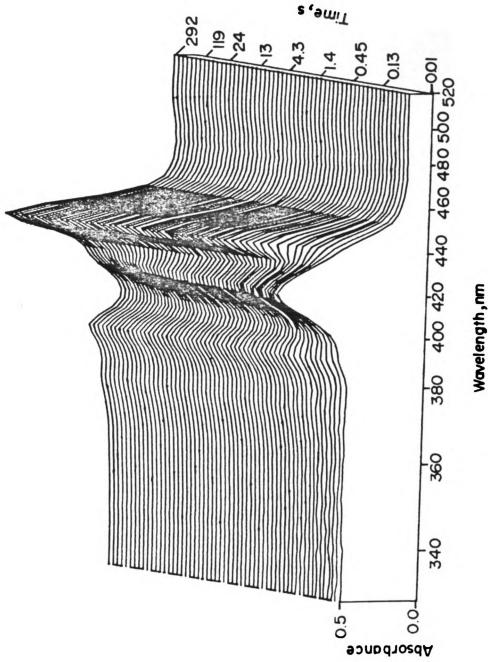


Figure V.2.--Experimental absorbance-wavelength-time surface for the anaerobic reduction of 3.78  $\mu\text{M}$  cytochrome oxidase by 8.4  $\mu\text{M}$  MPH. The data consisted of 60 wavelength "channels" and 56 scans. Medium was 50 mM HEPES containing 0.5% Tween 20, pH = 7.4. Cell path length = 1.85 cm; T = 21°C.

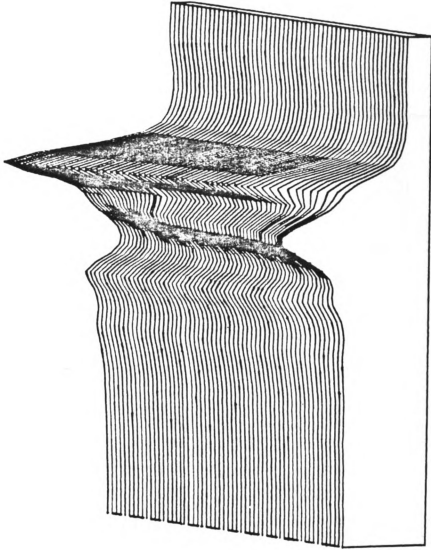


Figure V.3.---Principal component analysis (PCA) reconstructed surface using three eigenvectors in M-analysis. This figure is to be compared with the surface presented in Figure V.2.

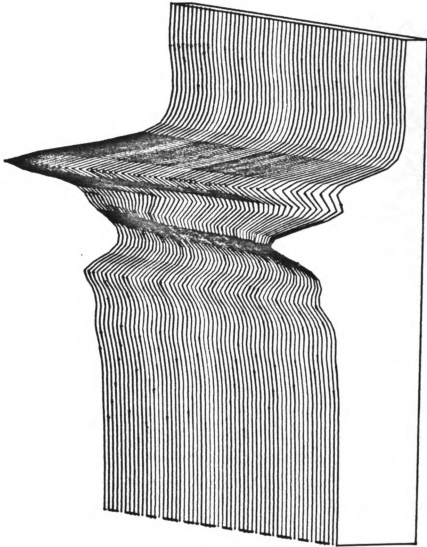


Figure V.4.--Reconstructed surface using only two M-analysis eigenvectors for the data in Figure V.2.

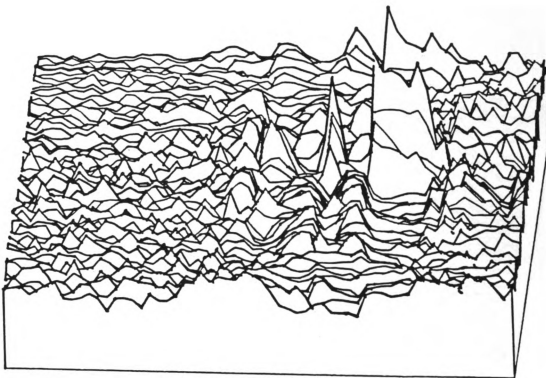


Figure V.5.--Residual surface  $(\hat{A}_{(3)}-A)$ , resulting from subtracting the matrix in Figure V.3 from the data in Figure V.2.  $\hat{A}_{(3)}$  refers to a reconstructed matrix in which 3-eigen-vectors were used,  $A$  is the experimental surface.

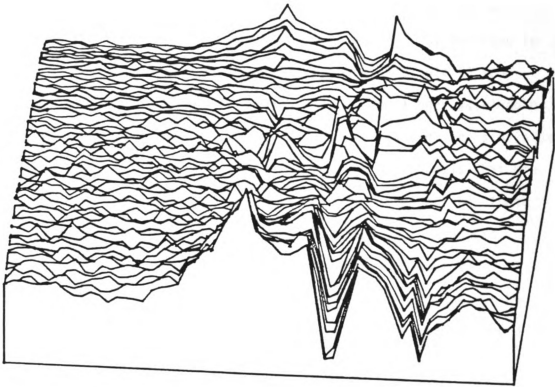


Figure V.6.--Residual surface  $(\hat{A}_{(2)} - A)$ .

$\underline{a}_3^{3+}$ ,  $\underline{a}_3^{2+}$  and MPMS and MPH. The absorbance changes due to MPH oxidation are very small compared to those of the heme moieties, and are also coupled to the reduction of the two cytochromes, since the concentrations were close to the stoichiometric ration (2 MPH: 1 Cytochrome oxidase, see Chapter IV). MPMS growth should also be coupled to the growth of the reduced heme bands. Because of limited wavelength resolution in the region of the Soret bands of the reduced enzyme and the fact that the region of the  $\alpha$ -band was not included in this experiment, the two reduced heme bands were difficult to separate, although they could be easily resolved in the longer wavelength region (Section C.2). The reduced resolution arises from the sinusoidal nature of the spread of the wavelength "channels." Channels that are near the beginning or the end of scan are closer together than those in the middle. In this experiment the Soret band of the reduced enzyme was near the middle of the scan (see Figure V.7 - V.9).

The three independent "absorbers" in this experiment can be identified as oxidized cytochromes  $\underline{a}$  and  $\underline{a}_3$  (together with MPH) and the spectrum containing the reduced heme band(s) and the MPMS (oxidized) spectral shapes. The latter composite spectrum is actually the last spectrum (scan) collected in the experiment (called the infinity spectrum).

C.1.2 Spectra of individual absorbers.--Making use of the assignments discussed above for the suspected absorbers, we try to fit these absorbers by the  $\underline{M}$  analysis eigenvectors. It is worth mentioning here that even when only a limited wavelength region is used for the

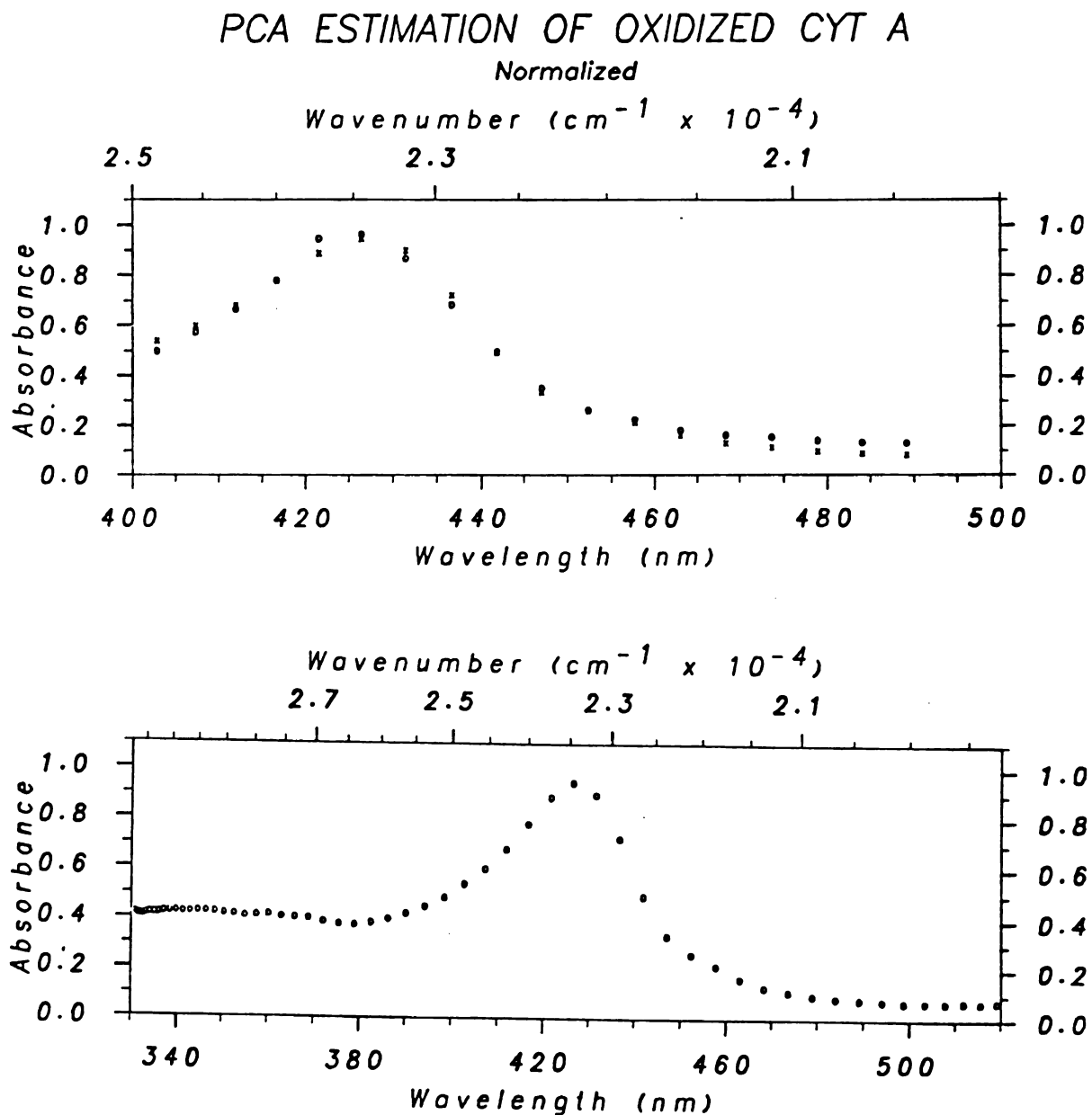


Figure V.7.--(a) M-analysis fit of oxidized cytochrome a spectra from the data presented in Figure V.2. X's are the proposed spectrum and O's are the estimated points. Three eigenvectors were used for this fit. (b) Estimated spectrum of cytochrome a for the entire wavelength region of the experiment presented in Figure V.2.

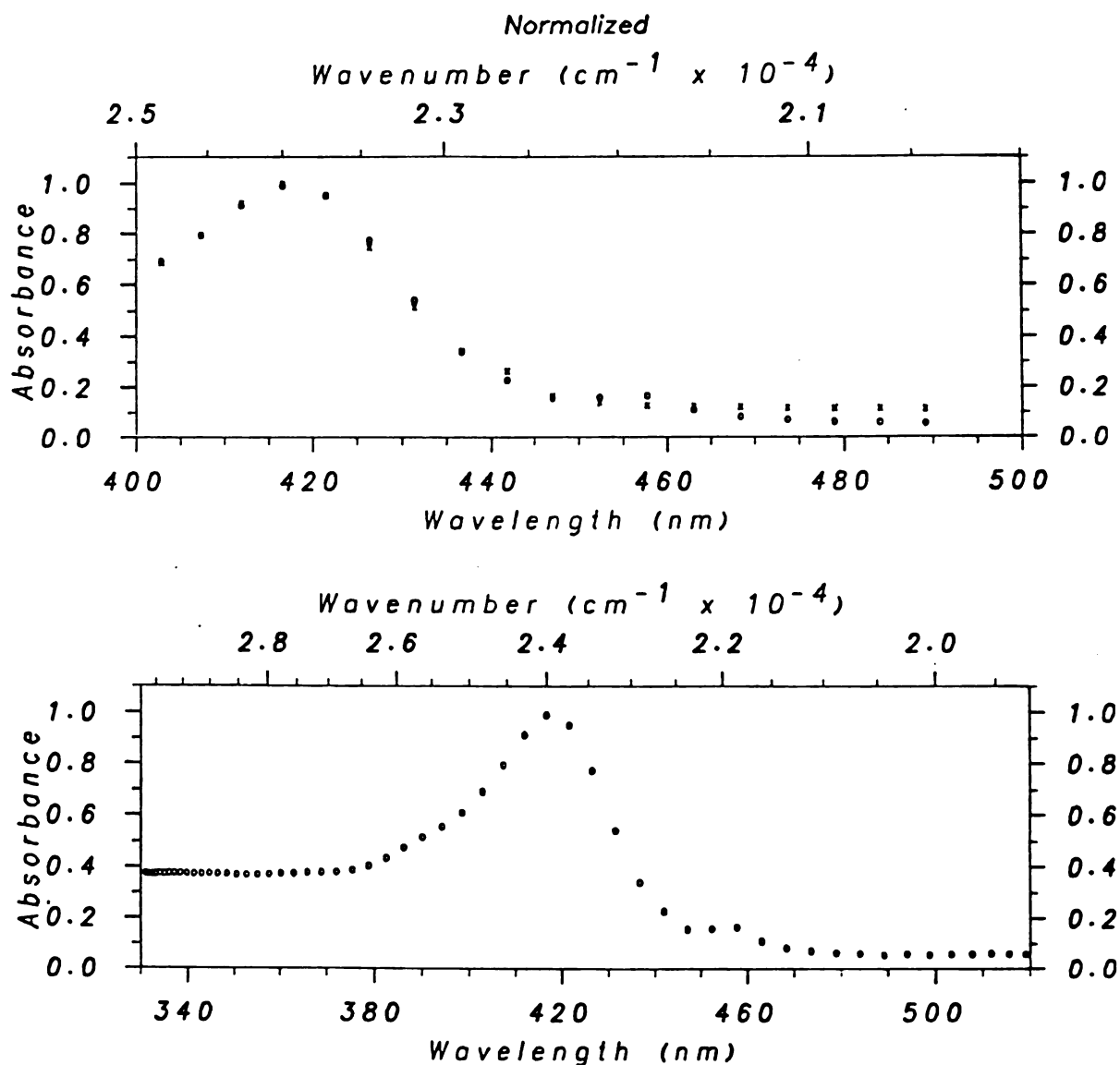
PCA ESTIMATION OF OXIDIZED CYT A<sub>3</sub>

Figure V.8.--(a) M-analysis fit of oxidized cytochrome a using three eigenvectors. X's: Proposed spectrum, O's; calculated. (b) Estimated spectrum of cytochrome a<sub>3</sub> for the wavelength region spanned in the experiment presented in Figure V.2.

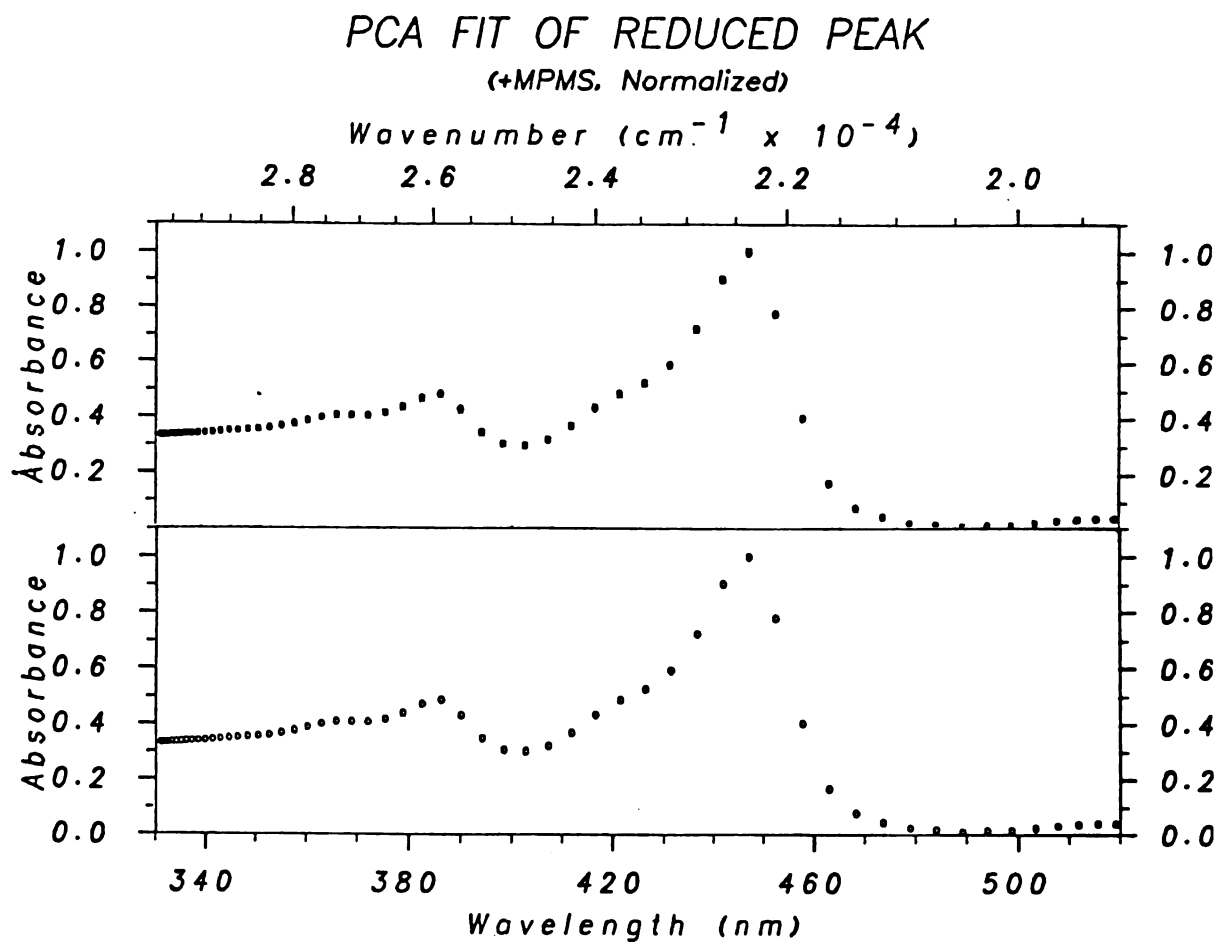


Figure V.9.--(a) M-analysis fit of the reduced oxidase (+ MPMS contribution, taken from the last spectrum in Figure V.2). Using three eigenvectors in M-analysis (b) estimated spectrum.

shape of a suspected absorber, the spectral shape of that absorber, which best fits the surface, is calculated for the entire set of experimental wavelength channels. We shall focus here on the fit of proposed spectra to the M-analysis eigenvectors.

The M-analysis fit to the proposed spectral shapes of the oxidized cytochromes  $\underline{a}$ ,  $\underline{a}_3$  and of the reduced oxidase (+ MPMS contribution) are shown in Figure V.7a, 8a, 9a. In Figure V.7b, 8b, 9b the calculated spectral shapes for the entire wavelength region are displayed for these three absorbers. It is significant that the program "corrects" minor deviations of the proposed spectra from the true spectra so that the best least-squares estimates of the spectral shapes of the independent absorbers are extracted from the wavelength-time-absorbance surface. The final spectra are the same even when different proposed spectra are tested as long as the proposed spectral shapes are close to the true shapes.

C.1.3 Concentration profiles.--Since it was possible to account for all the  $m$  ( $= 3$ ) eigenvectors in the M analysis, it was a straightforward problem to calculate the concentration profiles of the three absorbers. The results, shown in Figure V.10, provide a striking confirmation of the observations described in Chapter IV, that the decay of the oxidized cytochrome  $\underline{a}_3$  lags that of the oxidized  $\underline{a}$  (Figure V.10). Also, the growth of the reduced heme ( $\underline{a} + \underline{a}_3$ ) band results from an "averaging" of the two profiles. Without the results of PCA we were only able to conclude that the reduction of cytochrome  $\underline{a}$  is faster than that of  $\underline{a}_3$ . Now we can conclude that the fast phase

TIME COURSES OF OXIDASE COMPONENTS  
( Wavelength Region 330-520 nm )

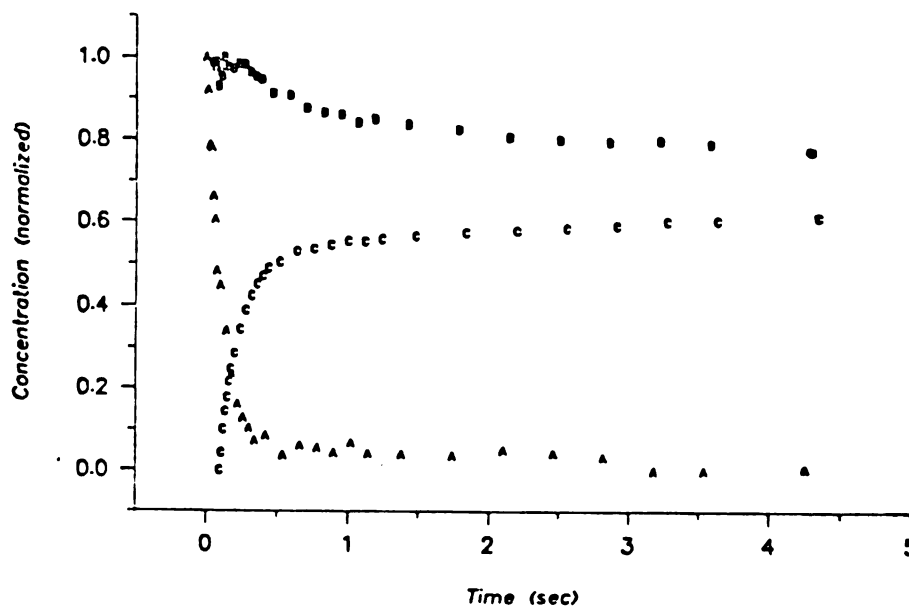
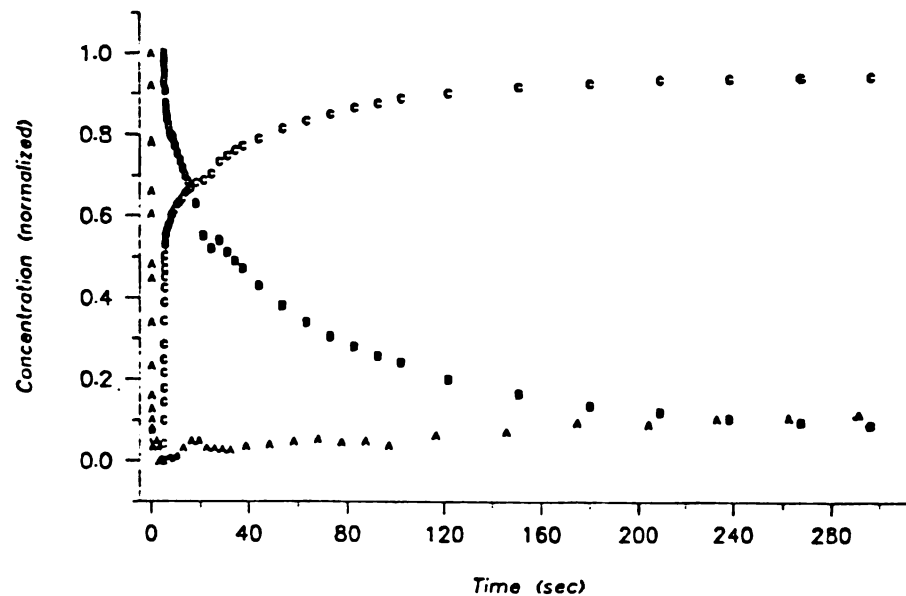


Figure V.10.--Concentration-time profile for the disappearance of oxidized cytochrome a (A), oxidized cytochrome a<sub>3</sub> (B) and the growth of the combined reduced peak, (C). Concentrations are in arbitrary units, time is in s. Bottom figure is the first 5 seconds of the reaction.

consists exclusively of the reduction of cytochrome a and that the slow phases represent the slower reduction of cytochrome a<sub>3</sub>. Thus cytochrome a is the site of the reduction by MPH and the slower reduction of cytochrome a<sub>3</sub> is most likely the result of an intramolecular electron transfer as proposed earlier (Halaka et al., 1981a).

C.2 PCA on the Reduction of the Oxygenated Enzyme by MPH (Wavelength Region 400 - 650 nm)

In this experiment we attempted to study the effect of "oxygenation" of the oxidase (see Chapter I, Section A.4.3). We also resolve the contribution of both reduced cytochromes a and a<sub>3</sub> to the reduced  $\alpha$ -band of the protein (around 600 nm). In this wavelength region (400 - 650 nm) the MPMS/MPH couple does not contribute appreciably to the absorbance (see Chapter III). The experimental absorbance-wavelength-time data surface is shown in Figure V.11 for the reduction of 3.32  $\mu$ M cytochrome oxidase by 26  $\mu$ M MPH.

C.2.1 Number of components.--M-analysis gave for the rank of M a value of 3. This is concluded from reconstructing the absorbance surface with  $r = 2$  (Figure V.12) and  $r = 3$  (Figure V.13). It can be seen that for  $r = 2$ , the reconstructed surface does not faithfully reproduce the data in Figure V.11. This is supported by the examination of the residual surfaces for  $r = 2$  and  $r = 3$ , which are shown in Figure V.14 and Figure V.15, respectively. Also, the values of the function  $Q_r/(N - r)(p - r)$  in Equation V.17 were 343, 8.4 and 1.6 for the first three eigenvectors for  $r = 3$ . The value of this

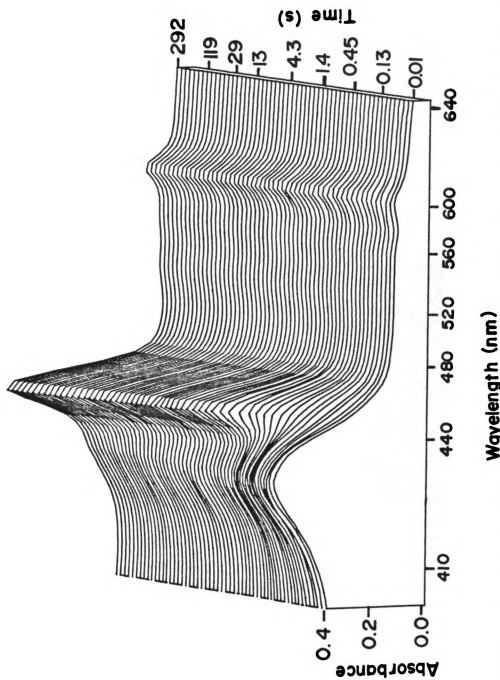


Figure V.11.--Experimental wavelength-absorbance-time data surface for the anaerobic reduction of the oxygenated form of the oxidase ( $3.32 \mu\text{M}$ ) by  $26 \mu\text{M}$  MPH. Other conditions were the same as in Figure V.2.

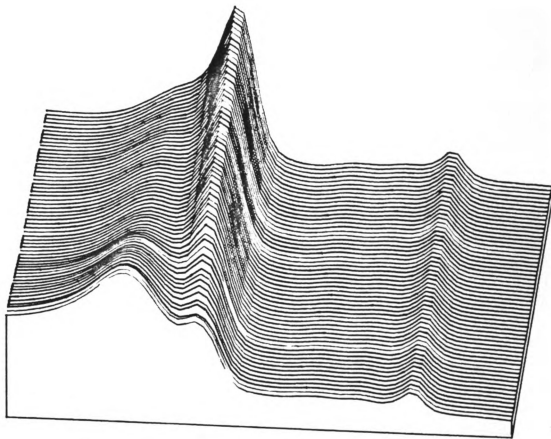


Figure V.12.--Reconstructed surface for the data presented in Figure V.11 using two eigenvectors.

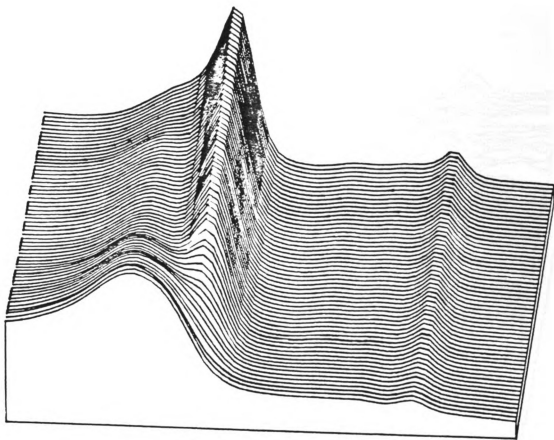


Figure V.13.--Reconstructed surface for the data in Figure V.11 using three eigenvectors.

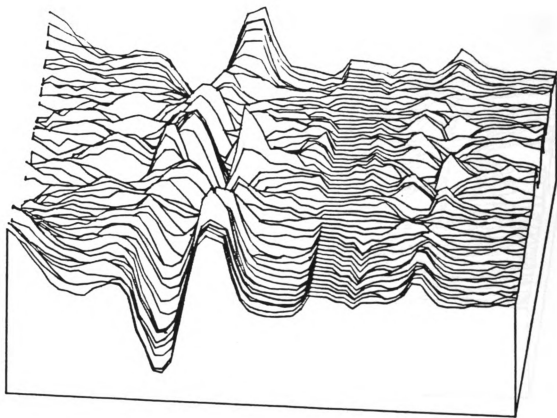


Figure V.14.--Residuals  $(\hat{A}_{(2)} - \underline{A})$  of the data presented in Figure V.11.

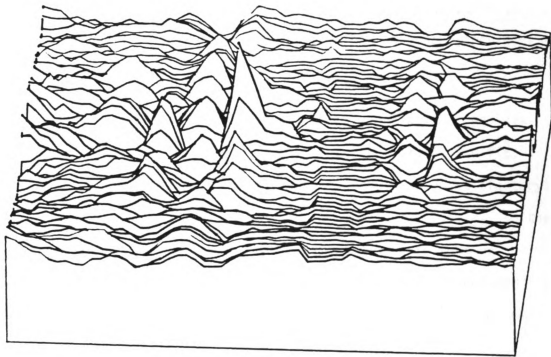


Figure V.15.--Residuals  $(\hat{A}_{(3)} - \underline{A})$  of the data presented in Figure V.11.

function for the fourth eigenvector was 0.67, indicating that  $r = 3$ . S-analysis of the same data indicated that there are only two components that independently change their concentrations with time,  $r_s = 2$ . This, again, was concluded from examination of the reconstructed absorbance surfaces and residuals. This value of  $r_s$  was further confirmed by the values of  $Q_r/(N-r)(p-r)$  for  $r_s = 1, 2$  and  $3$ , which were 19, 1.8 and 0.7, respectively, indicating  $r_s = 2$ .

The target absorbers for the fitting of the eigenvectors in this case (M-analysis) are four: The oxidized and reduced cytochromes a and a<sub>3</sub>.

C.2.2 Spectra of individual absorbers.--Unlike the case discussed for the shorter wavelength setting (Section C.1.1), the fit to the oxidized cytochrome a<sub>3</sub> (from Vanneste, 1966) was unsatisfactory. This is explainable, however, by postulating that cytochrome a<sub>3</sub><sup>3+</sup> in the "oxygenated" enzyme must have its peak shifted closer to that of cytochrome a<sup>3+</sup>. This is supported by the fact that the "oxygenated" enzyme has a combined peak for cytochromes a<sup>3+</sup> and a<sub>3</sub><sup>3+</sup> at 424 nm compared to about 418 nm in the resting enzyme.

The oxidized cytochrome a spectrum was found to fit as one of the M-analysis eigenvectors (Figure V.16). It should be pointed out, however, that this really represents both oxidized cytochromes (combined). The other two suspected absorbers (reduced cytochromes a and a<sub>3</sub>) were found to fit to the M-analysis eigenvectors. The reduced forms of the two cytochromes were resolvable in this case because of the better wavelength resolution in the Soret region, as well as the

## PCA ESTIMATION OF REDUCED CYT A

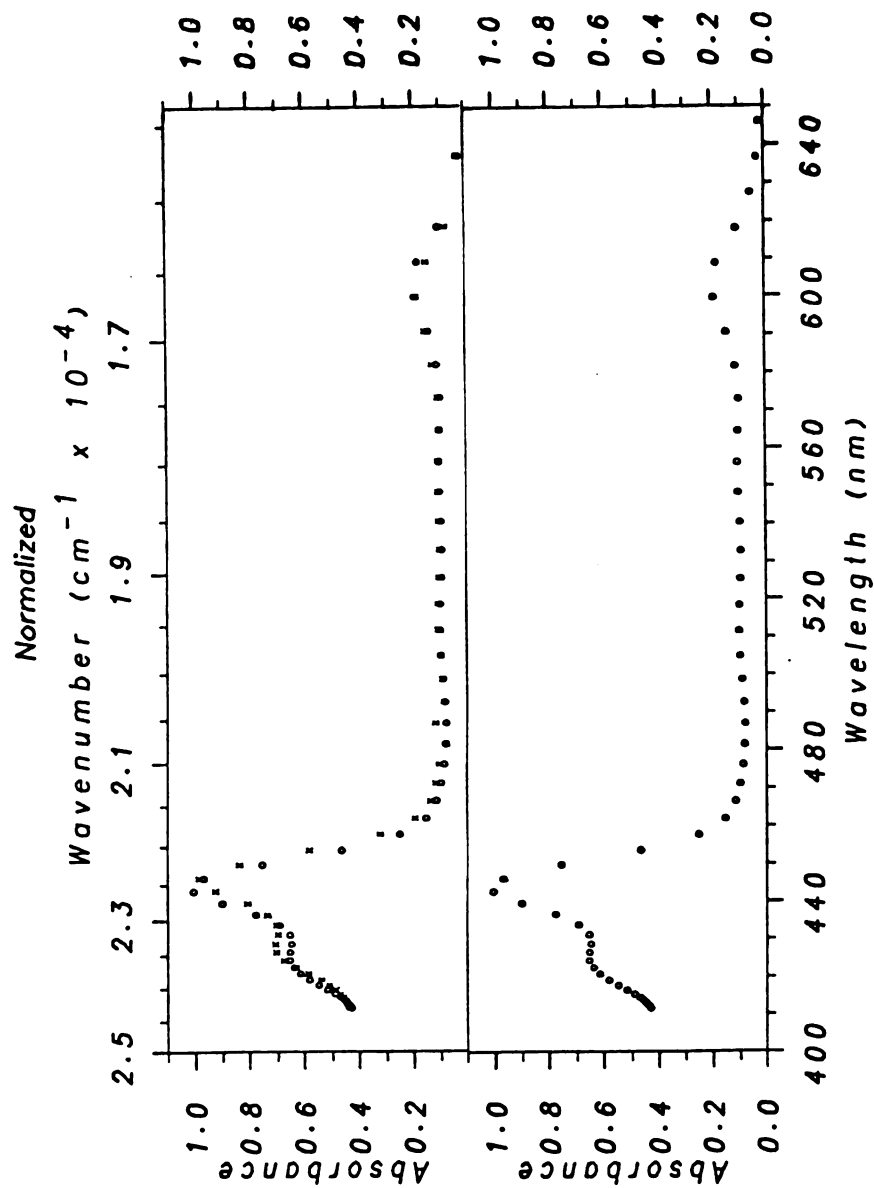


Figure V.16.--(a) M-analysis fit of the combined oxidized cytochromes a and a<sub>3</sub> spectrum for the oxygenated oxidase. X's are the proposed points and O's are the three eigenvectors estimation of spectrum. (b) the estimated spectrum.

contribution of the  $\alpha$ -band. It is important to note that reduced cytochrome a (Figure V.17) has a much higher absorption at around 600 nm than does reduced cytochrome a<sub>3</sub> (Figure V.18). This has been suspected for some time, but the present data provide experimental proof that the contribution of heme a in this region strongly predominates.

C.2.3 Concentration profiles.--The concentration-time profiles of the three absorbers are in general agreement with those obtained for the shorter wavelength setting. Again, cytochrome a<sub>3</sub><sup>3+</sup> reduction lags the reduction of cytochrome a<sup>3+</sup>, again confirming that MPH reduces a<sup>3+</sup> first (Figure V.19). Note that in this wavelength setting, we have the concentration-time profile for the appearance of cytochromes a<sup>2+</sup> and a<sub>3</sub><sup>2+</sup>, which can be compared to those of the disappearance of the oxidized forms of the two cytochromes in the shorter wavelength setting. Once again, we can conclude unequivocally that the fast phase represents reduction of cytochrome a<sup>3+</sup>. In spite of strongly overlapping bands, PCA has provided both wavelength and time resolution of the contributions from the separate chromophores.

#### D. Conclusions

The work presented here, although starting with known or postulated spectral shapes of the oxidase components, provides resolution of the independent spectral shapes of the components of the protein. We have not only proven that the oxidase has two different cytochromes, and given a "hands-off" estimation of their spectral shapes, but also

PCA ESTIMATION OF REDUCED CYT A<sub>3</sub>

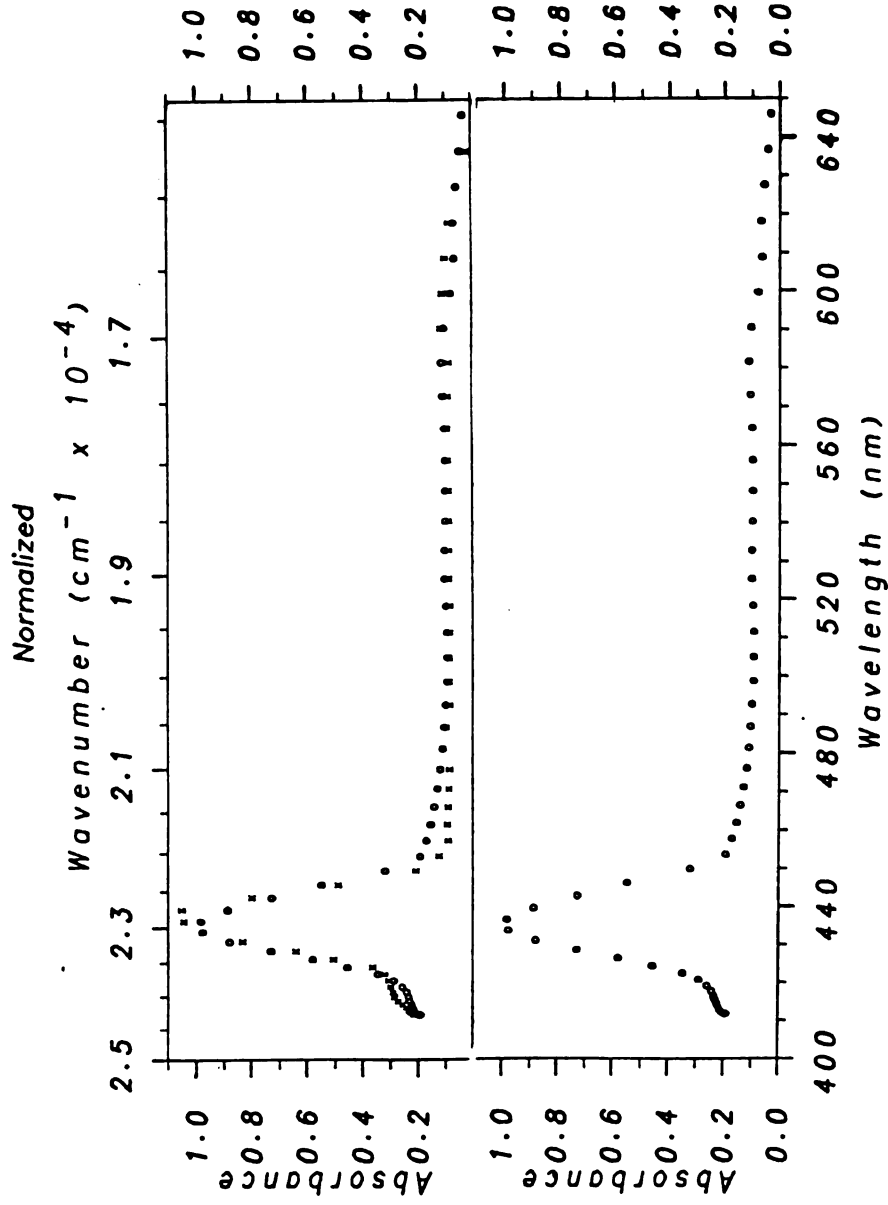


Figure V.17.--(a) Three eigenvectors M-analysis fit to the spectrum of reduced cytochrome a<sub>3</sub>.  
 X's: Prepared points, O's: Estimated points (b) estimated spectrum.

# PCA FIT OF OXIDIZED CYT ( A + A<sub>3</sub> )

( Oxygenated Oxidase, Normalized )

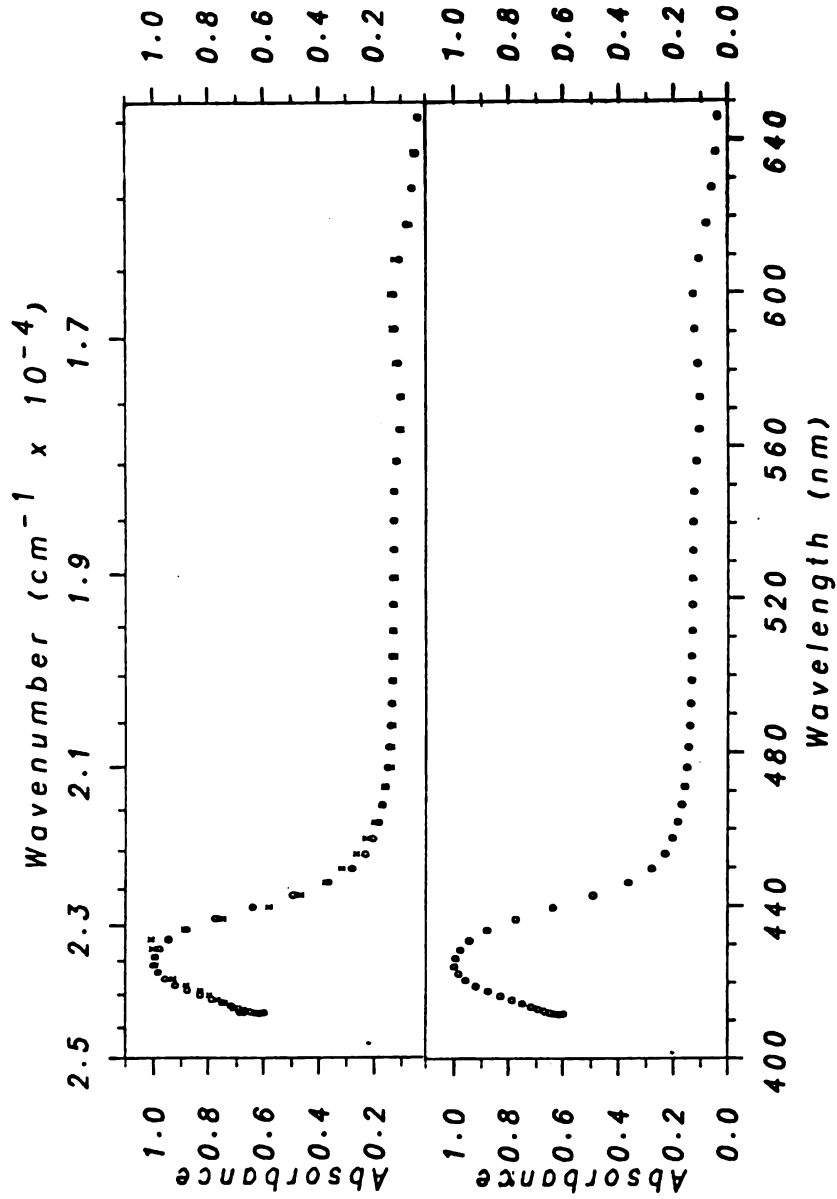


Figure V.18.--(a) Three eigenvectors M-analysis fit to the spectrum of oxidized a + a<sub>3</sub>  
 X's are the prepared points and O's are the calculated points. (b) estimated spectrum.

TIME COURSES OF OXIDASE COMPONENTS  
(Oxygenated. Wavelength Region 400-650 nm )

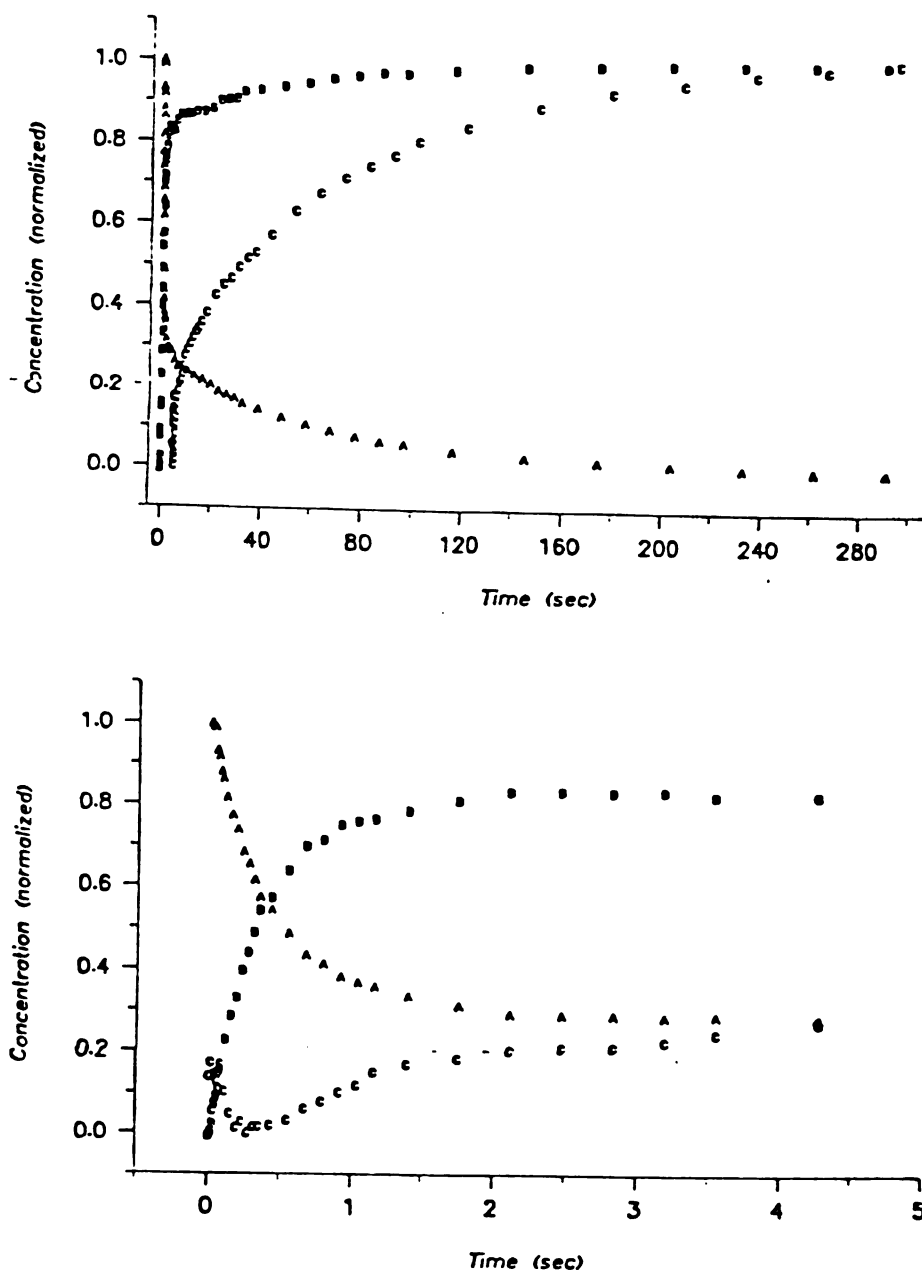


Figure V.19.--Concentration-time profile for the growth of reduced cytochrome  $a$ , (B); reduced cytochrome  $a_3$  (C); and for the disappearance of the combined oxidized ( $aa_3$ ), (A). Bottom figure is the first 5 seconds of the reaction.

resolved their separate reduction-time profiles by MPH. This work shows that principal component analysis is a powerful tool toward the goal of separating strongly overlapping spectral components, which show different temporal characteristics.

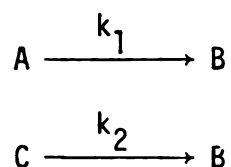
From data obtained in the long wavelength region (Figure V.17) PCA shows that the reduced cytochrome a spectrum has a shoulder in the Soret region and also a higher contribution to the  $\alpha$ -band than does reduced cytochrome a<sub>3</sub>, in agreement with previous suggestions. The analysis in this wavelength region also showed that in the "oxygenated" enzyme, the spectral shapes of the oxidized cytochromes a and a<sub>3</sub> are similar, and thus become difficult to separate.

The concentration-time profiles of the components of the oxidase, which were deduced from PCA, without any mechanistic assumptions, agree well with our previous assignments for the reduction of the oxidase by MPH. We have previously assigned cytochrome a<sup>3+</sup> to be the primary reduction site by MPH (Halaka et al., 1981a; see also Chapter IV). That was based on difference spectral shapes during the reduction. PCA not only confirmed this observation, but indicated a clean separation between the time-courses of the reduction of a<sup>3+</sup> and a<sub>3</sub><sup>3+</sup>. In the two wavelength regions examined, we have found the same concentration-time profiles: Cytochrome a<sub>3</sub><sup>3+</sup> reduction lags that of cytochrome a<sup>3+</sup>. This, of course, explains the multiphasic kinetics of the growth in absorbance at 444 nm upon reduction because growth at this wavelength results from contributions from both cytochromes.

In the M-analysis for each of the two wavelength regions studies here, three independent absorbers were the minimum number of

components that allowed reproduction of the absolute experimental data surfaces. S-analysis gave only two components that change concentrations independently with time. For the short wavelength setting the M-analysis components were interpreted to be the reduced peak of both cytochromes a and a<sub>3</sub> (combined, + MPMS) and oxidized cytochromes a and a<sub>3</sub>. Those for the long wavelength setting, when "oxygenated" protein was used, were interpreted as the shapes of the separate reduced cytochromes a and a<sub>3</sub> and a combined shape for the two oxidized cytochromes.

The  $r_s = 2$  results can be interpreted by a simplified scheme for both cases: For example, in the long wavelength region, there is the condition that the disappearance of the (combined) oxidized peak must appear in either the reduced cytochromes a or a<sub>3</sub>. A similar situation was illustrated by Cochran and Horne (1977) for the mechanism:



For which they illustrated that the rank of  $\underline{M} = 3$  and that of  $\underline{S} = 2$ .

The previously published spectra of cytochromes a and a<sub>3</sub> (Vanneste, 1966), which were deduced from ligand binding studies and have been questioned (Caughey et al., 1976), proved to be good approximations to the spectral shapes of these components. Note that in the scanning stopped-flow data discussed here, only reductions of these chromophores takes place; there is no ligation at either site. The

power of the method of PCA is exemplified by the fact that it gives the spectral shape for the whole wavelength region of the experiment, even though only a limited range of wavelength channels is used for the proposed spectra.

## CHAPTER VI

### REDUCTION OF CYTOCHROME OXIDASE BY SODIUM DITHIONITE

#### A. Introduction

Sodium dithionite ( $\text{Na}_2\text{S}_2\text{O}_4$ ) is a widely used reducing agent in biology. The dithionite ion dissociates in aqueous solutions to give  $\text{SO}_2^-$  (Equation VI.1).



Lambeth and Palmer (1973) studied the reduction of several biological molecules by dithionite by using stopped-flow techniques. Their findings indicate that although  $\text{S}_2\text{O}_4^{2-}$  can act as a reductant,  $\text{SO}_2^-$  is generally more reactive than  $\text{S}_2\text{O}_4^{2-}$ . They reported a value of  $1.4 \pm 0.4 \times 10^{-9} \text{M}$  for the equilibrium constant in Equation V.1,  $K_1 = k_1/k_{-1}$  from EPR measurements. The value of the rate constant for the dissociation of  $\text{S}_2\text{O}_4^{2-}$ ,  $k_1$ , was found by the same authors to be  $1.7 \text{ s}^{-1}$ .

Mayhew (1978) calculated a value for the mid-point redox potential,  $E^{0'}$ , for the  $\text{SO}_2^-/\text{HSO}_3^-$  couple at  $\text{pH} = 7$  and  $25^\circ\text{C}$  of  $-0.66\text{V}$ . The theoretical potential for the redox couple  $\text{S}_2\text{O}_4^{2-}/\text{H}_2\text{SO}_3$  at  $\text{pH} = 7$  was estimated to be  $-0.386 \text{ V}$ . Studies on the reduction by dithionite of

metmyoglobin derivatives (Olivas et al., 1977) and methemerythrin (Harrington et al., 1978) showed that  $\text{SO}_2^-$  is the reducing species for those oxidants.

The fact that sodium dithionite, as  $\text{SO}_2^-$  or  $\text{S}_2\text{O}_4^{2-}$ , carries negative charge is of importance in understanding the role of electronic charge of the reductant on the kinetics and site of the reduction of the oxidase. This is particularly true owing to the fact that the interaction between cytochrome oxidase and its physiological reductant, cytochrome c, is thought to be controlled by electrostatic phenomena (Wilms et al., 1981). Sodium dithionite has been sporadically used to study the reduction of cytochrome oxidase (Lemberg and Mansley, 1965; Lemberg and Gilmour, 1967). Orii (1979) recently reported scanning stopped-flow experiments on the reduction of the oxidase by dithionite in an air-saturated system. Also, dithionite was used for anaerobic reductive titration studies of the oxidase (Babcock et al., 1978).

### B. Spectral Shape Analysis

The spectral changes as a function of time on anaerobically mixing cytochrome oxidase with sodium dithionite are presented in Figure VI.1. Concentrations of the oxidase and dithionite after mixing were 3.78 and 47  $\mu\text{M}$ , respectively. These spectra were selected from 57 spectra collected by using the scanning stopped-flow system described in the experimental chapter. The spectra represent the "simultaneous" spectral changes of both the Soret and the  $\alpha$ -bands due to the reduction of the oxidase.

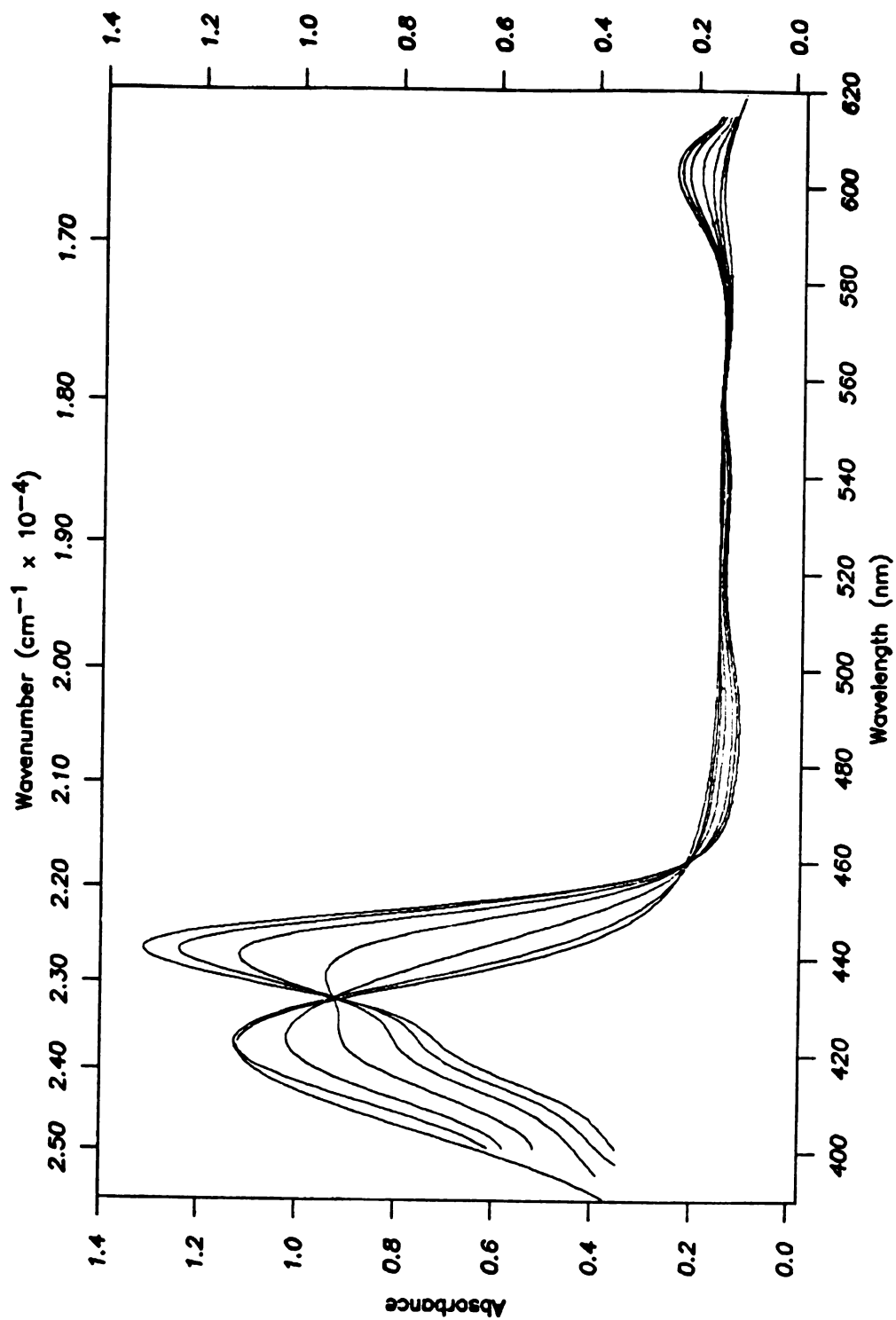


Figure VI.1.1.--Spectral shapes during the anaerobic reduction of 3.78  $\mu\text{M}$  cytochrome oxidase by 47  $\mu\text{M}$  sodium dithionite (concentration after mixing) in 50 mM HEPES buffer containing 0.5% Tween 20, pH = 7.4. Cell path length = 1.85 cm, T = 21°C. Times, in seconds for the selected spectra (at 444 nm from the bottom to the top) are, in seconds, 0, .01, 0.43, 4.2, 12.9, 38.8, 97.2, 292.

On subtracting the first spectrum collected (which, due to the slowness of the reduction by dithionite, is virtually identical to the sum of the spectra of the reactants), the resulting difference spectra are displayed in Figure VI.2. These show, in contrast to the reduction by MPH (Chapter IV), that the short wavelength side of the oxidized Soret region decays first. This can be taken as an indication that the reductant in this case reacts with cytochrome  $\underline{a}_3^{3+}$  faster than it does with cytochrome  $\underline{a}^{3+}$ . The shift of the "isosbestic" point from  $\sim 420$  nm to  $\sim 432$  nm at later times during the reduction supports this conclusion.

Another interesting feature of this reaction is also apparent in Figure VI.2. Examination of spectra in the 590 - 605 nm ( $\alpha$ -absorption band) shows that in the beginning of the reduction the  $\alpha$ -band has its peak at around 595 nm, which shifts to 604 nm at later stages of the reduction. The opposite effect, faster reduction of the  $\underline{a}^{3+}$  site, was observed in the case of the reduction of the oxidase by MPH (Chapter IV). Therefore, we conclude that  $\underline{a}_3^{2+}$  peak in the  $\alpha$ -region is blue shifted with respect to the  $a^{2+}$  peak.

### C. Kinetics of the Reduction of Cytochrome by Sodium Dithionite

The kinetics of the reduction of the oxidase by sodium dithionite were found to be triphasic, resembling the kinetics of reduction by MPH. However, since the electrons enter the  $\underline{a}_3(\text{Cu}_{a_3})$  site faster than they reduce the  $\underline{a}^{3+}$  site, the intramolecular electron flow should be in the opposite direction to that which occurs upon reduction by MPH.

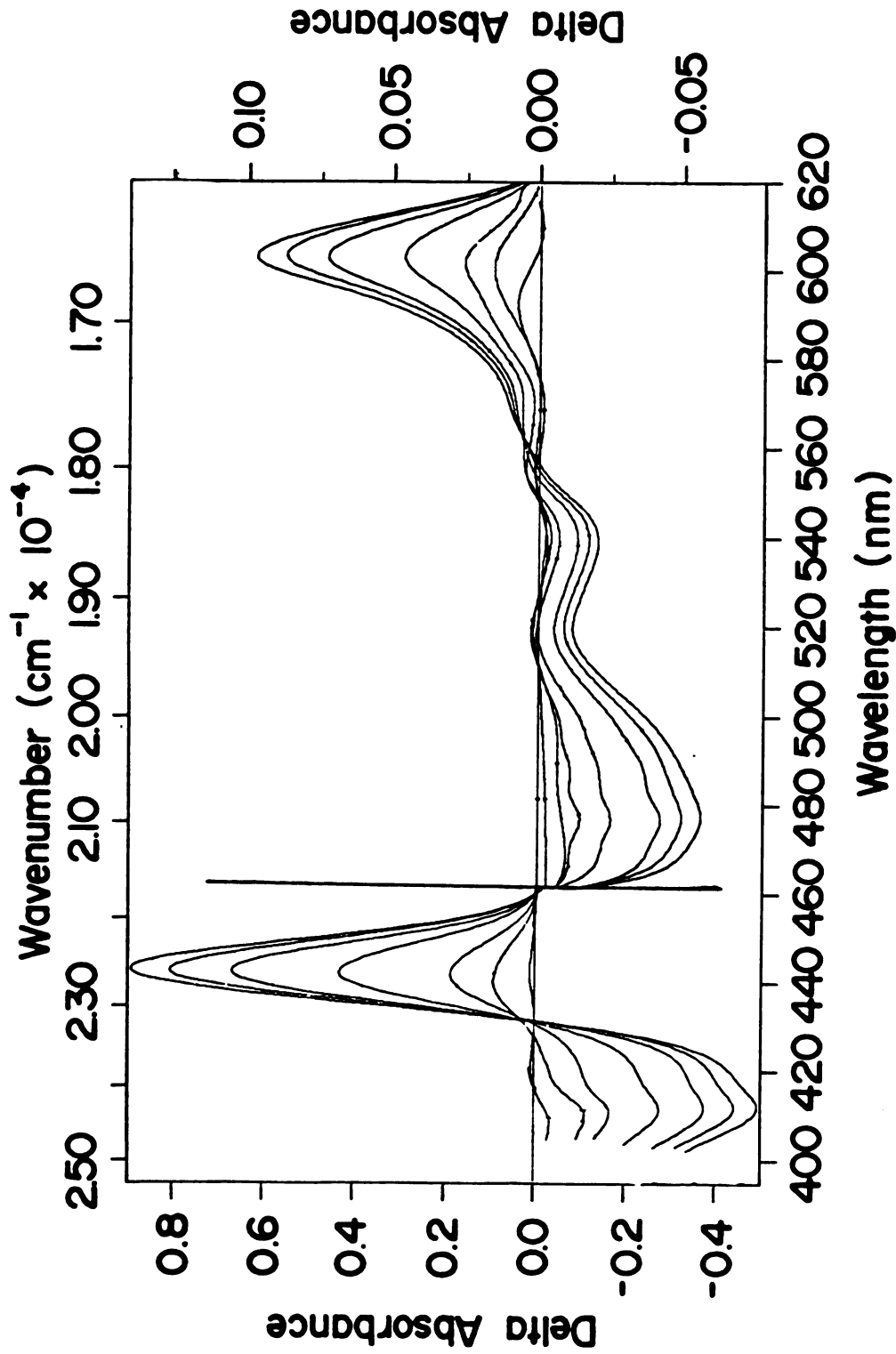


Figure VI.2.--Selected difference spectra during the reduction of cytochrome oxidase by sodium dithionite. The first spectrum collected was subtracted from the data shown in Figure VI.1 (original contained 57 spectra). All conditions are the same as in Figure VI.1. Times for the spectra, in sec, from bottom at 444 nm are: 0.11, 4.27, 12.91, 32.4, 68, 116, 292.

The conclusion that the cytochrome a site is being reduced by dithionite, but at a slower rate, is drawn from the data presented above and from the fact that the CN<sup>-</sup> complex of the oxidase undergoes reduction by sodium dithionite with a slower rate than that observed for the native protein in the absence of the inhibitor (see below).

Since the sodium dithionite concentration was much higher than that of the oxidase in all of the experiments reported here, full time courses were analyzed by using three exponentials which gave, for example, very small and random residuals for the decay at 410 nm (Figure VI.3). Table VI.1 summarizes results on the rate constants of the reduction by sodium dithionite.

Analysis of the fast phase, which is interpreted as a bimolecular encounter of the reductant with the oxidase, has revealed that the actual reducing species is  $\text{SO}_2^{\dot{-}}$ , since the observed pseudo-first order rate constant for that phase varied linearly with the square root of the dithionite concentration (Figure VI.4). The second order rate constant for the reduction of the oxidase (a<sub>3</sub> site) by  $\text{SO}_2^{\dot{-}}$  was calculated to be  $k = 3.4 \pm 0.8 \times 10^6 \text{ M}^{-1} \text{ s}^{-1}$ . This value was obtained from the slope of Figure VI.4 and the equilibrium  $\text{S}_2\text{O}_4^{\dot{+}} \xrightleftharpoons{K_1} 2\text{SO}_2^{\dot{-}}$  with an equilibrium constant,  $K_1 = 1.4 \pm 0.4 \times 10^{-9} \text{ M}$  (Lambeth and Palmer, 1973). The rates of the slow processes showed slight increase on increasing the dithionite concentration (Table IV.1), which may be attributed to some reduction at the a site by dithionite. No systematic study was done on the dependence of the rate of these processes on the protein concentration. However, by analogy to the reduction by

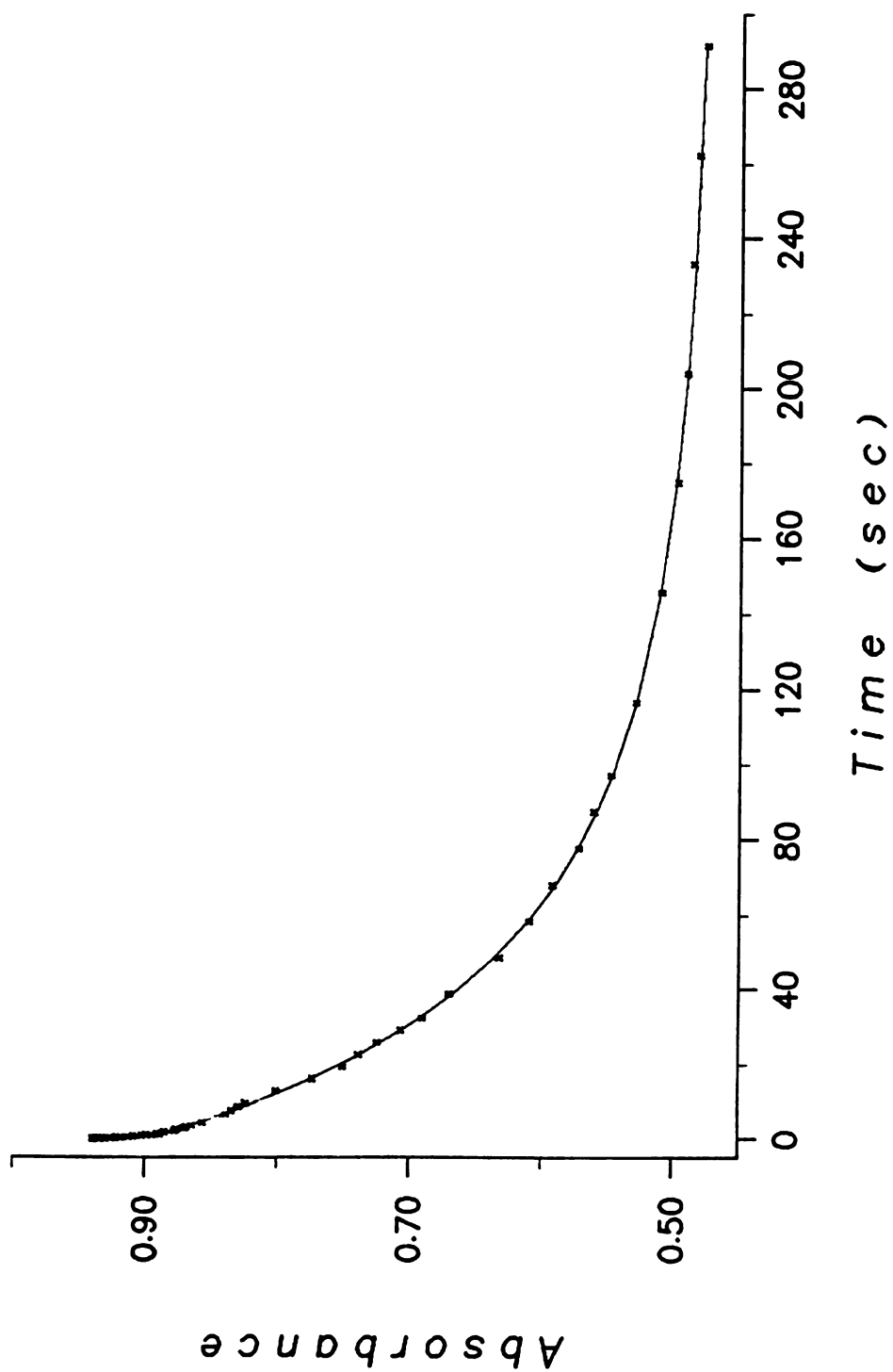


Figure VI.3.--Fit of the absorbance-time data at 410 nm of the reduction of cytochrome oxidase by sodium dithionite. Concentration after mixing were  $3.78 \mu$  and  $91 \mu\text{M}$ , solid line is the calculated curve by three exponentials. All other conditions are the same as in Figure VI.1.

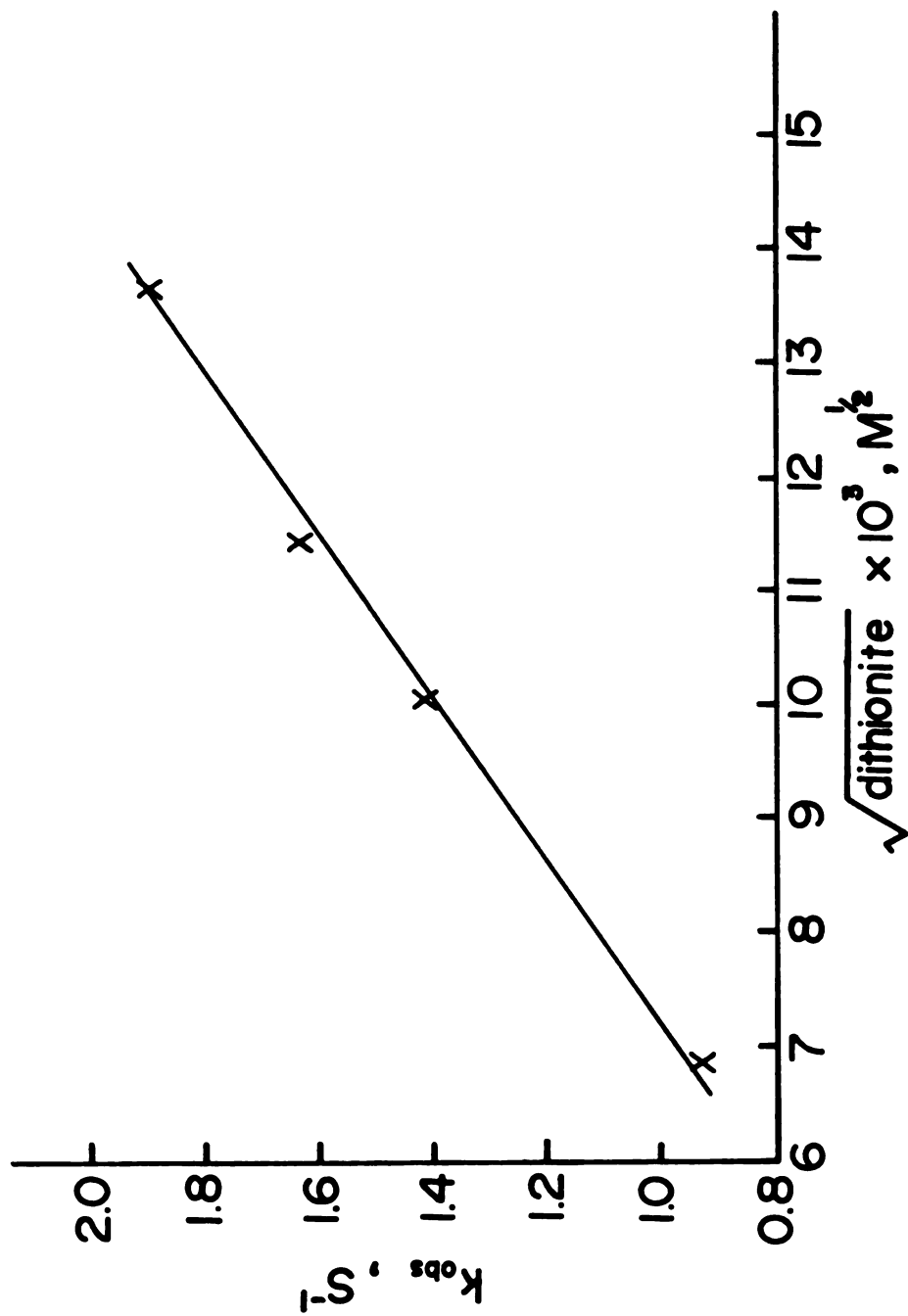


Figure VI.4.--Dependence of the pseudo first-order rate constant of the fast phase.  $k_1$  in Table VI.1 on the square root of sodium dithionite concentration.

TABLE VI.1 -- Rate constants for the reduction of cytochrome oxidase by sodium dithionite in HEPES buffer containing 0.5% Tween 20, pH = 7.4, T = 21°C. Rate constants are the observed first-order rate constants from the analysis of data by three exponentials.

[dithionite], $\mu\text{M}$	[oxidase], $\mu\text{M}$	$k_1, \text{s}^{-1}$	$k_2, \text{s}^{-1}$	$k_3, \text{s}^{-1}$
187	3.78	$1.9 \pm 0.2$	$0.039 \pm 0.05$	$0.0178 \pm .0005$
131	3.78	$1.6 \pm 0.2$	$0.032 \pm 0.009$	$0.0140 \pm 0.0005$
91	3.78	$1.41 \pm 0.2$	$0.030 \pm 0.004$	$0.0130 \pm 0.0002$
47	3.78	$.92 \pm 0.2$	$0.029 \pm 0.0004$	$0.0132 \pm 0.0003$

MPH, one might expect the two slow processes to be independent of the enzyme concentrations.

#### D. Effect of Cholate

When cholate was used as the detergent instead of Tween 20, the reduction of the oxidase by sodium dithionite was slowed considerably. Figure VI.5 presents the spectral changes in the wavelength range from 400 to 620 nm that occurred on anaerobically mixing cytochrome oxidase with sodium dithionite in HEPES buffer containing 0.5% cholate. Concentrations after mixing of the oxidase and dithionite were 0.92  $\mu\text{M}$  and 317  $\mu\text{M}$ , respectively. The spectra have qualitatively the same shape as those in Figure VI.1 (where Tween 20 was present as detergent). However, these spectra show that the reduction is incomplete, even after more than five minutes. The difference spectra (Figure VI.6) taken from Figure VI.5, show that  $\underline{a}_3$  is the principal reduced species with some reduction at the  $\underline{a}$  site, as indicated from the shift in the "isosbestic" point in the Soret region. The indication that cytochrome  $\underline{a}_3$  is more quickly reduced than  $\underline{a}$  results from the minimum in the difference spectra (Figure VI.6), which occurs at about 410 nm, near the "classical"  $\underline{a}_3^{3+}$  peak (Vanneste, 1966). This can also be seen from the spectra of Figure VI.5, where the decay on the short wavelength side of the oxidized peak (~410 nm) is much greater than that at the peak itself (420 nm).

The rate data were analyzed in a manner similar to the case when Tween 20 was used as the detergent (Section VI.C). The analysis was based upon program KINFIT4 (Dye and Nicely, 1971) and showed that

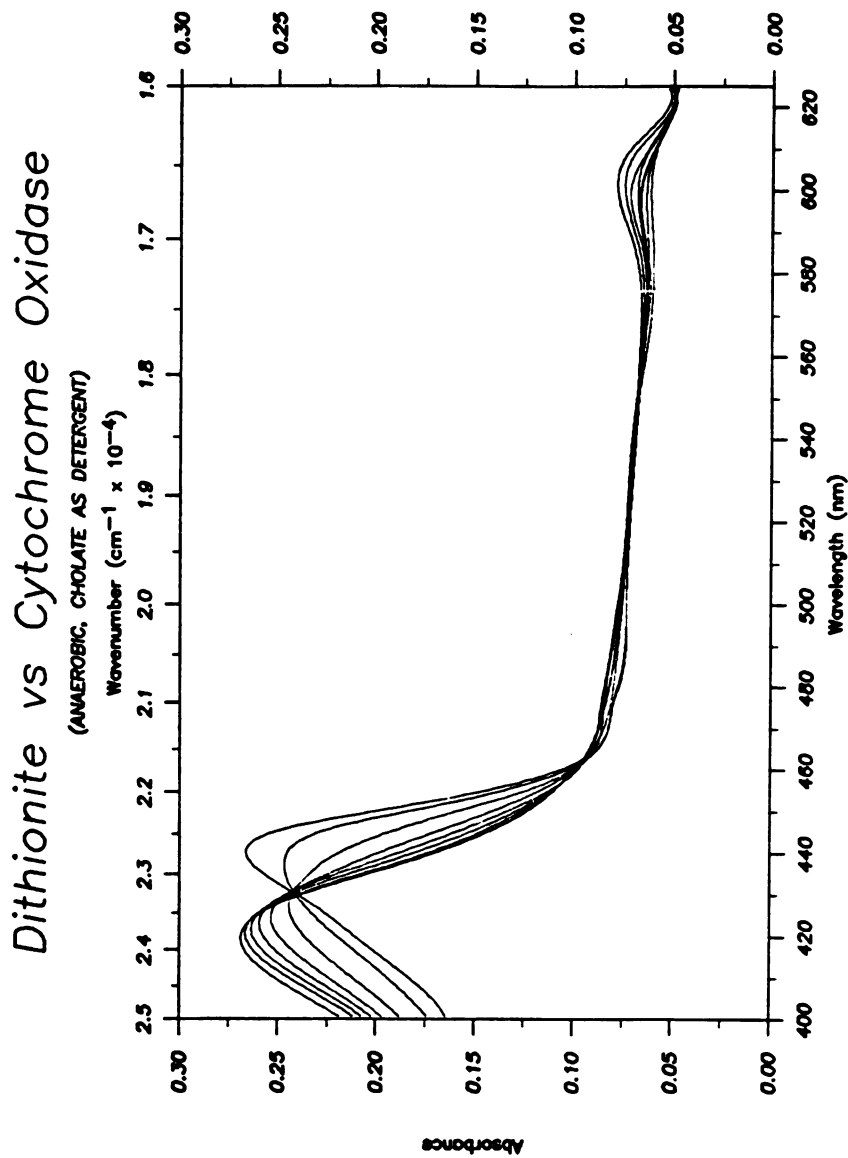


Figure VI.5.--Selected spectra during the reaction of 0.92  $\mu\text{M}$  cytochrome c oxidase with 317  $\mu\text{M}$  sodium dithionite (after mixing). Conditions were the same as those in Figure VI.1 except that 0.5% cholate was present as the detergent instead of Tween 20. Times, from bottom to top at 444 nm, in seconds, are: 0.01, 0.24, 0.43, 1.4, 4.2, 12.9, 48.6, 292.

## Dithionite vs Cytochrome Oxidase

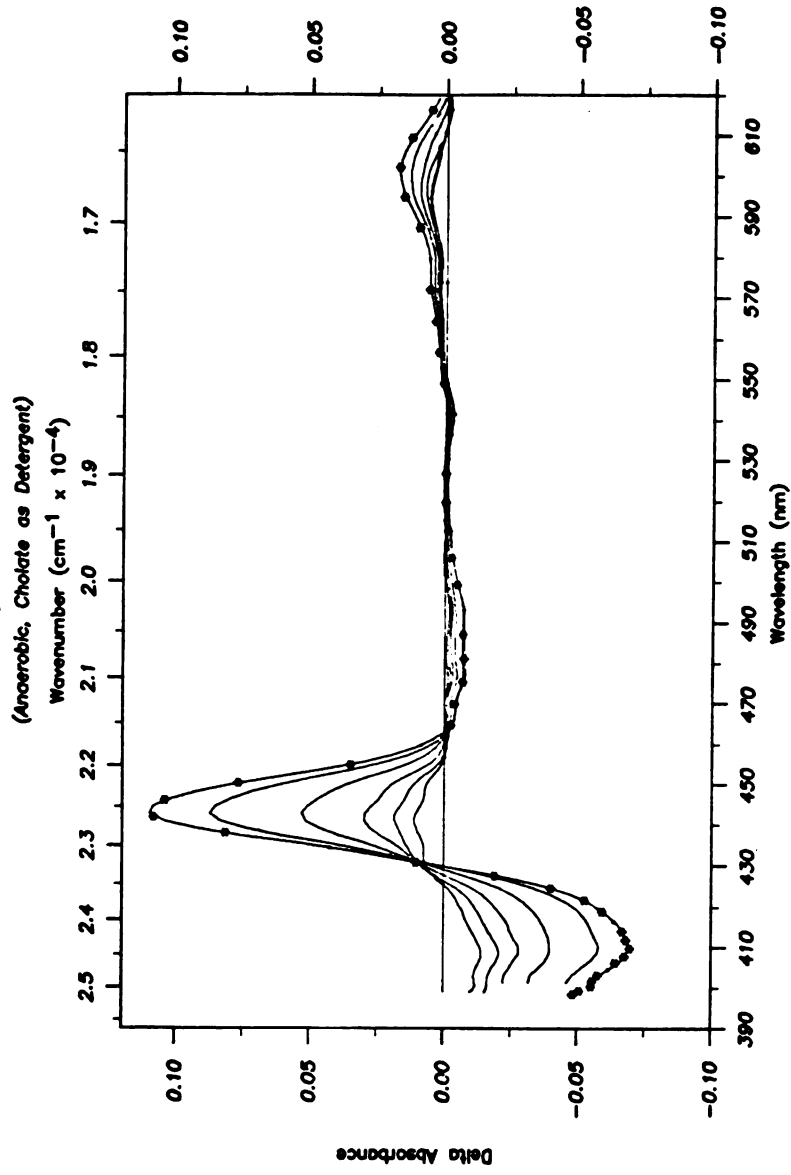


Figure VI.6.--Selected difference spectra from the same data shown in Figure VI.5. The first spectrum collected was subtracted from subsequent spectra. Times in seconds (from bottom to top at 444 nm are 0.43, 1.4, 4.2, 12.9, 48.6, 292.

the time dependence of the absorbance at 410 nm and 444 nm is biphasic. A two exponential fit to the data at 410 nm (Figure VI.7) gave two first order rate constants of  $0.38 \pm 0.04 \text{ s}^{-1}$  and  $0.0134 \pm 0.0004 \text{ s}^{-1}$ . Similar analysis at 444 nm (Figure VI.7) gave rate constants of  $0.42 \pm 0.05 \text{ s}^{-1}$  and  $0.0121 \pm 0.0003 \text{ s}^{-1}$ . The rate constant for the first phase, a pseudo first order rate constant, and the equilibrium constant for dithionite disproportionation (Equation VI.1) were used to calculate the second order rate constant for the reduction of the oxidase ( $\underline{a}_3$ ) by  $\text{SO}_2^{\cdot-}$ . The second order rate constant was found to be  $5.3 \pm 0.5 \times 10^5 \text{ M}^{-1} \text{ s}^{-1}$  when cholate was used as the solubilizing agent compared to a value of  $3.5 \pm 0.8 \times 10^6 \text{ M}^{-1} \text{ s}^{-1}$  when Tween 20 was present as the detergent.

#### E. Reduction of the Cyanide-Bound Cytochrome Oxidase by Dithionite

Figure VI.8 displays spectral changes as a function of time when  $2.75 \mu\text{M}$  cytochrome oxidase solution was mixed anaerobically with  $350 \mu\text{M}$  sodium dithionite (concentrations after mixing). The major changes in the absorbance are those due to the reduction of cytochrome  $\underline{a}^{3+}$ . The oxidized cytochrome  $\underline{a}$  band (maximum at 430 nm) decays as the reduced  $\underline{a}$  absorbance band (at 444 nm) grows in. The reduced  $\alpha$ - band also grows in at 605 nm due to the reduction. Figure VI.9 shows kinetic difference spectra, in the wavelength range 370 - 510 nm, under conditions similar to those of Figure IV.8.

Analysis of the absorbance-time data at 444 nm and 430 nm shows, in contrast to the reduction of the cyanide-bound enzyme by MPH which followed monophasic kinetics, by the criteria of small and random

**REDUCTION OF CYTOCHROME OXIDASE BY DITHIONITE**  
*Kinetics at 444.415 nm. Chololate as Detergent*

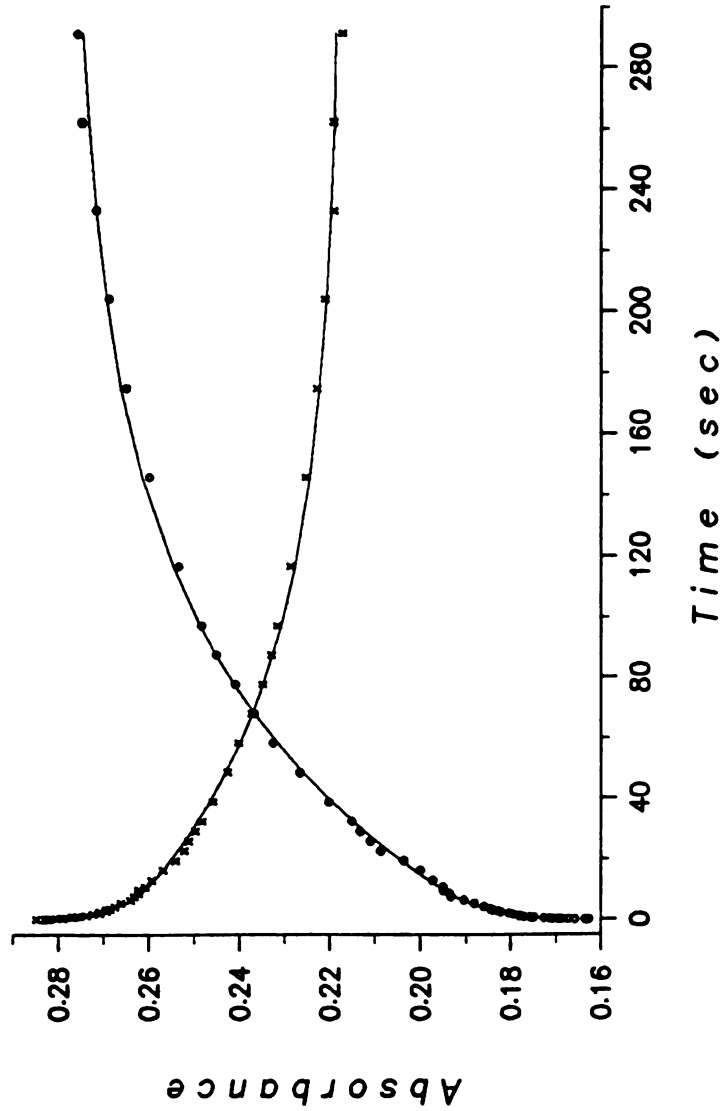


Figure VI.7.--Two-exponential fit to the absorbance-time data at 410 and 444 nm for the anaerobic reduction of cytochrome oxidase by sodium dithionite (after mixing). X's are data at 410 nm, O's at 444 nm; solid lines are two exponential calculated curves. Data from the same scanning experiment shown in Figure VI.5.

## Dithionite vs Cyano Oxidase

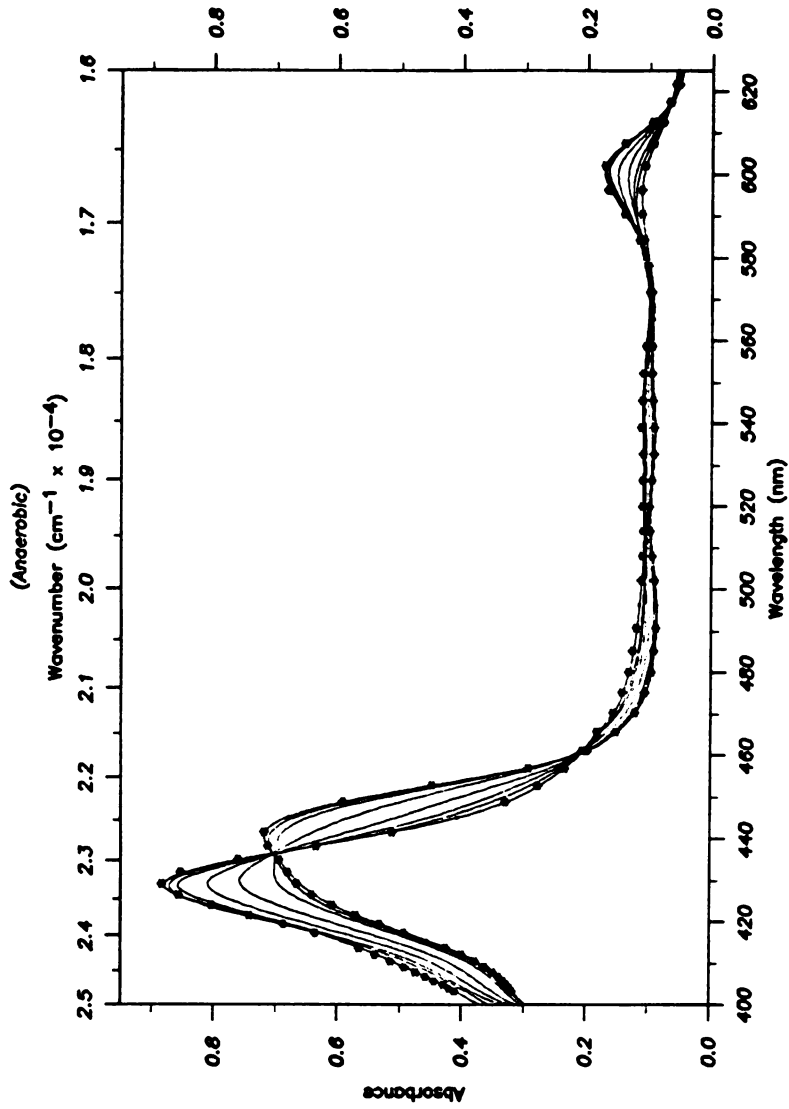


Figure VI.8.--Spectral changes as a function of time on the reduction of 2.75  $\mu\text{M}$  cyanide-bound cytochrome oxidase by 350  $\mu\text{M}$  sodium dithionite (after mixing). Buffer was 50 mM HEPES containing 0.5% Tween 20 (pH = 7.4), cell path length = 1.85 cm. Times from bottom to top at 444 nm are, in seconds, 0.01, 0.43, 1.4, 4.3, 12.9, 38.9, 116, 145, 292. \*'s are the actual stored points.

## Dithionite vs Cyano Oxidase

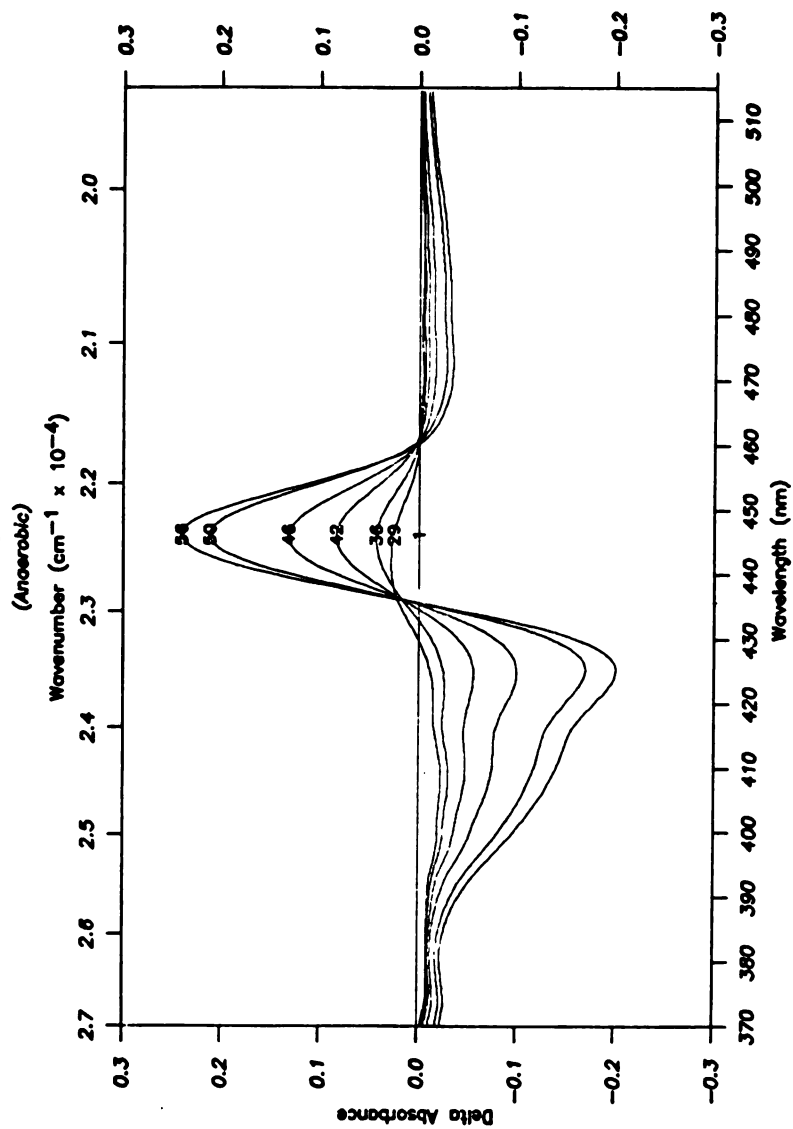


Figure VI.9.---Selected kinetic difference spectra in the Soret region during the reduction of 2.75  $\mu\text{M}$  cyanide bound cytochrome oxidase by 350  $\mu\text{M}$  sodium dithionite (after mixing). The first spectrum collected was subtracted from subsequent spectra. Times, in seconds are: 1, 0.01; 29, 4.3; 36, 12.9; 42, 48.6; 50, 146; 56, 292.

residuals, that the reduction by dithionite is biphasic. A two exponential fit for the data at 444 nm gave two observed first order rate constants (Figure VI.10) of  $0.21 \pm 0.04 \text{ s}^{-1}$  and  $0.0176 \pm 0.006 \text{ s}^{-1}$ . Treating the first of these as a pseudo first order rate constant as in Sections VI. B and C gave a second order rate constant for the reduction of the cyanide-bound cytochrome oxidase by  $\text{SO}_2^{\cdot-}$  of  $2.9 \times 10^5 \text{ M}^{-1} \text{ s}^{-1}$ .

#### F. Discussion

The anaerobic reduction of cytochrome oxidase by sodium dithionite provides several interesting insights into the spectral and electron transfer properties of the oxidase. The data presented here show that dithionite, reacting as the negatively charged  $\text{SO}_2^{\cdot-}$ , reduces the cytochrome  $\underline{a}_3^{3+}$  site faster than it does the  $\underline{a}$  site under our conditions. This can be viewed as resembling the reactions of ligands such as cyanide, formate or oxygen with the  $\underline{a}_3$  site. It can be argued that there is some "steric hindrance" in the accessibility to the cytochrome  $\underline{a}_3$  site, since, judging from the redox potentials of the  $\text{Fe}_{\underline{a}_3}^{3+}/\text{Fe}_{\underline{a}_3}^{2+}$  couple ( $\sim 0.35\text{V}$ , Babcock et al., 1978) and the  $\text{SO}_2^{\cdot-}/\text{HSO}_3^-$  ( $-0.66\text{V}$ , Mayhew, 1978) one would expect this reaction to be much faster. This argument is supported by the fact that the neutral molecule MPH, reacts primarily at the  $\underline{a}$  site. This is also supported by the fact that MPH is a bigger molecule than  $\text{SO}_2^{\cdot-}$ .

It is known that positively charged donors react mainly at the cytochrome  $\underline{a}$  site of the oxidase. Examples are the reduction by cytochrome  $\underline{c}^{2+}$  (cytochrome  $\underline{c}^{2+}$  carries a net positive charge at neutral

**REDUCTION OF CN-OXIDASE BY DITHIONITE**  
*Two exponential fit at 444 and 430 nm*

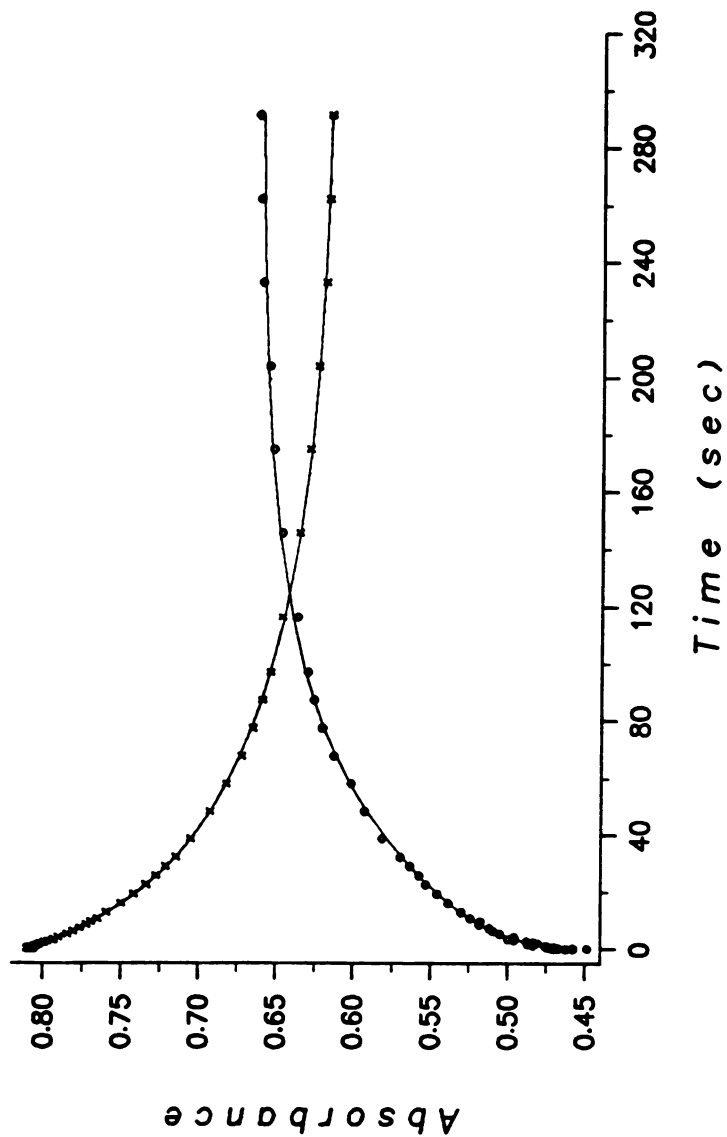


Figure VI.10.--Two-exponentials fit of the absorbance-time data at 444 and 430 nm for the reduction of 2.75  $\mu\text{M}$  cyanide-bound oxidase by 350  $\mu\text{M}$  sodium dithionite (after mixing). X's are 444 nm, o's are 430 nm data, and solid lines are calculated curves. Conditions are the same as in Figure VI.8.

pH; Koppenol et al., 1974), ruthenium (II) hexaamine (Scott and Gray, 1980), and hexaaquochromium (II) (Greenwood et al., 1977). Combination of this fact with the present work, which shows that MPH also reacts with the cytochrome a while  $\text{SO}_2^{\cdot-}$  reacts at the a<sub>3</sub> site suggests that cytochrome a has some net negative charge near the active site and is more accessible than cytochrome a<sub>3</sub>. Any reaction of  $\text{SO}_2^{\cdot-}$  with the cytochrome a site could then be viewed as largely electrostatic, and can be accelerated by increasing the ionic strength of the medium, since both reactants carry negative charges. Thus, Lemberg and Mansley (1965) who worked at higher ionic strength (approximately 0.2 M compared with about 0.025 M in the present work) and with high lipid content cytochrome oxidase, observed that cytochrome a reacts with dithionite faster than cytochrome a<sub>3</sub> does. It may also be concluded that this presumed negative charge on the a site is the reason that many negatively charged donors are not effective as reducing agents for the oxidase in the absence of a mediator. Examples include ascorbate and NADH (both are negatively charged at neutral pH). A report on the reduction of the oxidase by hydrated electrons also shows there is no appreciable reduction in the absence of cytochrome c. (Van Buuren et al., 1974).

The spectral shapes during the reduction are in agreement with the hypothesis mentioned above and confirm the classical assignments of the a and a<sub>3</sub> bands (Vanneste, 1966). The spectra also show complementary results to the reduction by MPH, in that the reduced  $\alpha$ -band of cytochrome a<sub>3</sub> has a peak at 595 compared to 604 for the reduced a.

The observed multiphasicity in the reduction of the oxidase by dithionite (triphasic when Tween 20 was present as the detergent) can be interpreted as a consequence of intramolecular electron transfer. This may be complicated, however, by direct reduction at the cytochrome a site. It is interesting to note that the two intramolecular rate constants for the reduction by dithionite ( $0.03 \text{ s}^{-1}$  and  $0.013 \text{ s}^{-1}$ ) are slightly smaller than those observed in the case of the reduction by MPH ( $0.19$  and  $0.02 \text{ s}^{-1}$ ). No attempt is being made, however, to determine equilibrium constants for separate intramolecular steps, since there is no evidence that electrons follow the same intermediate steps. However, by comparing the intramolecular rate constants for the two cases, one can argue that these equilibrium constants are not far from unity.

In the presence of cholate as the detergent instead of Tween 20, the reaction becomes slower and involves mainly the reduction of the a<sub>3</sub> site. Cholate is known to inhibit the activity of the protein (as measured by activity assay) (see Experimental chapter). The present results on the reduction by dithionite suggest that cholate may hinder the intramolecular electron transfer from a<sub>3</sub> to a.

The reduction of the CN-bound oxidase by dithionite was found to be biphasic in contrast to the case of the reduction of the complex by MPH where it was found to be monophasic. There are two possible explanations for this biphasicity. (1)  $\text{SO}_2^{\cdot-}$  is a one electron electron donor, unlike MPH which is essentially a two electron donor (see Chapter III), so that addition of two electrons to the oxidase may be

biphasic. This was observed with another one electron donor reduction of the CN-complex using  $\text{Ru}(\text{NH}_3)_6^{2+}$  (Scott and Gray, 1980); (2) There might have been some uncomplexed  $\text{a}_3^{3+}$ . This is less likely, since the same procedure of preparing the CN-oxidase was followed in both cases.

## CHAPTER VII

### SUGGESTIONS FOR FUTURE WORK

The work presented here has shown the usefulness of artificial electron donors in the study of the reduction of cytochrome c oxidase. MPH, in particular, has proven to be a useful reductant because of its low redox potential and spectral properties. Extension of this work and application to other systems are feasible in the following areas:

#### A. Effect of Detergents

The kind of detergent used to maintain the protein in solution is found to be extremely important in determining the stability and the activity of the oxidase. There are suggestions that the state of aggregation of the protein affects its activity (Robinson and Capaldi, 1977). Rosevear et al. (1980) have shown that the detergent lauryl maltoside is very effective in keeping a uniform (mono-disperse) solution of the protein, while retaining high activity. It is, in particular, the state of homogeneity of the cytochrome c oxidase solution that is important in the study of the kinetics. A preliminary experiment was done (in collaboration with Zexia Barnes) on the reduction of oxidase solution prepared in lauryl maltoside by MPH. Although the kinetics of the fast phase seem similar to those discussed in the text for solutions prepared in Tween 20, analysis of the full time

course is not complete. Study of the detergent effects are important in determining if the state of aggregation of the oxidase plays a role in its inter- and intra-molecular electron transfer.

### B. Partial Reduction of Cytochrome c Oxidase

The work presented in this text involved only the full reduction of cytochrome c oxidase (4 e/molecule of oxidase). A study of the anaerobic partial reduction (less than 4 electrons) should be very helpful in understanding the electron redistribution among the protein metal centers. Comparing the transient state spectra to those obtained under equilibrium conditions (Babcock et al., 1978) should reveal possible electron pathways through the protein. Preliminary work on partial reduction (particularly 2 e/oxidase molecule) produced some interesting results. We have found that with only two electrons, there are still slow phases of electron redistribution. Careful analysis of the extent of these phases and the exact counting of electrons (which could be obtained by comparing final "kinetic" spectra to those obtained under equilibrium titrations) have not been done.

### C. Aerobic Experiment

Although data on many "aerobic" experiments on the reduction of the oxidase by MPH were obtained by accident or by design, only the anaerobic kinetics were studied in detail. Data from experiments with oxygen present should have an enormous amount of information about the rates of the intra-molecular electron transfer in the protein.

Specifically, when the MPH concentration is higher than that of oxygen, the continuation of the reduction of the oxidase after oxygen exhaustion should reveal information on the effect of "oxygenation" (directly following catalytic cycles) on the intramolecular electron transfer. These are to be compared with the rates in the strictly anaerobic cases discussed in the present work. It has been suggested that the oxidized form can exist in three (or more) different conformations (see, for example, Brudvig et al., 1981). One of these forms is the "oxygenated" oxidase (Okunuki et al., 1958), which is formed when the reduced protein is subjected to reoxidation. The experiments (when oxygen is present) can then provide an answer to another question: Does this conformational change occur simultaneously upon reoxidation, or is it a slow process? The answer to this question is to be found by comparing the experiments mentioned above to those of anaerobic experiments on previously prepared (anaerobic) "oxygenated" protein.

#### D. Cytochrome $c_{552}$

Cytochrome  $c_{552}$ : flavocytochrome  $c_{552}$  is a heme protein that has a molecular weight of about 72,000 D and contains two moles of heme and one of flavin (FAD) per mole of enzyme (Bartsch and Kamen, 1960). The protein is believed to play a role in bacterial  $H_2S$  oxidation (Dickerson and Timkovich, 1975; Streckas, 1976). A number of EPR and Raman studies have appeared on the properties of this protein (Ondrias, 1979; Ondrias et al., 1980). An important observation from the limited kinetic studies on this enzyme (Vorkink, 1972) is that the rates of the reduction of the hemes are different from that of the

flavin. A preliminary study of the anaerobic reduction of the protein with sodium dithionite revealed that the reduction is fast, with  $t_{\frac{1}{2}} \sim 50$  ms when dithionite is present in slight excess. This  $t_{\frac{1}{2}}$  appears to be smaller than that reported earlier (Vorkink, 1972) for the same system. A study of this reduction at lower temperatures (to make use of the scanning mode) should be useful in resolving spectral shapes of the hemes and the flavin. Also, the use of other reductants, especially those of biological interest such as sulfide, may prove helpful in understanding the role of this protein. Flavocytochrome c<sub>552</sub> is analogous to cytochrome c oxidase in that it accumulates a total of four reducing equivalents, shows evidence of interaction between redox centers and can react with exogenous ligands, such as CO.

#### E. The Application of Principal Component Analysis to Other Systems

In Chapter V, a scheme for the statistical weighting of principal component analysis (PCA) was discussed. The application of PCA to resolve the spectral shapes and time courses of the strongly interacting chromophores of cytochrome c oxidase proves the power and the applicability of this method. The application of PCA to other enzymatic systems--particularly heme proteins--may prove to be useful in understanding the spectral and kinetic properties of these enzymes. PCA, when supplied with reasonable target spectral shapes or concentration profiles, can completely resolve scanning stopped-flow kinetic experiments.

REFERENCES

## REFERENCES

- Adar, F., and Yonetani, T. (1978). *Biochem. Biophys. Acta*, 502, 80.
- Anderson, R. F. (1980). *Biochem. Biophys. Acta*, 590, 277.
- Andreasson, L. E. (1975). *Eur. J. Biochem.*, 53, 591.
- Andreasson, L. E., Malmstrom, B. G., Stromberg, C., and Vanngard, T. (1972) *FEBS Lett.*, 28, 297.
- Antonini, E., Brunori, M., Colosimo, A., Greenwood, C., and Wilson, M.T. (1977). *Proc. Natl. Acad. Sci. U.S.A.*, 74, 3128.
- Antonini, E., Brunori, M., Greenwood, C., and Wilson, M. T. (1973). *Biochem. Soc. Trans.* 1, 34.
- Assa, R., Albracht, S. P. J., Falk, K. E., Lanne, B., and Vanngard, T. (1976). *Biochem. Biophys. Acta* 422, 260.
- Awasthi, Y. C., Chuang, T. F., Keenan, T. W., and Crane, F. L. (1971). *Biochim. Biophys. Acta* 226, 42.
- Babcock, G. T., Callahan, P. M., Ondrias, M. R., and Salmeen, I. (1981). *Biochemistry* 20, 959.
- Babcock, G. T., and Salmeen, I. (1979). *Biochemistry* 12, 2493.
- Babcock, G. T., Vickery, L. E., and Palmer, G. (1978). *J. Biol. Chem.* 253, 2400.
- Babcock, G. T., Vickery, L. E., and Palmer, G. (1976). *J. Biol. Chem.* 251, 7907.
- Bartsch, R. G., and Kamen, M. D. (1960). *J. Biol. Chem.* 235, 825.
- Beinert, H., Shaw, R. W., Hansen, R. E., and Hartzell, C. R. (1980). *Biochim. Biophys. Acta* 591, 458.
- Beinert, H., and Shaw, R. W. (1977). *Biochim. Biophys. Acta* 462, 121.
- Bellman, R. (1970). Introduction to Matrix Analysis, 2nd ed., McGraw-Hill, New York.

- Bergmeyer, U. H., and Bernt, E. (1974). in Methods of Enzymatic Analysis (Bergmeyer, U.H., Ed.) Vol. 2, pp. 579-582, Academic Press, New York.
- Birchmeier, W., Kohler, C. E., and Schatz, G. (1976). Proc. Natl. Acad. Sci. U.S. 73, 4334.
- Bisson, R., Azzi, A., Gutweniger, H., Colonna, R., Montecucco, C., and Zanotti, A. (1978). J. Biol. Chem. 253, 1874.
- Briggs, M. M., and Capaldi, R. A. (1978). Biochem. Biophys. Res. Commun. 80, 553.
- Briggs, M., Kamp, P. F., Robinson, N. C., Capaldi, R. A. (1975). Biochemistry 14, 5123.
- Brittain, T., and Greenwood, C. (1976). Biochem. J., 155, 453.
- Brudvig, G. W., Stevens, T. H., Morse, R. H., and Chan, S. I. (1981). Biochemistry 20, 3912.
- Blumer, J. T., and Shurvell, H. F. (1973). J. Phys. Chem, 77, 256.
- Callahan, P. M., and Babcock, G. T. (1981). Biochemistry 20, 952.
- Caughey, W. S., Wallace, W. J., Volpe, J. A., and Yoshikawa, S. (1976). in "The Enzymes," Vol. 13 (Boyer, P.D., ed.), pp. 299-344, Academic Press, New York.
- Caughey, W. S., Smythe, G. A., O'Keefee, D. H., Maskasky, J. G., and Smith, M. L. (1975). J. Biol. Chem. 250, 7602.
- Challoner, D. R. (1963). Nature, 217, 72.
- Chance, B., and Powers, L. (1981). Biophys. J. 33, 95a.
- Chance, B., Saronio, C., Waring, A., and Leigh, J. S. Jr. (1978). Biochim. Biophys. Acta, 503, 37.
- Chance, B., Saronio, C., and Leigh, J. S., Jr. (1975). J. Biol. Chem. 250, 922b.
- Chance, B., and Leigh, J. S., Jr. (1977). Proc. Natl. Acad. Sci. U.S., 74, 4777.
- Chew, V. S. F., and Bolton, J. R. (1980). J. Phys. Chem. 84, 1903.
- Chew, V. S. F., Bolton, J. R., Brown, R. G., and Porter, G. (1980). J. Phys. Chem. 84, 1909.

- Clore, G. M., and Chance, E. M. (1979). *Biochem. J.*, 177, 613.
- Clore, G. M., and Chance, E. M. (1978). *Biochem. J.* 173, 799.
- Clore, G. M., and Chance, E. M. (1978). *Biochem. J.* 173, 811.
- Clore, G. M., and Chance, E. M. (1978). *Biochem. J.* 175, 709.
- Cochran, R. N., and Horne, F. H. (1980). *J. Phys. Chem.*, 84, 2561.
- Cochran, R. N., Horne, F. H., Dye, J. L., Ceraso, J., and Suelter, C. H. (1980). *J. Phys. Chem.* 84, 2567.
- Cochran, R. (1977). Ph.D. Dissertation, Michigan State University, East Lansing, MI. 48824, USA.
- Cochran, R. N., and Horne, F. H. (1977). *Anal. Chem.* 49, 846.
- Coolen, R. B., Papadakis, N., Avery, J., Enke, C. G., and Dye, J. L. (1975). *Anal. Chem.* 47, 1649.
- Cox, R. P., and Hollaway, M. R. (1977). *Eur. J. Biochem.* 74, 575.
- Dearman, M., Rao, N. A., and Yagi, K. (1972). *Biochem, Biophys. Res. Comm.* 46, 849.
- Dickerson, R. E., and Timkovich, R. (1975). in "The Enzymes," Vol. 11 (P. D. Boyer, ed.) Academic Press, New York, pp. 497.
- Downer, N. W., Robinson, N. C., and Capaldi, R. A. (1976). *Biochemistry* 15, 2930.
- Dutton, P. L., and Wilson, D. F. (1974). *Biochim. Biophys. Acta* 346, 165.
- Erecinska, M. (1975). *Arch. Biochem. Biophys.* 169, 199.
- Errede, B., and Kamen, M. D. (1979). in "Symposium on Cytochrome Oxidase" (King, T. E., Orii, Y., Chance, B., and Okunuki, K., eds), pp. 269-280. Elsevier/North-Holland Biomedical Press, Amsterdam.
- Errede, B., and Kamen, M. D. (1978). *Biochemistry*, 17, 1015.
- Falk, K. E., Vanngard, T., and Angstrom, J. (1977). *FEBS Lett.* 75, 23.
- Farrington, J. A., Land, E. J., and Swallow, A. J. (1980). *Biochim. Biophys. Acta* 590, 273.

- Ferguson-Miller, S., Brautigan, D. L., and Margoliash, E. (1976). *J. Biol. Chem.*, 251, 1104.
- Fry, M., Zande, H. V., and Green, D. E. (1978). *Proc. Natl. Acad. Sci. U.S.* 75, 5908.
- Ghosh, R., and Quayle, J. R. (1979). *Anal. Biochem.* 99, 112.
- Gibson, Q. H., Greenwood, C., Wharton, D. C., and Palmer, G. (1975). *J. Biol. Chem.* 240, 888.
- Gibson, Q. H., Palmer, G., and Wharton, D. C. (1965). *J. Biol. Chem.* 240, 915.
- Gibson, Q. H., Greenwood, C. (1963). *J. Biol. Chem.* 86, 541.
- Gouterman, M. (1959). *J. Chem. Phys.* 30, 1139.
- Greenwood, C., Brittain, T., Brunori, M., and Wilson, M. T. (1977). *Biochem. J.* 165, 413.
- Greenwood, C., Wilson, M. T., and Brunori, M. (1974). *Biochem. J.* 137, 205.
- Greenwood, C., and Gibson, Q. H. (1967). *J. Biol. Chem.* 242, 1782.
- Griffiths, D. E., and Wharton, D. C. (1961). *Biochim. Biophys. Res. Commun.* 4, 199.
- Griffiths, D. E., and Wharton, D. C. (1961a). *J. Biol. Chem.* 236, 1850.
- Griffiths, D. E., and Wharton, D. C. (1961b). *J. Biol. Chem.* 236, 1857.
- Gutteridge, S., Winter, D. B., Bruzninck, W. J. A., and Mason, H. S. (1977). *Biochem. Biophys. Res. Commun.* 78, 945.
- Halaka, F. G., Babcock, G. T., and Dye, J. L. (1981a). *J. Biol. Chem.* 256, 1084.
- Halaka, F. G., Babcock, G. T., and Dye, J. L. (1981b). *J. Biol. Chem.*, in press.
- Harrington, P. C., DeWaal, D. J. A., and Wilkins, R. G. (1978). *Arch. Biochem. Biophys.* 191, 444.
- Hartzell, C., and Beinert, H. (1975). *Biochim. Biophys. Acta*, 368, 318.
- Henderson, R., Capaldi, R. A., and Leigh, J. S. (1977). *J. Mol. Biol.* 112, 631.

- Hisada, R., and Yagi, T. (1977). *Biochemistry* 82, 1649.
- Hochli, L., and Hackenbrock, G. R. (1978). *Biochemistry*, 17, 3712.
- Hu, V. W., Chan, S. I., and Brown, G. S. (1977). *Proc. Nat'l Acad. Sci. USA* 74, 3821.
- Jacobs, E. E., Jacob, M., Sanadi, D. R., and Bradley, L. B. (1950). *J. Biol. Chem.* 6223, 147.
- Jagendorf, A., and Margulies, L. (1960). *Arch. Biochem. Biophys.* 90, 184.
- June, D. S., Kennedy, B., Pierce, T. H., Elias, S. V., Halaka, F. G., Behbahani-Nejad, I., El-Bayoumi, A., Suelter, C. H., and Dye, J. L. (1979). *J. Am. Chem. Soc.* 101, 2218.
- Kearney, E. B., and Singer, T. P. (1956). *J. Biol. Chem.* 219, 963.
- Kellin, D., and Hartree, E. F. (1938a). *Proc. R. Soc. (B)*, 125, 171.
- Keilin, D. (1966). *The History of Cell Respiration and Cytochromes*, Keilin, J., ed., Cambridge Univ. Press.
- Keilin, D., and Hartree, E. F. (1954). *Proc. R. Soc. (B)* 127, 167.
- Keilin, D., and Hartree, E. F. (1938b). *Nature* 141, 870.
- Komai, H., and Capaldi, R. (1973). *FEBS Lett.* 30, 273.
- Koppenol, W. H., Van Buuren, K. J. H., Butler, J., and Braams, R. (1976). *Biochim. Biophys. Acta* 449, 157.
- Lambeth, D. O., and Palmer, G. (1973). *J. Biol. Chem.*, 248, 6095.
- Lanne, B., and Vanngord, T. (1978). *Biochim, Biophys. Acta*, 501, 449.
- Lanne, B., Malmstrom, B. G., and Vanngord, T. (1977). *FEBS Lett.*, 77, 146.
- Leigh, J. S. Jr., Wilson, D. F., Owne, C. S., and King. T. E. (1974). *Arch. Biochem. Biophys.* 160, 476.
- Lemberg, M. R. (1969). *Physiol. Rev.* 49, 48.
- Lemberg, R., and Gilmour, M. W. (1967). *Biochim. Biophys. Acta.*, 143, 500.
- Lemberg, M. R., and Mansley, G. E. (1965). *Biochim. Biophys. Acta*, 96, 187.

- Low, H., and Villain, I. (1963). *Biochim. Biophys. Acta*, 69, 361.
- Malinowski, E. R., and Howery, D. G. (1980). in Factor Analysis in Chemistry, Wiley--Interscience.
- Malkin, R., and Malmstrom, B. G. (1970). *Adv. Enzymes*, 33, 177.
- Malmstrom, B. G. (1979). *Biochim. Biophys. Acta*, 549, 281.
- Malmstrom, B. G. (1973). *Q. Rev. Biophysics*, 6, 389.
- Marzotko, D., Wachowiak, R., and Warchol, J. B. (1973). *Acta Histochemica*, 76, 150.
- Mayhew, S. (1978). *Eur. J. Biochem.* 85, 535.
- McIlwin, H. J. (1937). *Biochem. Soc. Part 2*, 1704.
- Minnaert, K. (1961). *Biochim. Biophys. Acta*, 50, 23.
- Nakamura, S., Arimura, K., Ogawa, K., and Yagi, T. (1980). *Clinica Chimica Acta*, 101, 321.
- Nakano, S., Kimura, K., Inskuchi, H., and Yagi, T. (1975). *Biochem.* 78, 1347.
- Nicholls, P., and Hildebrandt, V. (1978). *Biochim. Biophys. Acta* 504, 457.
- Nicholls, P., and Chance, B. (1974). in Molecular Mechanisms of Oxygen Activation (Hayaishi, O., ed.) pp. 149, Academic Press, New York.
- Nicholls, P., and Petersen, L. C. (1974). *Biochim. Biophys. Acta* 357, 462.
- Nishiki, M., Rao, N. A., and Yagi, K. (1972). *Biochem. Biophys. Res. Comm.* 46, 849.
- Ohno, A., Kimura, T., Oka, S., Ohnishi, Y., and Kagami, M. (1975). *Tetrahedron Letters* 28, 2371.
- Okunuki, K., Hagihar, B., Sekuzu, I., and Horio, T. (1958). *Proc. Int. Symp. Enzyme Chemistry, Tokyo and Kyoto*, Maruzen, Tokyo, p. 264.
- Olivas, E., DeWaal, D. J. A., and Wilkins, R. G. (1977). *J. Biol. Chem.* 252, 4038.
- Ondrias, M. R., Findson, E. W., Leroi, G. E., and Babcock, G. T. (1980). *Biochemistry* 19, 1723.

- Ondrias, M. (1979). Ph.D. Dissertation, Michigan State University, East Lansing, Michigan.
- Orii, Y. (1979). in "Symposium on Cytochrome Oxidase" (King, T. E., Orii, Y., Chance, B., and Okunuki, K., eds.) pp. 331-340, Elsevier/North-Holland Biomedical Press, Amsterdam.
- Ozawa, T., Suzuki, H., and Tanaka, M. (1980). Proc. Nat'l Acad. Sci., USA, 77, 928.
- Papadakis, N., Coolen, R. B., and Dye, J. L. (1975). Anal. Chem. 47, 1644.
- Peisach, J., and Blumberg, W. E. (1974). Arch. Biochem. Biophys. 165, 591.
- Penttila, T., Saraste, M., and Wikstrom, M. F. K. (1979). FEBS Letts. 101 295.
- Petersen, L. C., and Cox, R. P. (1980). Biochim. Biophys. Acta 590. 128.
- Petersen, L. C., and Cox, R. P. (1980). Eur. J. Biochemistry, 105, 321.
- Petersen, L. C., Nicholls, P., and Degn, H. (1976). Biochim. Biophys. Acta 452, 59.
- Phan, S. H., and Mahler, H. R. (1976a). J. Biol. Chem. 251, 257.
- Phan, S. H., and Mahler, H. R. (1976b). J. Biol. Chem. 251, 270.
- Powers, L., Chance, B., Ching, Y., and Angiolillo, P. (1981). Biophys. J. 33, 95a.
- Powers, L., Blumberg, W. E., Chance, B., Barlow, C. H., Leigh, J. S., Jr., Smith, J., Yonetani, T., Vik, S., and Peisach, J. (1979). Biochim. Biophys. Acta 546, 520.
- Poyton, R. O., and Schatz, G. (1975). J. Biol. Chem. 250, 752.
- Rao, P. S., and Hayon, E. (1976). Anal. Chem. 48, 564.
- Ritter, G. L., Lowry, S. R., Isenhour, T. L., and Wilkins, C. L. (1976). Anal. Chem. 48, 591.
- Robinson, N. C., and Capaldi, R. A. (1977). Biochemistry 16, 375.
- Rosevear, P., Van Aken, T., Baxter, J., and Ferguson-Miller, S. (1980). Biochemistry, 19, 4108.

- Rubaszewska, W., and Grabowski, Z. R. (1975). *J. Chem. Soc., Perkin Trans.* 2, 417.
- Rubin, M. S., and Tzagoloff, A. (1973). *J. Biol. Chem.* 248, 4269.
- Scott, R. A., and Gray, H. B. (1980). *J. Am. Chem. Soc.* 102, 3219.
- Sebald, W., Machleidt, W., and Otto, J. (1973). *Eur. J. Biochem.* 38, 311.
- Seiter, C. H. A., Margolit, R., and Perreault, R. A. (1979). *Biochem. Biophys. Res. Commun.* 86, 473.
- Sekuzo, I., Takemori, S., Yonetani, T., and Okunuki, K. (1959). *J. Biochem., Tokyo*, 46, 43.
- Shroedl, N. A., and Hartzell, C. R. (1977a). *Biochemistry*, 16, 1327.
- Shroedl, N. A., and Hartzell, C. R. (1977b). *Biochemistry*, 16, 4961.
- Shroedl, N. A., and Hartzell, C. R. (1977c). *Biochemistry*, 16, 4966.
- Singer, T. P., and Kearney, E. B. (1957). in Methods of Biochemical Analysis (Glick, D., ed.) Vol. 4, pp. 307, Interscience, New York.
- Slater, E. C. (1949). *Biochem. J.* 44, 305.
- Smith, L., in "Methods of Biochemical Analysis," Glick, D. E., ed., Interscience, New York, 1955, Vol. II, p. 427.
- Steffens, G. J., and Buse, G. (1979). in "Cytochrome Oxidase" (King, T. E., Orii, Y., Chance, B., and Okunuki, K., eds.) pp. 79-90, Elsevier/North-Holland, Amsterdam.
- Strekas, T. C. (1976). *Adv. Enzymol. Relat. Areas Mol. Biol.* 42, 287.
- Sturtevant, J. M. (1964) in Rapid Mixing and Sampling Techniques in Biochemistry, Chance, B., Eisenhardt, R. H., Gibson, Q. H., and Lonberg-Holm, K. K., eds. Academic Press, New York, pp. 89.
- Suelter, C. H., Coolen, R. B., and Dye, J. L. (1975). *Anal. Biochem.* 69, 155.
- Sylvestre, E. A., Lawton, W. H., and Maggio, M. S. (1974). *Technometrics* 16, 353.

- Tanaka, M., Hanin, M., and Yasunobo, K. T. (1977). *Biochem. Biophys. Res. Commun.* 76, 1014.
- Tiesjema, R. H., Muijsers, A. O., and van Gelder, B. F. (1973). *Biochim. Biophys. Acta*, 305, 19.
- Tiesjema, R. H., Muijsers, A. O., and van Gelder, B. F. (1972). *Biochim. Biophys. Acta* 256, 32.
- Tracy, R. P., and Chan, S. H. P. (1979). *Biochim. Biophys. Acta*, 576, 109.
- Tucker, A. (1966). *Science*, 154, 150.
- Tweedle, M. F., Wilson, L. J., Gracia-Iniguez, L., Babcock, G. T., and Palmer, G. (1978). *J. Biol. Chem.* 253, 8065.
- Vadasdi, K. (1974). *J. Phys. Chem.* 78, 816.
- Vanneste, W. H., Yseback-Vanneste, M., Mason, H. S. (1974). *J. Biol. Chem.* 249, 7390.
- Van Buuren, K. J. H., van Gelder, B. F., Wilting, J., and Braams, R. (1974). *Biochim. Biophys. Acta* 333, 421.
- Van Buuren, K. J. H., van Gelder, B. F., Wilting, J., and Braams, R. (1974). *Biochim. Biophys. Acta* 333, 421.
- Van Gelder, B. F., Tiesjema, R. H., Muijesers, A. O., and Van Buuren, K. J. H. (1973). *Fed. Proc.* 32, 1977.
- Van Buuren, K. J. H., Zuurendonk, P. F., van Gelder, B. F., Muijsers, A. O. (1972). *Biochim. Biophys. Acta* 256, 243.
- Van Buuren, K. J. H., van Gelder, B. F., and Eggelte (1971). *Biochim. Biophys. Acta* 234, 468.
- Vernon, L. P., Zaugg, W. S., and Shaw, E. R. (1963). in Photosynthetic Mechanisms of Green Plants, pp. 504, National Academy of Science, National Research Council, Washington.
- Volpe, J. A., and Caughey, W. S. (1974). *Biochem. Biophys. Res. Commun.*, 61, 502.
- Vorkink, W. P. (1972). Ph.D. dissertation, University of Arizona, Tuscon.
- Wharton, D. C., and Gibson, Q. H. (1976). *J. Biol. Chem.* 251, 2861.

- Wharton, D. C., and Tzagoloff, A. (1964). *J. Biol. Chem.* 239, 2036.
- Wharton, D. C., and Tzagoloff, A. (1963). *Biochem. Biophys. Res. Commun.* 13, 121.
- Wikstrom, M. K. F., and Krab, K. (1979). *Biochim. Biophys. Acta* 549, 177.
- Wilhelm, E., Battino, R., and Wilcock, R. (1977). *Chemical Reviews*, 77, 219.
- Wilms, J., Veerman, E. C. I., Konig, B. W., Dekker, H. L., and van Gelder, B. F. (1981). *Biochim. Biophys. Acta* 635, 13.
- Winter, D. B., Bruyninckx, W. J., Foulke, F. G., Grinich, N. P., and Mason, H. S. (1980). *J. Biol. Chem.* 255, 11408.
- Wiskind, H. K., and Burger, R. L. (1964). Appendices I and II in *Rapid Mixing and Sampling Techniques in Biochemistry*, Chance, B., Eisenhardt, R. H., Gibson, Q. H., and Lonberg-Holm, K. K., eds., Academic Press, New York.
- Yang, E. K., Adar, F., Leigh, J., and Chance, B. (1981). *Biophys. J.* 33, 949.
- Yonetani, T. (1962). *J. Biol. Chem.*, 237, 550.
- Yonetani, T. (1961). *J. Biol. Chem.* 236, 1680.
- Yoshikawa, S., Shoc, M. G., O'Toole, M. C., and Caughey, W. S. (1977). *J. Biol. Chem.* 252, 5498.
- Yu, C., and Yu, L. (1977). *Biochim. Biophys. Acta* 495, 248.
- Zaugg, W. S. (1964). *J. Biol. Chem.* 239, 3964.
- Zaugg, W. S., Vernon, L. P., and Tripack, A. (1964). *Proc. Nat'l Acad. Sci. USA*, 51, 232.

